CHARACTERIZATION AND SELECTIVE TARGETING
OF ANEUPLOID HUMAN COLONIC EPITHELIAL CELLS

APPROVED BY SUPERVISORY COMMITTEE

Jerry W. Shay, Ph.D. (Advisor)

Lawrence Lum, Ph.D. (Chairman)

Gray W. Pearson, Ph.D.

Tej K. Pandita, Ph.D.

DEDICATION

Dedicated to beautiful wife Lenh for her everlasting love and support.

CHARACTERIZATION AND SELECTIVE TARGETING OF ANEUPLOID HUMAN COLONIC EPITHELIAL CELLS

by

PETER LY

DISSERTATION

Presented to the Faculty of the Graduate School of Biomedical Sciences

The University of Texas Southwestern Medical Center at Dallas

In Partial Fulfillment of the Requirements

For the Degree of

DOCTOR OF PHILOSOPHY

The University of Texas Southwestern Medical Center at Dallas

Dallas, Texas

December 2012

ACKNOWLEDGEMENTS

I would first like to express my gratitude towards my research advisors, Jerry Shay and Woodring Wright, for their support and mentorship throughout my graduate career. You both undertook a young, naïve graduate student to develop into an independent scientist. For that, I could never thank you enough. I am also appreciative of the scientific freedom to find my own way, and not to mention, all the constructive criticism that came with it.

Next, I would like to thank members of my dissertation committee: Lawrence Lum, Gray Pearson, and Tej Pandita, for their valuable advice and contributions to my project and career over the years. An acknowledgement also goes to Chaitanya Nirodi for sharing experimental advice, as well as members of the UTSW HTS facility for always being so cooperative and helpful.

I would also like to recognize Kevin Kennon for providing outstanding administrative support, as well as all members of the Shay/Wright laboratory, both past and present, for sharing in this memorable experience with me. In particular, I would like to thank Ugur Eskiocak, Sang Bum Kim, and Oliver Delgado for their mentorship, advice, and contributions toward my scientific way-of-thinking and career. Thanks also goes to Lu Zhang, Crystal Cornelius, Andres Roig, Suzie Hight, Aadil Kaisani, Guido Stadler, Kim Batten, Stina Singel, Sebastian Biglioni, Phil Smiraldo, Jin Yong Kim, Chelsea Parker, and Kenneth Harris for being excellent friends and colleagues.

A special acknowledgement also extends to my childhood friends: Richard Quach, Tuan Chieu, Harrison Chow, and Raymond Chow, for being there with me every step of the way throughout the years. You are all brothers to me.

I am also especially grateful to my family: my father Sao Ly, my mother Leng Ly, my brother Bryan Ly, and my aunt Ngo Chiv, for their unconditional love and continuous support throughout my education, career, and life.

Last and not least, the appreciation I have for my wife and best friend, Lenh Ngo, cannot be expressed in words. Your never-ending love and support has guided me through life and has given me meaning for everything that I do and all that I am. Also, thanks to Toby for always being a good dog.

CHARACTERIZATION AND SELECTIVE TARGETING
OF ANEUPLOID HUMAN COLONIC EPITHELIAL CELLS

PETER LY

The University of Texas Southwestern Medical Center at Dallas, 2012

JERRY WILLIAM SHAY, Ph.D.

Aneuploidy, an abnormal number of chromosomes, occurs in the vast majority of sporadic colorectal cancer patients. Despite this observation, the cellular advantages conferred by recurring cytogenetic alterations are poorly understood and targeted therapies selective to aneuploid cells are currently non-existent. Here, we provide evidence that serum-free passage of originally diploid, immortalized human colonic epithelial cells give rise to the acquisition of trisomy 7 (1CT+7), an aneuploidy detected in over 40% of colorectal adenomas. Pre-existing 1CT+7 cells within the original population were undetectable through GTG-banding and fluorescent *in situ* hybridization analysis, suggesting a conversion of diploid cells to an aneuploid state. Compared to their

isogenic diploid counterpart, 1CT+7 cells express higher levels of the epidermal growth factor receptor (EGFR, located on chromosome 7p). Treatment with the pharmacological adenosine analog 5-aminoimidazole-4-carboxamide-1-β-D-ribofuranoside (AICAR) completely halted proliferation of 1CT+7 cells and reduced both metabolic consumption and production *in vitro*. Unexpectedly, treatment of 1CT+7 cells with AICAR led to a reversible 3.5-fold reduction in EGFR overexpression. AICAR-induced depletion of EGFR protein can be abrogated through inhibition of the proteasome with MG132. AICAR also heavily promoted EGFR ubiquitination in cell-based immunoprecipitation assays, suggesting enhanced degradation of EGFR protein mediated by the proteasome. Moreover, treatment with AICAR reduced EGFR protein levels in a panel of human colorectal cancer cell lines *in vitro* and in xenograft tumors *in vivo*. Our data collectively supports the compound AICAR as a novel inhibitor of EGFR protein abundance and as a potential anticancer agent for aneuploidy-driven colorectal cancer. In summary, we have isolated and characterized isogenic human colonic epithelial cells that represent recurrent chromosomal acquisitions in sporadic colorectal cancer and demonstrate how it may be possible to selectively target these cells for therapeutic intervention.

TABLE OF CONTENTS

PRIOR PUBLICATIONS

Ly P, Eskiocak U, Kim SB, Roig AI, Hight SK, Lulla DR, Zou YS, Batten K, Wright WE, Shay JW. (2011) Characterization of aneuploid populations with trisomy 7 and 20 derived from diploid human colonic epithelial cells. ***Neoplasia***; 13(4): 348-357.

Eskiocak U, Kim SB, **Ly P**, Roig AI, Biglione S, Komurov K, Cornelius C, Wright WE, White MA, Shay JW. (2011) Functional parsing of driver mutations in the colorectal cancer genome reveals numerous suppressors of anchorage-independent growth. ***Cancer Research***; 71(13): 4359-4365.

Ly P, Kim SB, Kaisani AA, Marian G, Wright WE, Shay JW. (2012) Aneuploid human colonic epithelial cells are sensitive to AICAR-induced growth inhibition through EGFR degradation. ***Oncogene***, Epub ahead of print.

Ly P, Eskiocak U, Parker CR, Harris KJ, Wright WE, Shay JW. (2012) RNAi screening of the human colorectal cancer genome identifies multifunctional tumor suppressors regulating epithelial cell invasion. ***Cell Research***; 22(11): 1605-1608.

Kim SB, Pandita RK, Eskiocak U, **Ly P**, Kaisani AA, Kumar R, Cornelius C, Wright WE, Pandita TK, Shay JW. (2012) Targeting of Nrf2 induces DNA damage repair and protects colonic epithelial cells from ionizing radiation. ***Proc Natl Acad Sci***; 109(43): 2949-2955.

Hernandez V, Weng J, **Ly P**, Pompey S, Dong HY, Mundy DI, Mishra L, Schwarz MA, Anderson RG, Michaely P. (2012) Cavin-3 controls signal transduction coupling to ERK and Akt via linkage between caveolae and the membrane cytoskeleton. (Manuscript submitted)

Kim SB, **Ly P**, Kaisani AA, Wright WE, Shay JW. (2012) Mitigation of radiation-induced damage by targeting EGFR in human colonic epithelial cells. (Manuscript submitted)

LIST OF FIGURES

LIST OF APPENDICES

LIST OF ABBREVIATIONS

+7	*trisomy 7*
+20	*trisomy 20*
ACF	*aberrant crypt foci*
AICAR	*5-aminoimidazole-4-carboxamide-1-β-D-ribofuranoside*
AMPK	*AMP-activated protein kinase*
APC	*adenomatosis polyposis coli*
CAN-genes	*candidate colorectal cancer genes*
CDK4	*cyclin dependent kinase 4*
cDNA	*complementary DNA*
CIN	*chromosomal instability*
CRC	*colorectal cancer*
CT	*Cdk4- and hTERT-immortalized*
CTRP	*HCEC CT with $KRAS^{V12}$ expression and TP53 knockdown*
EGF	*epidermal growth factor*
EGFR	*epidermal growth factor receptor*
FISH	*fluorescent in situ hybridization*
HCEC	*human colonic epithelial cells*
HSP90	*heat shock protein 90*
hTERT	*human telomerase reverse transcriptase*
LOH	*loss of heterozygosity*
MEF	*mouse embryonic fibroblast*

MIN	*microsatellite instability*
MMP	*matrix metalloproteinases*
PD	*population doubling*
RNAi	*RNA interference*
SILAC	*stable isotope labeling by amino acids in cell culture*
siRNA	*small interfering RNA*
shRNA	*short hairpin RNA*

CHAPTER ONE

ANEUPLOIDY AND COLORECTAL CANCER PATHOGENESIS

Colorectal Cancer

As the final part of the mammalian digestive system, the colon (or large intestine) is responsible for storing waste, absorbing nutrients, and maintaining water homeostasis. The human colon consists of millions of invaginated, finger-like structures, known as the crypts of Lieberkühn, which comprises the basic functional unit of the colon (Crosnier et al., 2006). With exception to the colonic stem cells, every cell within the intestinal epithelium undergoes continuous renewal approximately once each week, making the colon one of the most rapidly turned over human organs (Humphries et al., 2008). Multipotent stem cells are located at the bottom of the tubular crypt structures and give rise to transit amplifying cells that lead to further differentiated cell types, including absorptive, goblet, enteroendocrine, and Paneth cells (Ricci-Vitiani et al., 2009). These cells then migrate apically up the epithelium towards the intestinal lumen (**Figure 1.1**). At the apex of these crypts, terminally differentiated cells subsequently undergo apoptosis and/or shedding to create space for newly replenished epithelial cells arising from the basal portion of the crypt (Crosnier et al., 2006). Therefore, the colonic stem cell compartment and organization of the crypts are especially important in the maintenance and proper function of the colon (Humphries et al., 2008).

Cancer of the colon or rectum is collectively referred to as colorectal cancer (CRC). Over 140,000 cases of CRC are annually diagnosed in the United States alone

(Moran et al., 2010) and upwards to 900,000 cases are diagnosed worldwide each year (Rustgi 2007). Cancer generally arises from deregulated control of cell growth due to oncogene activation or tumor suppressor inactivation. The accumulation of genetic and epigenetic alterations forms the fundamental basis of tumorigenesis. According to the multiple-hit hypothesis proposed in 1971, genetic mutations gradually accrue and allow normal cells the ability to acquire pro-tumorigenic phenotypes that can then contribute towards cancer development (Fearon et al., 1990). Such phenotypes include, but are not limited to, resistance to apoptosis, enhanced cell proliferation, and/or improved adaptation to stressful conditions (Hanahan et al., 2011). Therefore, the acquisition of a series of specific mutations can alter the behavior of normal cells to progress towards malignancy. For example, mutations in the *RAS* oncogene or the *TP53* tumor suppressor are frequently detected among colorectal carcinoma samples (42% and 52%, respectively, The Cancer Genome Atlas), suggesting that these genes are critically involved in tumor regulation.

Both inherited and sporadic mutations contribute to different types of CRC, as well as dietary and lifestyle factors. Approximately 80% of CRC cases are sporadic, with a majority of sporadic patients also harboring karyotypic abnormalities in addition to genetic mutations (Grady et al., 2008). Hereditary colonic diseases include familial adenomatous polyposis, a predisposition in which the epithelium is lined with hundreds to thousands of benign polyps that can become malignant if left untreated. The basis of this disease led to the discovery of the adenomatous polyposis coli (*APC*) gene (Groden et al., 1991; Nishisho et al., 1991), the most frequently altered CRC gene. Mutations in

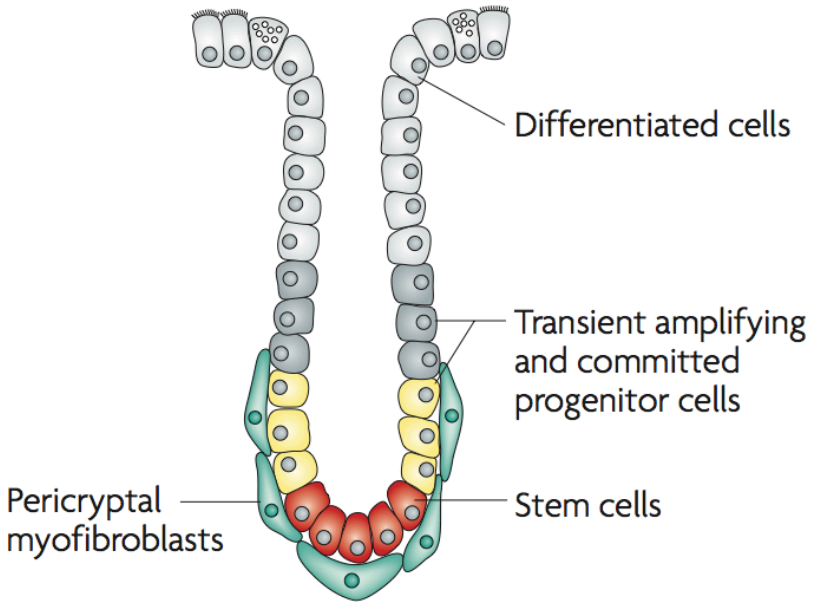

Figure 1.1. Organization of the colonic crypt. Stem cells located at the base of the crypt give rise to more differentiated transit amplifying and progenitor cells. Terminally differentiated cells at the apex of the crypts undergo apoptosis, and the entire epithelium is replenished approximately once a week.

Adapted from Humphries et al, *Nature Reviews Cancer* 2008

APC that confer a truncated protein product can be detected in a large fraction of sporadic and hereditary CRC patients.

In CRC, it is proposed that genetic and chromosomal alterations to the epithelial or stem cell compartments mark the initiation of tumorigenesis (Fearon 2011). The development of aberrant crypt foci (ACF) lining the gastrointestinal track can result in the appearance of benign colorectal polyps, or adenomas **(Figure 1.2)**. These precancerous lesions can potentially progress towards the malignant adenocarcinoma stage if not surgically removed during routine colonoscopy screening. Additional alterations then contribute towards metastasis, where cells from the primary tumor are able to spread and seed at distant organs. The median survival time of patients diagnosed with metastatic disease is nineteen months, with spreading to the liver accounting for one-third of all CRC-related deaths (Kopetz et al., 2009). Although the majority of sporadic CRC is preventable and can be surgically treated if detected early through routine surveillance screening, patients diagnosed with more advanced cancers typically undergo a combination of surgery and chemotherapy (Cunningham et al., 2010).

Chromosomal Instability and Aneuploidy

Maintenance of genomic integrity throughout cell division is critical for successful organismal development. Defects throughout mitotic division can lead to an inappropriate number of chromosomes per cell, a condition known as aneuploidy (Rajagopalan et al., 2004). Almost all germline aneuploidies occurring at an early developmental stage results in spontaneous abortions, with the exception of specific

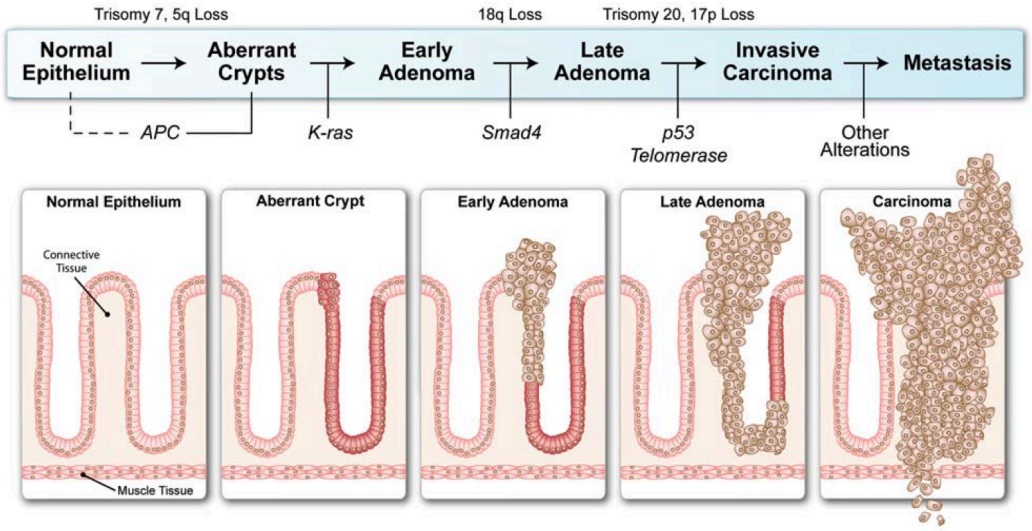

Figure 1.2. The current model for human colorectal cancer progression. Cells lining the gastrointestinal track undergo a variety of genetic alterations that gradually transitions a normal colonic epithelium towards the carcinoma stage. Aside from genetic alterations, there are also recurrent chromosomal alterations that occur in a presumably stepwise manner.

Adapted from Roig et al, *Current Colorectal Cancer Reports* 2009

autosomal trisomies (chromosomes 13, 18, and 21) that lead to severe birth defects, mental impairment, and shortened life expectancy (Patau, Edwards, and Downs syndrome, respectively) (Hassold et al., 1996). It has been proposed that aneuploidy is generally disadvantageous towards overall fitness at both the organismal and cellular level (Siegel et al., 2012). Therefore, one conundrum is that a large percentage of cancers, a disease characterized by unabated cell growth and division, typically exhibit some degree of aneuploidy. Since aneuploidy can be observed in the vast majority of solid human tumors and is especially apparent in specific tissue types, including the colon, several questions arise: How does aneuploidy contribute to cancer development despite being evolutionarily detrimental? What are the key biological differences between diploid and aneuploid cells? How do defects in proper mitotic division lead to aneuploidy and which genes or pathways are involved?

Through his experimentation with sea urchins, the German zoologist Theodor Boveri proposed over a century ago that cancer is a disease caused by chromosomal abnormalities (Boveri 2008), although this theory was generally disregarded at the time. Cells exhibiting chromosomal instability (CIN), a dynamic rate of aneuploidy accrual, can fluctuate chromosome numbers or become stably aneuploid once CIN is reduced. Translocations, deletions, and amplifications of specific loci or whole chromosome arms also contribute to the karyotypic diversity found in many tumors (Lengauer et al., 1998). According to the Mitelman Database of Chromosome Aberrations in Cancer, approximately 15% of carcinomas are diploid ($2n$), with the majority of tumors having either lost or gained a single chromosome, termed monosomy ($2n$-1) and trisomy ($2n$+1), respectively **(Figure 1.3)** (Weaver et al., 2008). Recent studies have also identified

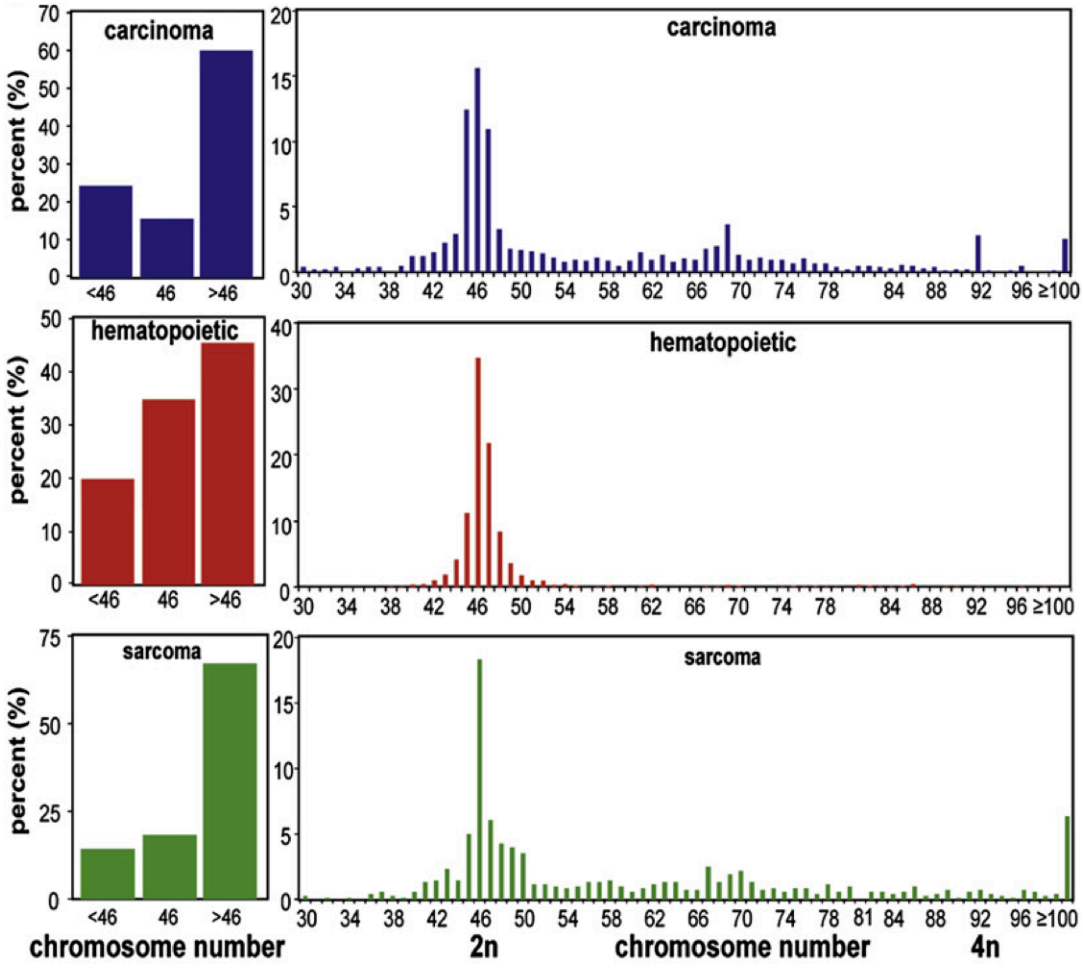

Figure 1.3. Percentage of cancers with a specific chromosomal content. According to the Mitelman Database of Chromosome Aberrations in Cancer, the majority of human tumors contain more than 46 chromosomes, most with the acquisition of a single chromosome (trisomic).

Adapted from Weaver and Cleveland, *Cancer Cell* 2008

chromothripsis as a new form of genomic abnormality, a chaotic chromosomal shattering event in which DNA fragments become stitched together in random order, causing massive chromosome rearrangements in a one-time cellular crisis event (Stephens et al., 2011). The research conducted as part of this dissertation will provide an in-depth study on recurring numerical CIN, how aneuploidy may affect normal cell behavior, and whether aneuploid cells can be specifically targeted through pharmacological inhibition for therapeutic purposes.

How exactly does aneuploidy arise? During mitosis, checkpoints are intact to ensure conditions are sufficient to proceed through cell division (Musacchio et al., 2007; Thompson et al., 2010). For example, these checkpoints can serve as a safeguard to confirm proper replication of the entire genome before entering the next cell cycle phase, or that all chromosomes are aligned prior to segregation (Silva et al., 2011). Defects in these checkpoints, such as a faulty signal to prematurely proceed towards anaphase, can result in a lagging chromosome that was incorrectly aligned at the metaphase plate (Bakhoum et al., 2009). This lagging chromosome can then serve as either a trisomic or monosomic chromosome in newly replicated daughter cells (**Figure 1.4**), although most cells with chromosomal missegregation events typically undergo apoptosis. The cells that do survive, however, now harbor an inappropriate number of chromosomes (McGranahan et al., 2012), potentially leading to the differential expression of thousands of genes compared to normal diploid cells.

The Cellular Response to Aneuploidy

In order to determine the role of aneuploidy in tumorigenesis, the effect of aneuploidy at the cellular level must first be elucidated. The most obvious response to aneuploidy would be changes in gene expression due to the addition or subtraction of chromosomes. Due to gene dosage effects, a trisomy should theoretically generate a one-third overexpression of gene products located on trisomic chromosomes compared to diploid cells. Oncogenes located on these respective chromosomes would therefore be expressed at higher levels, potentially leading to oncogenic transformation by perturbing a variety of pathways. In contrast, a monosomy is expected to reduce the expression of any possible tumor suppressors located on the monosomic chromosome to half that of karyotypically normal cells. Cells with a prior mutation in a tumor suppressor, combined with a monosomic loss of the specific chromosome, could lead to loss of heterozygosity (LOH) (Baker et al., 2009). However, not all genes located on aneuploid chromosomes follow these dosage effects, with some conflicting data suggesting that only a fraction of genes are actually affected (Platzer et al., 2002; Tsafrir et al., 2006). In particular, a more direct correlation exists between mRNA expression and chromosomal copy number alterations, whereas ~25% of proteins located on aneuploid chromosomes are expressed at levels similar to diploid cells (Stingele et al., 2012).

Recent studies have examined the effects of additional chromosomes in both yeast and mammalian cells. In the budding yeast *Saccharomyces cerevisiae*, strains with an extra copy of nearly any chromosome displays reduced proliferative capabilities, as well as increased metabolic demand and production (Torres et al., 2007). These

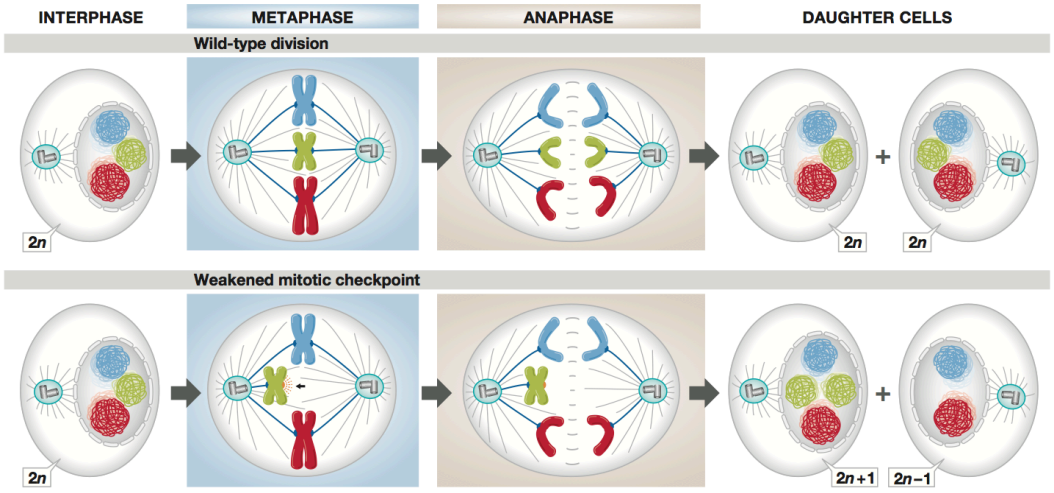

Figure 1.4. Premature procession through anaphase produces a lagging chromosome. A cell with a weakened mitotic checkpoint prematurely enters anaphase prior to proper chromosome alignment. A lagging chromosome becomes unequally partitioned to only one daughter cell, which becomes trisomic (*2n+1*), while the other daughter cell loses the chromosome and becomes monosomic (*2n-1*).

Adapted from McGranahan et al, *EMBO Reports* 2012

observations were also replicated in trisomic mouse embryonic fibroblasts (MEFs) (Williams et al., 2008). Aneuploid yeast strains harboring yeast artificial chromosomes containing mammalian DNA sequences, however, did not result in any proliferative or metabolic changes. These data suggest that the phenotypes shared among aneuploid strains are specific only to amplified yeast proteins (Torres et al., 2007). Further evidence indicates that the proliferative impairments of aneuploid cells are possibly due to slower progression through G1/S phases of the cell cycle (Stingele et al., 2012). In addition to proliferative impairments, both aneuploid models also undergo substantial transcriptomic alterations (Torres et al., 2007; Sheltzer et al., 2012). Additional proteins generated by extra chromosomes have been hypothesized to elicit a proteotoxic stress response (Torres et al., 2008). This response can become engaged when cells detect stoichiometric imbalances in the proteome, such as disproportionate levels of various protein complex subunits (i.e. ribosomal subunits, transcription factor complexes).

It is predicted that proteomic imbalances do not occur in cells with tetraploidy, or duplication of the entire genome (4*n*). Although extra chromosomes are present, all proteins within the genome are amplified to the same degree and, therefore, do not induce similar stress responses as the aneuploid state. Additional studies have also suggested that aneuploid yeast strains tend to evolve compensatory mutations in specific genes or pathways, in a chromosome-independent manner, which allows them to overcome aneuploidy-induced proliferative impairment. For example, yeast strains carrying an additional copy of one of several chromosomes tend to develop loss-of-function mutations in the *UBP6* gene, a deubiquitinating enzyme (Torres et al., 2010). These results suggest that cells are able to counter proteotoxic stress by allowing for increased

protein ubiquitination and degradation to return to growth rates comparable to normal diploid cells. In yeast models, aneuploidy has also been shown to reduce DNA repair kinetics and increase the rate of background mutations, also known as the mutator phenotype (Sheltzer et al., 2011).

Aneuploidy – Tumor Suppressor or Driver?

In some cases, aneuploidy is sufficient to induce tumorigenesis in mouse models. Induction of a wide range of stable chromosomal aberrations by overexpressing the mitotic checkpoint protein Mad2 is sufficient to drive a variety of tumor types (Sotillo et al., 2007). Furthermore, only transient expression of Mad2 is required for tumor progression and maintenance, as withdrawal of Mad2 still resulted in tumor growth due to the initial CIN (Sotillo et al., 2007). CIN can also cause tumor relapse following chemotherapy treatment. For example, aneuploidy induced by transient Mad2 expression in mice also harboring an inducible oncogenic *KRAS* allele causes an increased frequency of tumor recurrence following oncogene-withdrawal regression compared to *KRAS*-only mice (Sotillo et al., 2010). These data suggest that the generation of aneuploidy is sufficient to induce tumor relapse following potential targeted therapy against oncogene-driven cancers. Furthermore, CIN has also been associated with increased drug resistance in several organisms (Selmecki et al., 2009; Lee et al., 2011), as well as poor clinical outcome (Carter et al., 2006).

Since aneuploidy is observed in a large percentage of tumors, while also impairing normal cell proliferation, the question remains as to whether aneuploidy drives

or inhibits cancer development. Is aneuploidy simply a byproduct of tumorigenesis or does aneuploidy actually promote tumorigenesis? Addressing these questions appears to be surprisingly complex. Depending on the tissue type, aneuploidy can act as both a driver and inhibitor of transformation. For example, in mice heterozygous for the centromere motor protein CENP-E, in which the frequency of aneuploidy is higher compared to normal mice, aneuploidy promotes tumorigenesis in some organs (i.e. lung, spleen) while inhibiting malignant transformation in others (i.e. liver) (Weaver et al., 2007).

Along with tissue specificity, chromosomal specificity is also observed (Ried et al., 1996). Some aneuploidies tend to occur often in specific tumor types whereas others are observed infrequently (Meijer et al., 1998). An example of a recurrent aneuploidy in CRC is trisomy 7. Three copies of chromosome 7 can be detected in a wide range of epithelial cancers, including tissues such as the kidney (Zhuang et al., 1998), breast (Briand et al., 1996), and bladder (Berrozpe et al., 1990). Trisomy 7 can be detected in approximately 40% of colonic adenomas and increases to 80% in carcinomas (Ried et al., 1996; Bomme et al., 2001; Grade et al., 2006; Habermann et al., 2007), suggesting an early initiative event that can also potentially serve as a diagnostic biomarker. Due to gene dosage effects, it is presumed that genes located on chromosome 7 (*EGFR*, *c-MET*, *EPHB6*, etc.) will be expressed at higher levels compared to diploid cells. Interestingly, increased EGFR expression can be found in benign ACFs (Cohen et al., 2006), providing further evidence that the pathways affected by recurring aneuploidies can also contribute towards tissue-specific tumorigenesis.

Derivation and Applications of Human Colonic Cell Models

The long-term establishment of dependable *in vitro* models to study normal colonic biology has been technically challenging (Grossmann et al., 2003) and those that currently exist are inadequate. Until recently, almost all derived colonic cell lines were of malignant origin and contain numerous genetic alterations and abnormal karyotypes. Although these cells are useful as cancer lines, non-transformed colonic epithelial cells of adult human origin are required to properly investigate the effects of specific aberrations towards CRC development.

Recently, our laboratory has established normal human colonic epithelial cells (HCECs) as *in vitro* reagent to study intestinal cell biology (Roig et al., 2010). These cells were obtained from non-cancerous biopsy tissue of a previous adult CRC patient undergoing routine colonoscopy. HCECs were immortalized with ectopic expression of *CDK4* and *hTERT*, with immortalized cells from this patient termed HCEC 1CT. Importantly, these cells remain non-cancerous under a wide variety of tumorigenicity assays; testing negative for soft-agar growth, extracellular matrix invasion, and xenograft tumor formation in immunocompromised mice. These HCECs display a variety of epithelial (cytokeratin 18 and 20, ZO-1, villin, mucin, etc.) and stem cell markers (Lgr5), as well as differentiation capabilities into cyst-like structures in three-dimensional culture (Roig et al., 2010). Under 2% serum growth conditions, the HCEC 1CT line also remains fully diploid following long-term culture. Thus, these non-transformed cells provide a suitable *in vitro* model to investigate the tumorigenic effects of different genetic and epigenetic alterations to normal colonic cells.

These unique HCEC lines can be used for a variety of *in vitro* experiments. Such studies include three-dimensional culturing techniques to examine colonic differentiation, loss-of-function RNA interference (RNAi) or complementary DNA (cDNA) expression screening to identify novel cancer related genes, and high-throughput chemical compound screening for drug discovery. Importantly, our laboratory has generated a set of aneuploid HCEC lines that will serve as a valuable model to examine the effects of CIN and aneuploidy in normal cells (Ly et al., 2011). These HCECs can also be utilized to discover novel compounds to specifically target aneuploid cells (Ly et al., 2012), a potential therapeutic strategy for preventing or treating CRC.

CHAPTER TWO

DERIVATION AND CHARACTERIZATION OF ISOGENIC ANEUPLOID HUMAN CELLS

Introduction

Sporadic colorectal cancer (CRC) arises from the sequential accumulation of non-random genetic and epigenetic alterations that drive normal colonic epithelium towards neoplastic transformation (Fearon et al., 1990). A hallmark observed in the vast majority of epithelial cancers is the development of chromosomal instability (CIN) (Lengauer et al., 1997). CIN is prominent in sporadic CRC patients (Rajagopalan et al., 2003) and describes the rate at which cells accrue increasing amounts of aneuploidy, an abnormal number of chromosomes (Williams et al., 2009). As cells develop alterations in critical cell cycle control pathways, an increased incidence of aneuploidy can be detected as cells progressively become transformed (Sieber et al., 2003). This suggests that aneuploidy may be a key factor in the early events of CRC initiation that predisposes cells towards tumorigenesis (Komarova et al., 2002). Although CIN can be observed in ~85% of sporadic CRC cases (Grady et al., 2008), the causes and consequences of CIN and aneuploidy currently remain unknown (Weaver et al., 2008).

Improved human cellular reagents modeling early CIN events in CRC pathogenesis are required to more clearly characterize the biological effects of aneuploidy and to identify novel strategies for chemoprevention. Our laboratory has recently developed a method to isolate and immortalize human colonic epithelial cells

(HCECs) derived from non-cancerous tissues of patients undergoing routine screening or surveillance colonoscopy (Roig et al., 2010). Immortalized HCECs (termed HCEC CT for transduction with *Cdk4* and *hTERT*) remain diploid under long-term propagation in 2% serum growth conditions and do not exhibit any malignant phenotypes (e.g. anchorage-independent growth, invasion through extracellular matrices, tumor formation in immunocompromised mice).

The pattern of CIN leading to aneuploidy in CRC appears to be at least partially non-random. Specific chromosomal changes (such as trisomies or loss of chromosome arms) become apparent during the adenoma stage while other changes become evident in more advanced lesions (Habermann et al., 2007). One of the earliest alterations that occur in up to ~40% of colonic adenomas is the development of trisomy for chromosome 7 (+7) (Ried et al., 1996; Bomme et al., 2001; Grade et al., 2006; Habermann et al., 2007). A HCEC line propagated in our laboratory (HCEC 1CT) was derived from a patient with a previous history of sigmoid adenocarcinoma. Subsequent to immortalization, these non-cancerous cells were placed in serum-free culture for an extended period. The majority of emerged cells contained +7 as the sole cytogenetic abnormality. Experiments with these +7 cells (HCEC 1CT+7) have been conducted to elucidate if and how this single, but common, cytogenetic abnormality may confer a selective advantage to normal cells (Johansson et al., 1993). Experiments from yeast studies reveal that aneuploidy can be beneficial under a wide range of stress conditions by providing a growth advantage (Pavelka et al., 2010), although these findings have not been replicated using human cells.

Here, I report the isolation and initial characterization of 1CT+7 HCECs. I provide evidence that these aneuploid cells possess a measurable growth advantage under

serum-deprived conditions and acquire other phenotypes (e.g. defective cell migration) that may affect normal colonic physiology and promote tumorigenesis. In addition, the emergence of trisomy 20 (+20) HCEC sub-populations after introducing defined oncogenic changes into 1CT+7 HCECs is also described. Since +7 and +20 are common and recurrent chromosomal abnormalities frequently detected throughout various CRC stages (Meijer et al., 1998; Hoglund et al., 2002; Lassmann et al., 2007), these isogenically derived HCEC lines provide a valuable cell-based model to further dissect the biological consequences behind aneuploidy-driven CRC and may serve as useful reagents in the discovery of novel chemopreventive options.

Results

Emergence of HCEC 1CT+7 from diploid populations

The HCEC 1CT line used in these experiments were derived from normal tissue of a patient with a previous history of CRC and maintain a normal karyotype (46, XY) when continuously propagated in 2% oxygen and medium containing 2% serum (Roig et al., 2010). As a separate experiment, a subset of 1CT HCECs were cultured and passaged under serum-free conditions for a prolonged period and underwent a phase of slow growth. At approximately 40 population doublings (PD), 2% serum was added to the culture medium **(Figure 2.1, A)**. Cells that emerged from this population contained +7 as the sole cytogenetic change **(Figure 2.1, B)**. No distinct differences were observed in cell morphology between the two cell types. Although it is difficult to rigorously prove that an extremely rare +7 cell did not pre-exist in the population during the time of serum-free

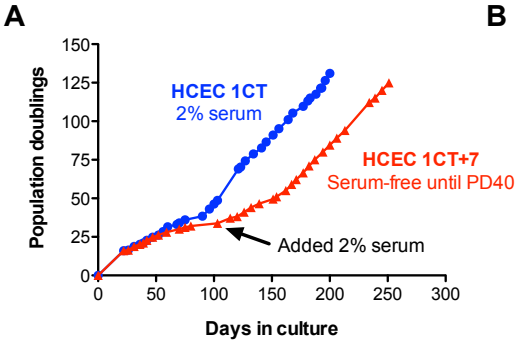

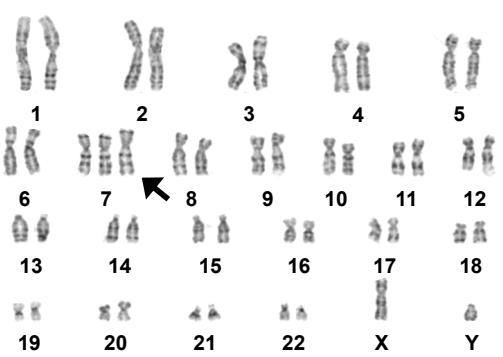

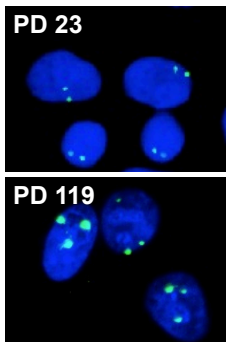

D

Population Doubling	Growth Condition	Method	Cells Analyzed	% Trisomy 7
20	0% Serum	GTG-Banding	*n* = 100	0%
20	0% Serum	FISH	*n* = 1000	0%
120	2% Serum	GTG-Banding	*n* = 50	100%
120	2% Serum	FISH	*n* = 500	100%

Figure 2.1. Trisomy 7 HCECs (HCEC 1CT+7) appeared under long-term culture in serum-free conditions.
(A) Growth curve of originally diploid cells propagated in either serum or serum-free conditions. Long-term culture of HCEC 1CT in serum stably maintains a diploid karyotype. Serum-free HCEC 1CT underwent a period of slow growth around PD30, in which case 2% serum was subsequently added to the culture at PD40.
(B) The emerged population of cells originally maintained under serum-free conditions displayed a trisomy for chromosome 7 by karyotypic analysis as the sole cytogenetic alteration.
(C) FISH analysis on early and late PD cells using a chromosome 7 centromere-specific probe.
(D) Trisomy 7 cells emerged from originally diploid HCECs with no evidence of a rare aneuploid population at an early PD.

culture, GTG-banding and fluorescent *in situ* hybridization (FISH) analysis of the original population at an early PD showed no evidence of a rare subpopulation of cells containing +7 (all 1000 interphase cells were diploid for chromosome 7 by FISH using a chromosome 7 specific probe) **(Figure 2.1, C-D)**. Emerged HCEC 1CT+7 populations were confirmed by analyzing metaphase cells by GTG-banding (50 out of 50 cells analyzed) and FISH (500 out of 500 cells analyzed) **(Figure 2.1, D)**. Array CGH analyses (NCBI GEO accession numbers: GSE24092 and GSM593069-GSM593070) also revealed no other large amplifications or deletions other than whole chromosome 7 amplifications.

Acquisition of trisomy 7 precedes loss or truncation of APC

Loss or truncation of the *APC* gene is believed to be the earliest genetic lesion responsible for the generation of CIN and initiation towards the adenoma stage (Rusan et al., 2008). HCEC 1CT and 1CT+7 both express abundant levels of full-length APC protein while DLD-1 cancer cells express the truncated form **(Figure 2.2)**. Furthermore, Axin2 is not detected in HCECs when examining the same lysates on a polyacrylamide gel, suggesting that APC is fully functional in these cells **(Figure 2.2)**. Axin2, a negative-feedback regulator of the Wnt signaling pathway, is upregulated in the presence of Wnt ligands and nuclear ß-catenin (Leung et al., 2002). With functional APC, downstream components of ß-catenin (such as Axin2) are not expressed. Therefore, the generation of CIN and subsequent acquisition of +7 appears prior to loss or truncation of APC in the HCEC 1CT line.

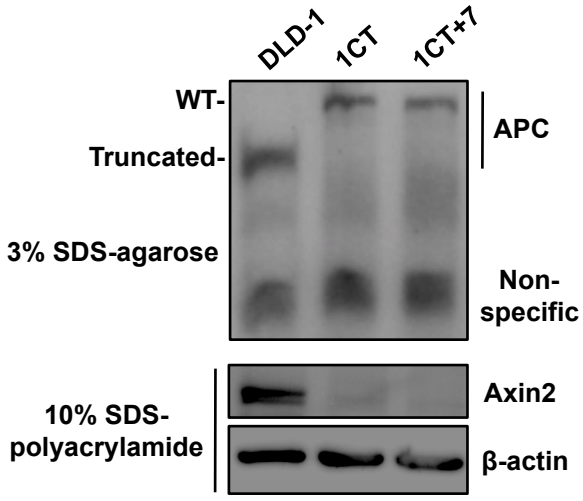

Figure 2.2. Expression of full-length, functional APC in both diploid and trisomy 7 HCECs. The colorectal cancer cell line DLD-1 is used as a positive control for truncated APC. The same lysates were also probed for Axin2, a protein upregulated in the presence of Wnt ligands and subsequent nuclear β-catenin localization.

Diploid HCECs lose growth advantages in serum-free conditions

Next, I tested whether serum has an effect on the clonogenicity of these cells **(Figure 2.3, A)**. Colony formation assays indicate that in the presence of serum, diploid cells have a higher percentage of colony forming cells as compared to 1CT+7. However, in serum-depleted conditions, the clonogenicity of 1CT HCECs significantly decreases while there are no obvious effects on 1CT+7 cells, suggesting that diploid cells lose proliferative advantages when shifting from more optimal (serum) conditions to more stressful (serum-free) conditions.

In agreement with previous reports using other models of aneuploidy (Torres et al., 2007; Williams et al., 2008), diploid 1CT HCECs proliferate more rapidly compared to 1CT+7 HCECs in the presence of 2% serum and growth supplements (0.9 PD/day [26.6 hours/doubling] as compared to 0.7 PD/day [34.3 hours/doubling], respectively). However, in defined medium only supplemented with growth factors, both cell types divide at approximately equal rates (0.3-0.4 PD/day [60-80 hours/doubling]). In order to differentiate the nearly identical growth rates between 1CT and 1CT+7 HCECs, equal numbers of non-labeled diploid cells and dsRed-labeled 1CT+7 cells were co-cultured for over a month in defined, serum-free medium. After 38 days, the majority of cells in culture were dsRed-positive 1CT+7 HCECs **(Figure 2.3, B)**. In control assays, co-culturing non-labeled 1CT+7 cells with dsRed-labeled 1CT+7 cells revealed no apparent differences after several weeks in culture **(Figure 2.3, B)**. In experiments with 2% serum, diploid cells quickly took over the culture (data not shown). Reversing the labeled cells also had no effect on these observations (data not shown).

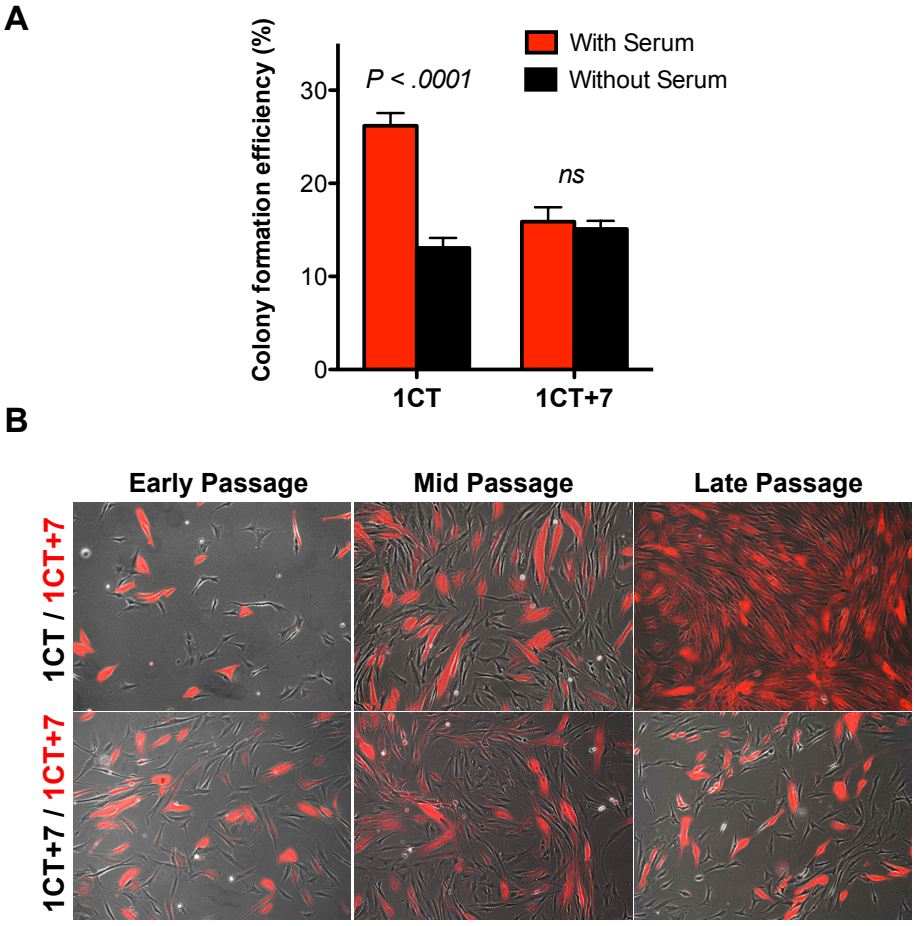

Figure 2.3. Diploid HCECs lose growth advantages under serum-free culture conditions.
(A) HCECs were plated at clonal density in serum or serum-free medium for 10 days. The absence of serum significantly reduces the clonogenicity of 1CT but has no effect on 1CT+7 cells.
(B) DsRed-labeled 1CT+7 cells were mixed with an equal number of non-labeled 1CT cells and passaged in serum-free growth medium. Late passage represents approximately 38 days in culture, splitting the cells once every 8 days. Control experiments with non-labeled 1CT+7 show no differences in the ratio of dsRed positive to negative cells.
Columns represent mean ± SEM. P-values obtained by two-tailed, unpaired Student's t-test.

Aberrant EGFR regulation in HCEC 1CT+7

Since the epidermal growth factor receptor (EGFR) is located on chromosome 7, I hypothesized that EGFR misregulation may be a critical alteration in +7 HCECs (Upender et al., 2004). Indeed, an increase in EGFR protein levels was found in 1CT+7 cells as compared to diploid HCECs in both serum and serum/EGF-free conditions after five days in culture **(Figure 2.4A)**. Analysis of fractionated lysates by western blotting also reveals the localization of EGFR to the cell membrane in both 1CT and 1CT+7 HCECs **(Figure 2.4, B)**.

Since a diverse range of cell types with varying EGFR levels respond differently to EGFR-targeting therapies, I decided to test whether there are disparate responses between HCEC 1CT and 1CT+7 to an EGFR inhibitor. Cetuximab, a monoclonal antibody targeting the extracellular domain of EGFR (Wong 2005), can equally and effectively inhibit EGFR activation induced by short-term EGF stimulation in both 1CT and 1CT+7 cells *in vitro* **(Figure 2.4, C)**. Interestingly, 1CT+7 cell proliferation, induced by various concentrations of EGF in the growth medium, is more potently reduced by five day cetuximab treatment compared to diploid cells **(Figure 2.4, D)**, perhaps indicating an augmented dependency on EGFR signaling in 1CT+7 HCECs. Additionally, no mutations were detected in the tyrosine kinase domains of EGFR by exon sequencing in both cell types.

HCEC 1CT+7 have defects in cell migration

To further characterize 1CT and 1CT+7 HCECs, I next investigated if there are any differences in cell motility. Cell migration is an important factor in the rapid turnover

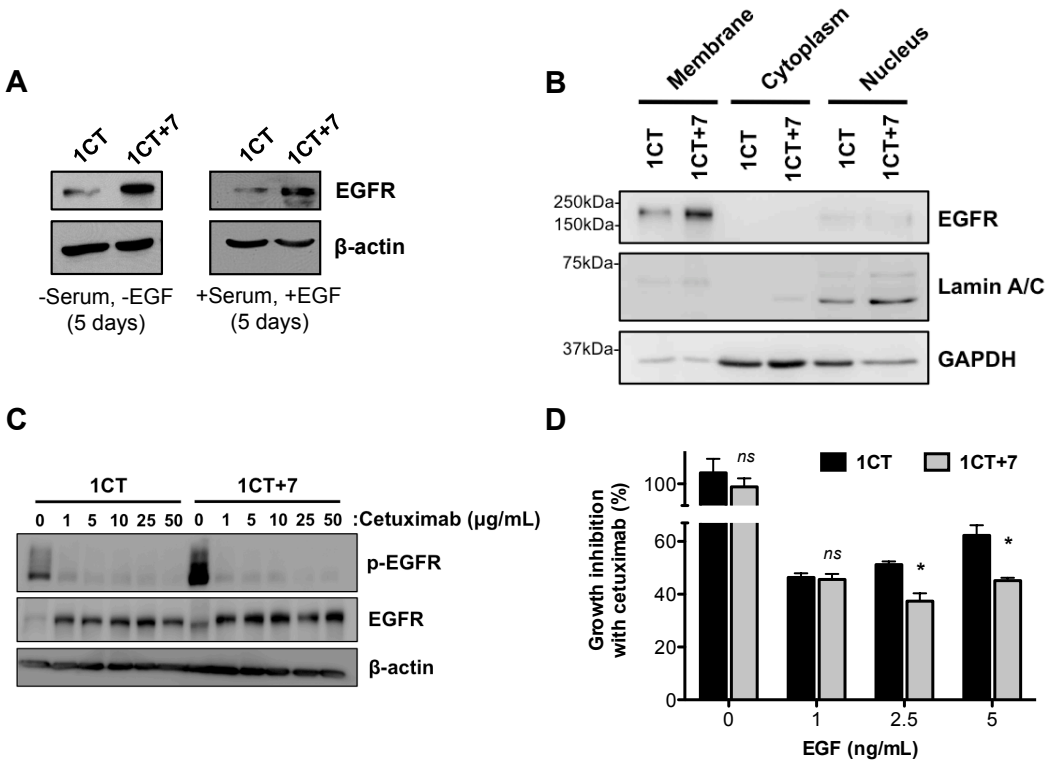

Figure 2.4. Trisomy 7 HCECs exhibits aberrant EGFR regulation and cell growth is more potently inhibited by cetuximab.
(A) HCEC 1CT+7 expresses higher levels of EGFR in serum and serum-free conditions as compared to 1CT as shown by western blot analyses.
(B) Expression of EGFR is localized to the cell membrane as shown by western blot analyses on fractionated lysates. Lamin A/C and GAPDH are used as non-membrane controls.
(C) Cetuximab, a monoclonal EGFR inhibitor, can effectively inhibit EGFR phosphorylation in both 1CT and 1CT+7 cells. Cells were treated with varying concentrations of cetuximab for 1 hour prior to stimulation with 5ng/mL EGF for 15 mins.
(D) Treatment with cetuximab more effectively reduces 1CT+7 cell proliferation induced by EGF as compared to diploid cells. Cells were cultured for 5 days in various concentrations of EGF in the presence of 50μg/mL cetuximab or saline (n=3).
Columns represent mean ± SEM. Asterisks (*), $P < .05$ (by two-tailed, unpaired Student's t-test).

of colonic crypts (Boman et al., 2008), and defects in cell motility could thus provide an initial survival advantage in the early stages of CRC (e.g. retention of epithelial cells within the crypt compartment, increased time-frame to accumulate mutations). Using a transwell migration assay, 1CT+7 HCECs exhibited defects in cell migration through a porous membrane towards serum-containing medium **(Figure 2.5, A-B)**. This loss in migration ability is also recapitulated in a two-dimensional wound migration assay **(Figure 2.5, C-D)**. In contrast to diploid cells, 1CT+7 HCECs have a decreased ability to migrate into the wound area. These results suggest a disruption in the highly regulated process of cell migration (Frey et al., 2004). Analysis of matrix metalloproteinases (MMPs) by gelatin zymography also reveals a significant repression of pro-MMP-2 levels in HCEC 1CT+7 as compared to HCEC 1CT and 2CT (an immortalized normal cell line from a non-CRC patient) (data not shown).

Emergence of trisomy 20 in HCEC 1CT+7 expressing KRAS^{V12} and TP53-knockdown

Next, I attempted to experimentally transform these HCECs *in vitro* by recapitulating commonly detected genetic events in CRC progression. This work was started by introducing the *KRAS^{V12}* oncogene and stably depleting *TP53* levels using shRNAs (Eskiocak et al., 2010) in both 1CT and 1CT+7 HCECs (termed HCEC 1CTRP and 1CTRP+7, respectively) **(Figure 2.6, A)**. Interestingly, metaphase spreads revealed that only 1CT+7 HCECs (and not the 1CT diploid cells) displayed a trisomy for chromosome 20 (+20) in 20% of the population (7 out of 35 cells analyzed by GTG-banding) **(Figure 2.6, B)**. After isolating a clonal population of +20 cells, it was determined that +20 had no obvious effects on clonogenicity in anchorage-dependent

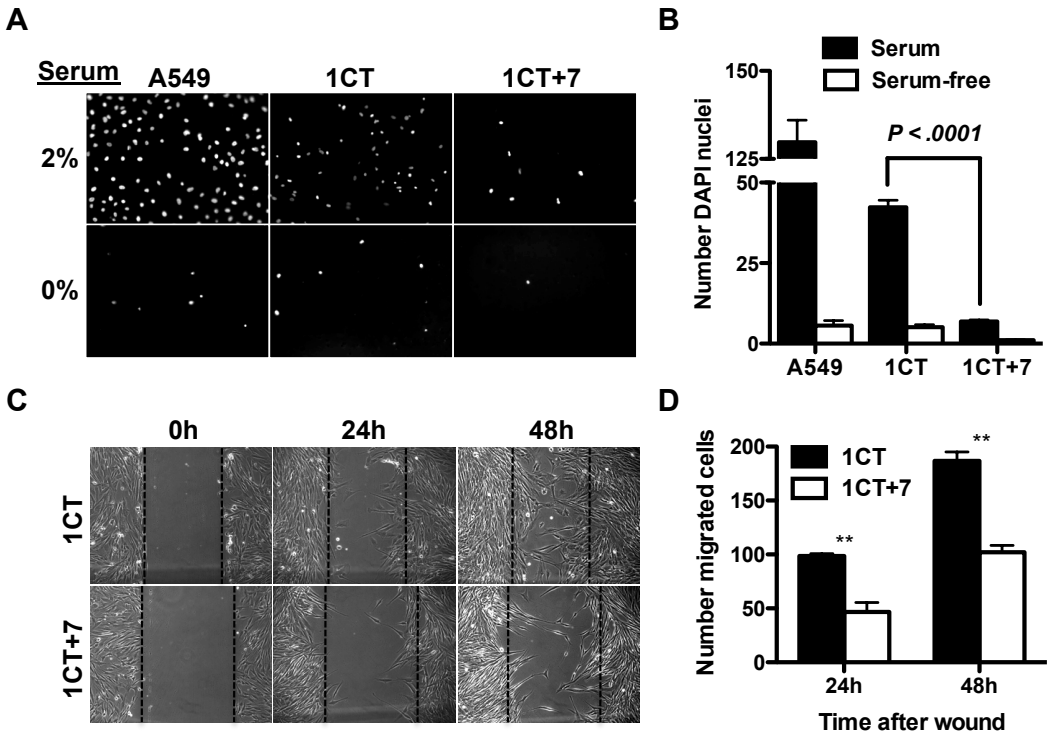

Figure 2.5. 1CT+7 HCECs are impaired in cell migration.
(A) In a transwell migration assay, cells were seeded in serum-free medium and allowed to migrate through an 8μm pore membrane towards medium containing 0% or 2% serum. Migrated cells were stained with DAPI. A549 lung cells were used as a positive control for cell migration.
(B) Quantification of **(A)** by averaging the number of cells per 20x magnification (n=15).
(C) HCEC 1CT+7 are slower to migrate into a gap created by an experimental wound to the cell monolayer.
(D) Quantification of **(C)** by averaging the number of cells that migrated into the gap as compared to 0h (n=3).
All columns represent mean ± SEM. Asterisks (**), $P < .005$ (by two-tailed, unpaired Student's t-test).

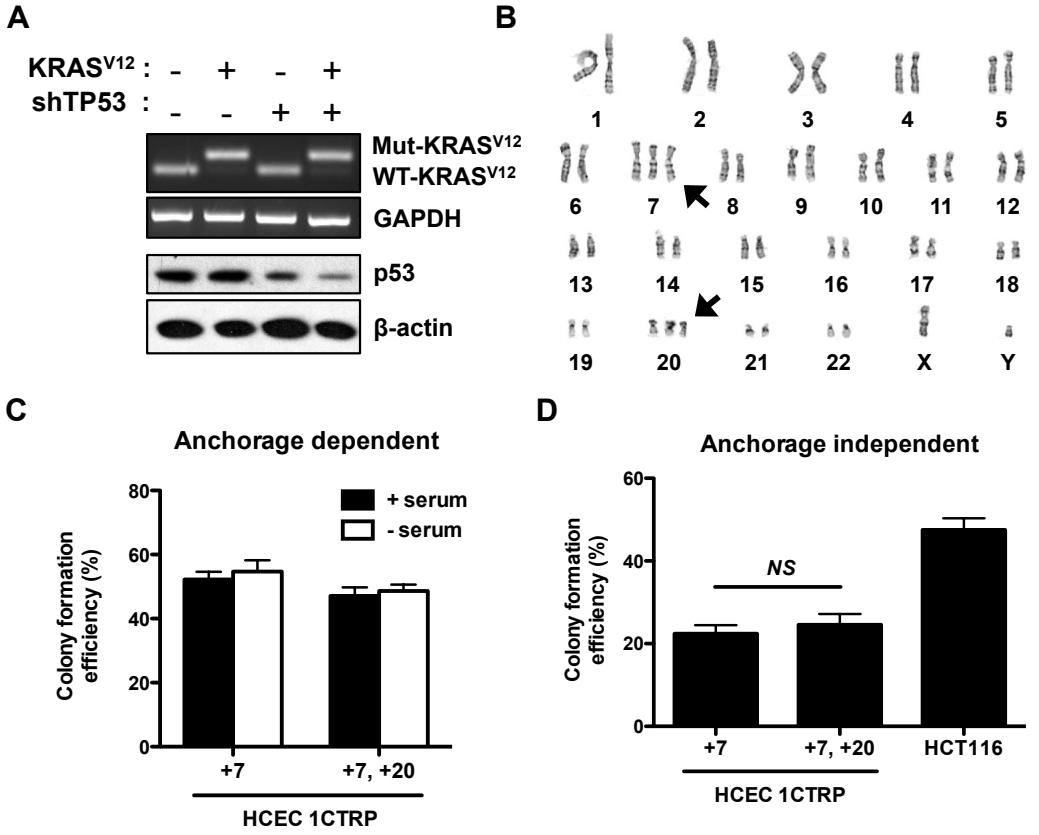

Figure 2.6. Introduction of a constitutively active *KRAS^{V12}* oncogene and shRNA-mediated depletion of *TP53* induces the emergence of trisomy 20.
(A) Knockdown of *TP53* and expression of *KRAS^{V12}* in HCEC 1CT+7.
(B) Karyotypic analysis reveals +20 in 7 out of 35 cells analyzed by GTG-banding. No +20 cells were detected in diploid HCECs under the same conditions. Neither knockdown of *TP53* nor expression of *KRAS^{V12}* alone was sufficient to induce +20 in HCEC 1CT+7.
(C-D) The addition of an extra chromosome 20 has no effect on **(C)** anchorage dependent (adherent culture) and **(D)** independent (soft agar) clonogenicity. HCT116 colon cancer cells were used as a positive control for anchorage independent growth.
All columns represent mean ± SEM.

colony formation assays **(Figure 2.6, C)** or anchorage-independent assays in soft-agar **(Figure 2.6, D)**. Alterations to *KRAS* and *TP53*, however, increases serum-free anchorage-dependent clonogenicity from ~15% in 1CT and 1CT+7 cells **(Figure 2.3, A)** to ~50-55% in 1CTRP+7 and 1CTRP+7, +20 cells **(Figure 2.6, C)**. Unlike diploid 1CT cells, it appears that the absence or presence of serum has no effect on clonogenicity in aneuploid HCECs. These 1CTRP +7, +20 HCECs could further serve as models to study CIN-mediated CRC progression, most likely representing later-staged adenomas. However, these cells still do not fully represent the transformed state as they lack the ability to form tumors in immunocompromised mice (data not shown).

Discussion

Isogenic derivatives of HCECs have been isolated from the same biopsy tissue that are either diploid when maintained in 2% serum or acquire +7 trisomy under serum-free conditions. Analysis of a large sampling of cells by GTG-banding and FISH detected no pre-existing trisomy cells in the original population, arguing for conversion rather than selection. While I cannot formally prove that rare +7 cells did not pre-exist in the original diploid population, it's frequency is less than 1 out of a 1000 cells (0.1%). This data supports the hypothesis that in the initial stages of culture, a cell from an originally diploid population underwent CIN and subsequent *de novo* conversion to a +7 cell. This was followed by a selective growth advantage for the rare +7 cell type in serum-deprived culture conditions to eventually outcompete diploid cells within the population. A hypothetical model of these events, under specific assumptions, is shown in **Figure 2.7**.

For example, it is possible to calculate the percentage of 1CT+7 cells within a population using the equation $(y(2^{0.4}))/(x(2^{0.3})+y(2^{0.4}))$ where x equals the initial number of 1CT cells dividing at 0.3 doublings/day and y equals the initial number of 1CT+7 cells dividing at 0.4 doublings/day. Under the assumption of 99.9% 1CT cells and 0.1% 1CT+7 cells in the initial population (percentages inferred from FISH analysis of early PD populations), it would take approximately 125-150 days for a minute fraction of 1CT+7 cells to saturate an originally diploid culture. This intrinsic defect leading to CIN appears to be specific to the HCEC 1CT line, as cells from another patient (HCEC 2CT) do not possess any chromosomal alterations under the same experimental conditions. **Figure 2.8** provides a schematic placing these observations in the context of the current CRC progression paradigm.

Mutation or epigenetic misregulation of the *APC* gene is one of the earliest known alterations in CRC progression and has been shown to be a significant factor in the generation of CIN (Rusan et al., 2008). APC mutations can be detected in ~85% of CRC tumor samples (Wood et al., 2007). Although APC has many known functions, it is currently unclear exactly how its loss can lead to aneuploidy. Truncation events are the main cause in a majority of APC-inactivated CRC cases (Tighe et al., 2004), followed by promoter hypermethylation (Esteller et al., 2000). I have shown that both 1CT and 1CT+7 HCECs express full-length APC protein. Additionally, DNA sequencing of the *APC* mutation cluster region reveals no pre-existing mutations. Pyrosequencing was also used to confirm hypomethylated promoters in both the diploid and trisomy lines (0-2% methylation in 1CT, 1CT+7, and 2CT cells) (data not shown). Contrary to other reports (Fodde et al., 2001; Kaplan et al., 2001; Hadjihannas et al., 2006; Aoki et al., 2007), these

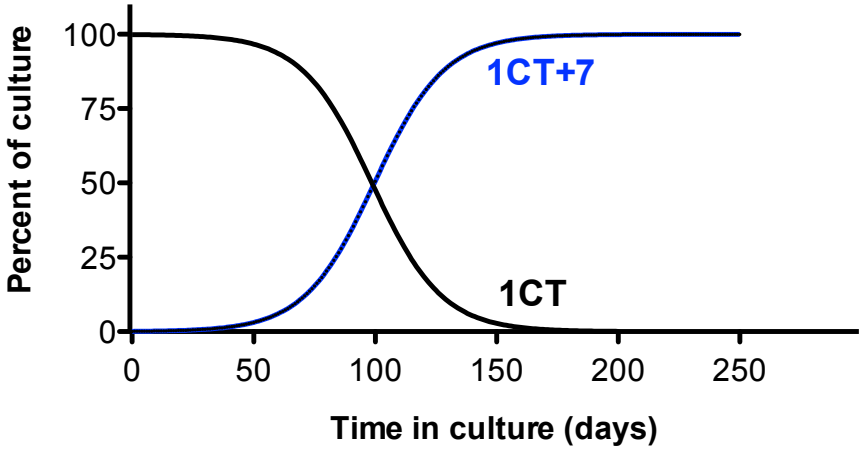

Figure 2.7. Mathematical model depicting how rare trisomy 7 cells are able to overtake a culture of diploid cells. Here, the following three assumptions are made: 1) An initial ratio of 99.9% to 0.1% 1CT cells to 1CT+7 cells, respectively, exists in the population at t = 0. 2) 1CT cells proliferate at 0.3 doublings/day. 3) 1CT+7 cells proliferate at 0.4 doublings/day.

results suggest that APC loss is not required for the onset of CIN in the HCEC 1CT line. Additionally, there were no observable differences in messenger RNA transcript levels for Sgo1 and Bub1 by quantitative PCR (data not shown), two frequently down-regulated genes in CRC associated with increased levels of CIN (Iwaizumi et al., 2009; Pino et al., 2010).

Aneuploidy is generally disadvantageous to cells in non-stressful environments. For example, under normal growth conditions, aneuploid MEFs have an overall decreased cellular fitness compared to diploid fibroblasts (Williams et al., 2008). This suggests that cells may develop other changes to overcome the initial chromosomal aberration to prevent elimination from the population (Torres et al., 2010). This mechanism of compensation for additional chromosomes may confer unknown fitness advantages under specific conditions which allow aneuploid cells to outcompete diploid cells (Pavelka et al., 2010). I hypothesize that under stressful or non-optimal growth conditions, 1CT+7 HCECs gained a growth advantage over their diploid counterparts and this gain may act as a mechanism for cancer initiation (Zhang et al., 2006). When shifted to serum-free conditions, diploid HCECs lose growth advantages while aneuploid cells gain a slight growth advantage (**Figure 2.3**). Thus, the emergence of an extra chromosome could confer a selective advantage to 1CT+7 cells to outcompete normal cells and could provide one explanation for early CRC pathogenesis events in terms of cell competition within colonic crypts. It is currently unknown whether the aberrant EGFR regulation exhibited by 1CT+7 HCECs contributes to the conversion or selection pressures for +7 cells.

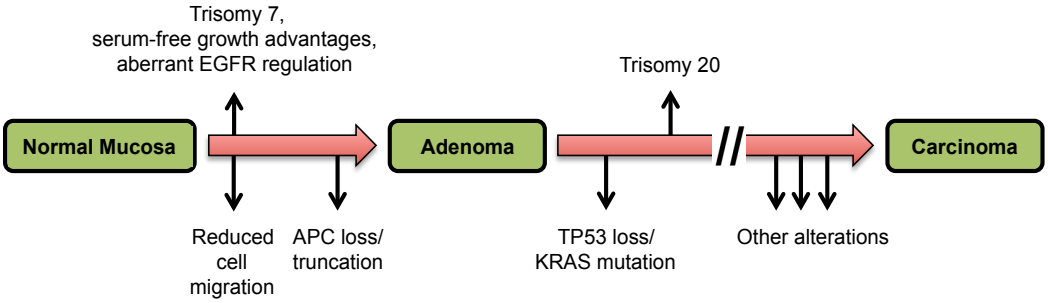

Figure 2.8. Updated schematic to the current colorectal cancer progression paradigm. In the HCEC 1CT model, the appearance of trisomy 7 coinciding with aberrant EGFR regulation and defects in cell migration precedes the loss or truncation of APC. Trisomy 20 also appears following alterations to *KRAS* or *TP53*. Since these cells still do not form tumors in mice, there must be other alterations that drive the progression towards the carcinoma phenotype. The identification of such potential driver alterations is discussed in Chapter 5.

Another difference between diploid and trisomy 7 HCECs is a defect in cell migration in 1CT+7 cells. Proper cell migration is a coordinated and dynamic process in the physiological turnover of the colonic epithelium (Humphries et al., 2008). Stem cells at the bottom of the colon crypts give rise to progenitor cells that differentiate as they migrate towards the lumen of the colon. As differentiated cells reach the apex of the crypt, they undergo apoptosis and are shed into the lumen to make way for newer cells emerging from the base (Stappenbeck et al., 1998). Thus, the strict regulation in the number of cells gained at the bottom of crypts roughly equals the number of cells lost at the apex (Nowak et al., 2002). Even partial loss of cell migration within the epithelium could therefore be disruptive to normal colon crypt physiology (Lamprecht et al., 2002). A decrease can be seen in the motility of 1CT+7 HCECs as compared to their diploid counterparts **(Figure 2.4)**. These results suggest that, *in vivo*, +7 HCECs may be slightly impaired in crypt migration and could lead to interference with normal colonic turnover (Frey et al., 2004). This may predispose cells to the accumulation of tumorigenic alterations due to prolonged retention of cells within the crypt. This defect in 1CT+7 cell migration also correlates with a decrease in pro-MMP-2 levels (data not shown). MMP-2 is expressed in non-tumorigenic mouse colonic epithelial cells (Fenton et al., 2002) and is associated with normal cell migration and physiological wound healing processes (Murphy et al., 1999). Although aberrant MMP-2 expression has been implicated in disease progression and metastatic potential of cancer cells (Seiki 2002), MMP-2 is required and sufficient to initiate the migration of normal epithelial cells (Giannelli et al., 1997). These results suggest a possible association between decreased MMP-2 levels and reduced +7 epithelial cell migration that may exist within colonic crypts. Additionally,

cell models of Down syndrome (human trisomy 21, mouse trisomy 16) also display perturbed migratory abilities (Leffler et al., 1999; Delom et al., 2009), although the mechanistic link between aneuploidy and cell migration remains unclear.

Introduction of oncogenic *KRAS*^{V12} and stable knockdown of *TP53* in 1CT+7 HCECs (1CTRP+7) led to the emergence of another non-random aneuploidy, trisomy 20 (+20), appearing in 20% of the population (1CTRP+7, +20). A clonal isolate was selected and expanded to generate a pure population of 1CTRP+7, +20 HCECs. Neither expression of *KRAS*^{V12} nor *TP53* knockdown alone was sufficient to induce any chromosomal abnormalities. These events also could not be recapitulated in normal diploid 1CT or 2CT HCECs, suggesting an intrinsic defect within +7 HCECs upon experimental manipulation of both *KRAS* and *TP53*. These results also provide additional evidence for the conversion (rather than selection) of pre-existing aneuploid cells in the initial population, as there was no evidence of +20 chromosomes unless oncogenic changes were introduced into 1CT+7 cells. Although the EGFR pathway may contribute to the selective advantage of 1CT+7 HCECs over diploid cells, the mechanism by which +7, +20 begins to selectively outcompete +7 in 1CTRP HCECs remain unknown. Interestingly, +7 and +20 events are both frequently detected throughout CRC pathogenesis (Tsafrir et al., 2006) and these cytogenetic changes appear to be non-random. Since it is highly unlikely that such CRC specific chromosomal changes could be occurring by chance, I propose that these 1CTRP+7, +20 HCECs represent a further progressed cell type that may be recapitulating a hierarchy of frequently observed events throughout different stages of CRC. These cells with experimentally introduced oncogenic changes and spontaneous chromosomal abnormalities appearing within the

same population of initially diploid cells could also contribute to the cellular heterogeneity generally observed among tumor samples (Shackleton et al., 2009).

In summary, I describe the isolation and initial characterization of +7 and +20 HCEC lines derived from an originally diploid population. Although the underlying mechanism of CIN in the HCEC 1CT population has yet to be identified, these isogenic cells will be useful in studying CIN-mediated CRC initiation and progression in a genetically tractable human cell-based model. Furthermore, these cells could serve as reagents for the discovery of novel drug targets that can exploit specific vulnerabilities in aneuploid HCECs to inhibit their growth or induce apoptosis for therapeutic purposes.

Materials and Methods

Cell culture

The culture conditions of HCECs have been reported elsewhere (Roig A.I. 2010; Roig et al., 2010). Briefly, HCECs are maintained under 2% oxygen and 5% carbon dioxide on Primaria (BD Biosciences, San Jose, CA) plates in 4:1 high-glucose DMEM:medium 199 with 2% cosmic calf serum (Hyclone, Logan, UT) plus growth supplements: EGF (20ng/mL; Peprotech, Rocky Hill, NJ), hydrocortisone (1mg/mL), insulin (10mg/mL), transferrin (2mg/mL), and sodium selenite (5nM) (all Sigma, St. Louis, MO).

Karyotyping and fluorescent in situ hybridization (FISH)

HCECs at 70% confluency were treated with 0.01μg/mL colcemid (KaryoMax, Gibco/Invitrogen, Carlsbad, CA) for two hours and metaphase chromosomes were harvested under standard protocols. Slides were dropped using a Thermotron chamber (Thermotron, Inc, Holland, MI) and stained with G-bands by trypsin using Giemsa. The images of each metaphase were captured with a Zeiss Axioskop 2 microscope (Photometrics, Tucson, AZ) and Applied Imaging CytoVision Software (Applied Imaging Corp., Spring Valley, NY) was used to analyze these metaphase cells and each chromosome analysis was performed on at least 20 metaphases at each PD. DNA probes specific for human centromeres of chromosomes 7 and 20 (CEP7 and CEP20) were obtained from Abbott Molecular Inc. (Des Plaines, IL) for FISH analysis using a Zeiss Axioskop 2 fluorescent microscope with CCD camera (Photometrics). At least 500 interphase cells at each PD were examined.

Co-culturing competition assays

HCECs were labeled with dsRed by transduction with a pSSI-8018 lentiviral vector followed by blasticidin selection. Two hundred thousand non-labeled HCEC 1CT cells were mixed with equal numbers of dsRed-labeled HCEC 1CT+7 cells in a $10cm^2$ plate. Cells were cultured for at least 38 days in serum-free medium with growth supplements and passaged every eight days. Phase/fluorescence pictures are representative images from the center of triplicate culture plates. Control experiments represent the co-culturing of non-labeled and labeled HCEC 1CT+7 cells.

Western blotting

Total cell lysates were prepared by harvesting cells in Laemmli SDS reducing buffer. Protein concentrations were measured using a Pierce BCA protein assay kit (Thermo Scientific, Rockford, IL), resolved on an 8-10% polyacrylamide gel, and transferred to PVDF. Ultracentrifugation was used to fractionate lysates as specified. HRP-conjugated goat anti-mouse or -rabbit (Jackson Immunoresearch, West Grove, PA) were used as secondary antibodies at 1:5000 and detected with SuperSignal West Pico or Femto Chemiluminescent Substrate Kit (Thermo Scientific, Rockford, IL). Bands were quantified using a ChemiDoc™ XRS+ Imager with Image Lab™ software (Bio-Rad, Hercules, CA) and normalized to β-actin.

Response to EGF and cetuximab

For cell counting experiments, $8.0x10^4$ cells were cultured in the presence of 0, 1, 2.5, or 5ng/mL EGF in a six-well dish in serum-free medium with growth supplements with either 50μg/mL cetuximab (Erbitux®, ImClone Systems Inc., Branchburg, NJ) or saline. Cell numbers were obtained 5 days later. For western blots with cetuximab, serum/EGF-starved cells were treated with 0-50μg/mL cetuximab for one hour prior to stimulation with 5ng/mL EGF for 15 mins. Lysates were collected immediately and analyzed as previously described.

Colony formation assay

Cells were seeded in triplicate $10cm^2$ culture plates at three different clonal densities (50-400 cells/plates) in either serum or serum-free medium containing growth supplements. After ten days, colonies were washed with PBS, stained for 30 mins with 6% glutaraldehyde/0.5% crystal violet solution, and counted.

Migration assays

Transwell migration assays were performed using a modified Boyden chamber. Briefly, $4.0x10^4$ cells were serum-starved for six hours and plated into serum-free and GF-free medium onto 8.0μm pore transwell PET membranes (BD Biosciences, Bedford, MA). Five hundred μl of medium containing 2% serum and growth supplements were added to the bottom well. Non-migratory cells were scraped off 24 hours later and migratory cells were fixed in 100% methanol, washed, and DAPI stained. Experiments were performed in triplicate transwells and quantified by averaging the number of DAPI nuclei per 20x

field of view counting five fields per chamber (n=15). Wound migration assays were performed by plating cells to confluency in a six-well plate in serum-free medium with growth supplements. After 24 hours, three wounds per well were created by scratching the confluent monolayer with a P200 pipette tip and debris was removed by PBS washes. The wound was imaged by phase microscopy at the middle of the scratch line at different time points. Cells migrated into the wound were counted and averaged from triplicate wells.

CHAPTER THREE

SELECTIVE TARGETING OF ANEUPLOID HUMAN CELLS WITH AICAR

Introduction

Chromosomal instability (CIN) leading to aneuploidy, an abnormal number of chromosomes, has long been observed in solid human tumors throughout various tumorigenic stages. Aneuploidy arises when chromosomes fail to properly segregate during mitotic cell division (Gordon et al., 2012). While there is debate as to whether aneuploidy drives or merely serves as a consequence of cancer progression (Sheltzer et al., 2011), targeting cells with an inappropriate number of chromosomes may be a practical chemopreventive or therapeutic approach (Bakhoum et al., 2012; McGranahan et al., 2012). Tumors typically acquire non-random gains, losses, or translocations of chromosomes that may permit selective benefits that are currently not well understood (Weaver et al., 2007). One of the most common and recurrent cytogenetic alterations in sporadic colorectal cancer (CRC) is the appearance of trisomy for chromosome 7, detected in approximately 40% of early-staged adenomas and increases with disease progression (Bomme et al., 1994; Habermann et al., 2007). Although aneuploidy has been extensively studied in yeast and some mammalian cells, selective therapies targeting cells with such chromosomal abnormalities have only recently been explored (Manchado et al., 2011).

Our laboratory has previously described the spontaneous generation of a trisomy 7 cell line (1CT+7) derived from originally diploid (46,XY karyotype) human colonic epithelial cells (HCEC 1CT) (Ly et al., 2011). The HCEC 1CT line, which is stably diploid when propagated in 2% serum, originated from non-malignant tissue of a previous CRC patient undergoing routine colonoscopy and immortalized with ectopic expression of *CDK4* and *hTERT* (Roig et al., 2010). Under defined serum-free culture conditions, HCECs with the acquisition of a third copy of chromosome 7 emerged from the diploid 1CT line, thus representing an isogenic model to examine the effects of trisomy 7 *in vitro* **(Figure 2.1)**. Such isogenic cell lines can serve as useful cellular reagents to identify anti-growth or apoptosis-inducing compounds specific to aneuploid human cells. Interestingly, 1CT+7 HCECs (along with trisomy 7 cells derived from breast (Briand et al., 1996), brain (Sareen et al., 2009), and esophageal (Garewal et al., 1990) tissue) aberrantly overexpresses the epidermal growth factor receptor (EGFR) (Ly et al., 2011), conveniently located on chromosome 7p11 **(Figure 2.4, A).**

EGFR, a membrane-localized receptor tyrosine kinase, becomes activated in the presence of epidermal growth factor (EGF) ligands (Schlessinger 2000) and promotes cell proliferation through a cascade of signal transduction events. Upon ligand binding to the extracellular domain of the receptor, autophosphorylation of C-terminal tyrosine residues (Y1173) initiates EGFR activation and internalization through endocytosis. These events lead to the recycling of receptors back to the cell surface for re-use or receptor degradation by the ubiquitin-proteasome and/or -lysosomal pathways (Levkowitz et al., 1998; Levkowitz et al., 1999; Longva et al., 2002; Dikic 2003). Since many types of human cancers display overexpression (Cohen et al., 2006) or mutations in

the EGFR gene, a number of antibody-based therapies targeting EGFR are currently utilized for therapeutic purposes (Messersmith et al., 2008). For example, the EGFR inhibitor cetuximab is used in the treatment of metastatic colorectal and head/neck cancers. It was previously shown that cetuximab (trade name Erbitux) is more effective at inhibiting HCEC 1CT+7 proliferation compared to karyotypically normal cells **(Figure 2.4, C-D)**, suggesting that cells with trisomy 7 also acquire an increased dependency on EGFR signaling (Ly et al., 2011).

The adenosine analog compound AICAR (5-aminoimidazole-4-carboxamide-1-β-D-ribofuranoside) has recently been found to elicit a selective apoptotic response in trisomic mouse embryonic fibroblasts (MEFs) and CIN-driven CRC lines (Tang et al., 2011), as well as anti-growth responses in EGFR-vIII mutated glioblastoma cells (Guo et al., 2009). Immunocompromised mice treated daily with AICAR also displayed reduced xenograft tumor volume using a variety of cancer cell lines with abnormal karyotypes (Tang et al., 2011). The canonical effects of AICAR include a cellular energy stress response that induces AMP-activated protein kinase (AMPK) phosphorylation (T172) by the kinase LKB1 and subsequent inactivation of acetyl-CoA carboxylase (ACC). AMPK and ACC phosphorylation halts cell proliferation through inhibition of the mTOR pathway (Shackelford et al., 2009). For these reasons, AICAR has been extensively studied as a potential anti-cancer drug.

In the present study, the effects of AICAR on the growth of diploid versus trisomic HCECs were tested. These experiment reveal that AICAR is selectively and potently cytostatic towards 1CT+7 cells but largely ineffective against diploid 1CT cells. Surprisingly, treatment of 1CT+7 cells dramatically reduced EGFR overexpression and

inhibited proliferation in an EGF-dependent manner. I propose that AICAR accelerates ubiquitination and subsequent degradation of EGFR in 1CT+7 cells through an AMPK phosphorylation-independent mechanism. AICAR-mediated depletion of EGFR proteins is further confirmed *in vitro* with a panel of human CRC cells as well as in xenograft tumor models *in vivo*. Taken together, the anti-cancer properties of AICAR may be potentially beneficial as a chemopreventive agent to patients predisposed to sporadic CRC through the proliferative inhibition of trisomy 7 cells.

Results

AICAR induces selective cytostatic and metabolic effects on HCEC 1CT+7

Previous studies indicate that MEFs harboring one additional chromosome are more sensitive to apoptosis induced by AICAR exposure compared to diploid MEFs (Tang et al., 2011). To determine whether 1CT (diploid) or 1CT+7 (trisomy 7) HCECs are preferentially sensitive to treatment with AICAR, cells were cultured in increasing concentrations of AICAR for five days. This dose-response experiment revealed a four-fold lower EC_{50} value for 1CT+7 cells compared to 1CT (0.225 and 1.026mM, respectively) (**Figure 3.1, A**). The growth inhibitory potency of 0.25mM AICAR was further evaluated over a six-day period by collecting sequential cell counts every three days after treatment. These data indicated that AICAR completely prevented the proliferation of 1CT+7 but not 1CT cells compared to vehicle control (**Figure 3.1, B**). This block in cell cycling could be attributed to an increase in S-phase arrest in asynchronous cells (data not shown). Treatment with AICAR did not induce apoptosis, as

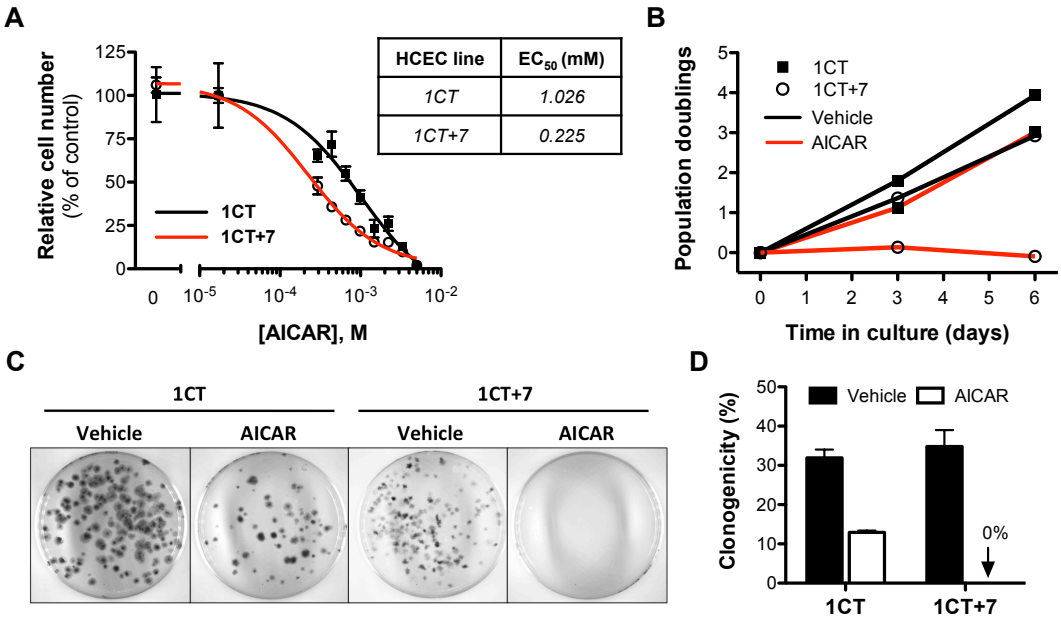

Figure 3.1. AICAR selectively and potently inhibits growth of 1CT+7 HCECs.
(A) HCEC 1CT and 1CT+7 were treated with the indicated concentrations of AICAR and cell numbers were assessed five days post-treatment by CTG assay. Cell viability is normalized to vehicle control.
(B) 1CT and 1CT+7 cells were cultured in 0.25mM AICAR or vehicle. Doublings were calculated from total cell counts obtained after 3 and 6 days of treatment.
(C) HCECs were seeded at clonal density (200-400 cells/10cm^2) and treated with 0.25mM AICAR 24 hours later. Colonies were stained after 2 weeks with crystal violet. Representative images of plates are shown.
D) Quantification of clonogenicity from **(C)**.
Columns represent mean ± SEM.

all cells remain attached to culture plate. When cells were plated at clonal density, AICAR completely and potently abolished the clonogenic potential of 1CT+7 cells compared to 1CT cells (**Figure 3.1, C-D**).

Since the metabolic effects of AICAR on mammalian cells have previously been investigated (Aschenbach et al., 2002), it was next inquired whether AICAR can selectively perturb critical metabolic processes in either of the HCEC lines. 1CT and 1CT+7 cells were treated with vehicle or AICAR-containing medium for 48 hours and cell culture supernatants were collected for analysis. Treatment with AICAR selectively decreased both the consumption of glucose (**Figure 3.2, A**) and the production of lactate (**Figure 3.2, B**) in 1CT+7 cells whereas no significant effects were observed in diploid cells. Furthermore, 1CT+7 cells have a noticeably higher basal rate of both metabolic processes compared to diploid cells, similar to observations published elsewhere (Williams et al., 2008).

AICAR negatively regulates EGFR protein levels in 1CT+7 HCECs

Since 1CT+7 cells express high levels of EGFR compared to 1CT cells, I tested whether the mechanism by which AICAR inhibits 1CT+7 proliferation could be mediated through EGFR. Both 1CT and 1CT+7 cells were treated for 24 hours with 0.25mM AICAR and whole cell lysates were probed for EGFR by western blot analyses. Surprisingly, I show that AICAR treatment led to a 3.5-fold decrease in 1CT+7 EGFR levels but had only marginal effects on diploid 1CT cells (**Figure 3.3, A-B**). Phosphorylation of well-known AICAR targets, such as AMPK, ACC, and mTOR **(Figure 3.3, A)**, were negligible between control and compound-treated cells (with slight

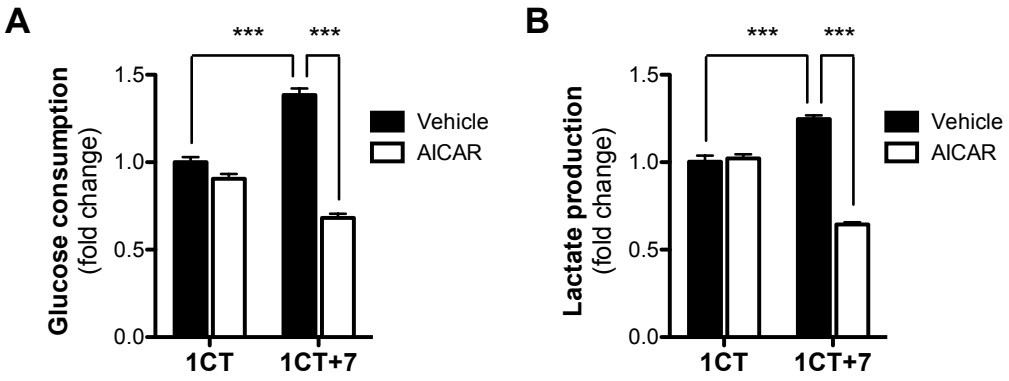

Figure 3.2. AICAR impairs the metabolism of 1CT+7 HCECs. AICAR treatment (0.25mM) selectively decreases (A) glucose consumption and (B) lactate production in 1CT+7 HCECs. Glucose/lactate levels were measured in cell culture supernatants collected after 48-hour treatment and normalized to both cell-free medium and cell counts. Columns represent mean ± SEM (***$p<0.0001$, by two-tailed, unpaired Student's *t* test).

increases in ACC phosphorylation in the presence of AICAR). To determine whether LKB1, the kinase responsible for AMPK activation during energy stress, is required for EGFR depletion, 1CT+7 cells were transfected with control or LKB1 siRNA for three days to deplete endogenous LKB1 levels. siRNA-transfected 1CT+7 cells were then treated with vehicle or AICAR for 24 hours and whole-cell lysates were resolved by SDS-PAGE. Since knockdown of LKB1 had no effect on EGFR levels regulated by AICAR treatment (**Figure 3.4**), this data suggests that AICAR-induced EGFR depletion is independent of the LKB1 pathway. In addition, treatment with AICAR for a short-term period (30 minutes) also did not alter EGFR levels in HCECs, suggesting that AICAR does not facilitate rapid EGFR turnover through ligand-independent receptor activation. The depletion of EGFR proteins is further verified by immunofluourescent staining on AICAR-treated 1CT+7 cells (**Figure 3.3, C**).

To determine whether depletion of EGFR by AICAR is a permanent or transient effect, HCECs were treated with AICAR for 24 hours, washed, and replaced with serum- and AICAR-free culture medium for the indicated time points. Twenty-four hour release of cells from AICAR resulted in the restoration of EGFR expression (**Figure 3.3, D**) by western blot analysis. AICAR also did not affect c-MET protein levels; another chromosome 7-located receptor tyrosine kinase overexpressed in 1CT+7 cells. These results support EGFR-specificity rather than a global repression of receptor tyrosine kinases.

To establish whether AICAR reduces EGFR at the transcriptional level, steady state EGFR mRNA transcripts by semi-quantitative RT-PCR were examined. Total RNA isolated from cells treated with AICAR was reverse transcribed and the EGFR tyrosine

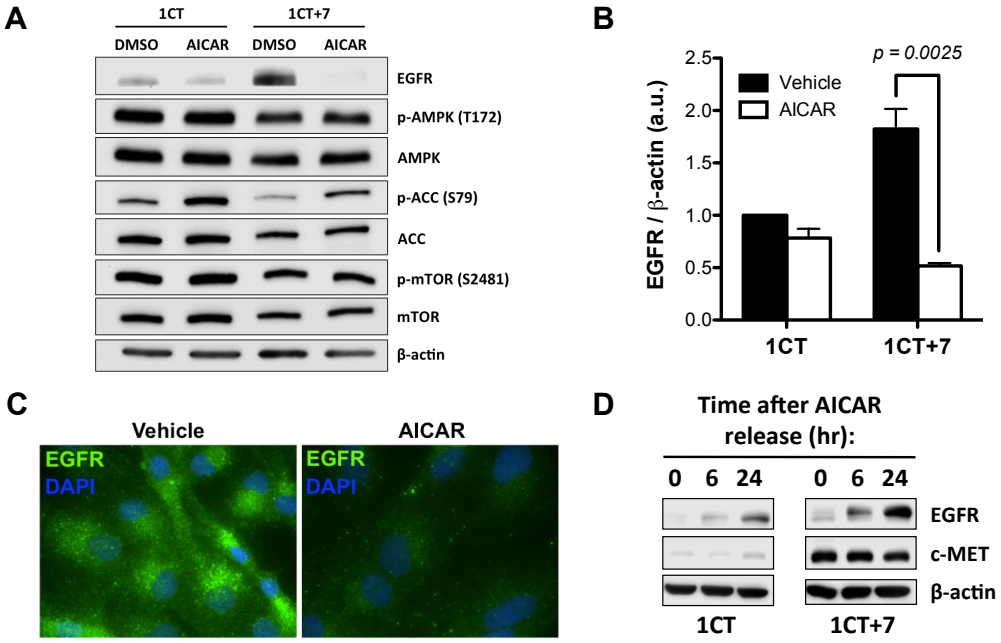

Figure 3.3. AICAR negatively regulates EGFR protein levels.
(A) HCECs were treated for 24 hours with 0.25mM AICAR. Whole cell lysates were resolved by SDS-PAGE and probed for the indicated proteins. No significant changes in the phosphorylation status of known AICAR targets were observed with the exception of slight increases in p-ACC levels.
(B) Quantification of **(A)** from three independent experiments and normalized to loading control. AICAR treatment induced a 3.5-fold reduction in EGFR protein levels. Columns represent mean ± SEM.
(C) Confirmation of EGFR repression by immunostaining (100x magnification) of 24-hour 0.25mM AICAR-treated 1CT+7 cells.
(D) EGFR levels are restored following 24-hour release from AICAR. Cells were treated overnight with AICAR, thoroughly washed, and replenished with fresh medium for the indicated time points.

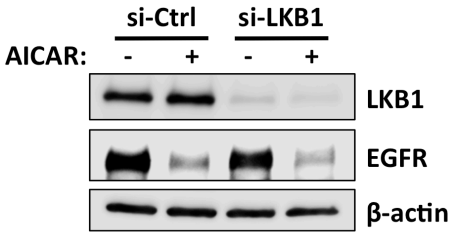

Figure 3.4. LKB1 is not required for AICAR-induced EGFR depletion. HCEC 1CT+7 were transfected with non-targeting control or LKB1 siRNA for three days prior to 24-hour treatment with 0.25mM AICAR. Whole-cell lysates were resolved by SDS-PAGE and probed for LKB1, EGFR, and actin loading control.

kinase domain was detected by PCR. EGFR transcripts were unaltered in both cell types following treatment with AICAR (data not shown), suggesting a regulation at the protein level.

AICAR treatment induces ligand-dependent EGFR degradation

I subsequently asked whether the availability of EGF ligands is required for AICAR-induced EGFR depletion in 1CT+7 cells. To determine if the presence of EGF is necessary for this mechanism of action, EGFR protein levels in 1CT+7 cells treated with AICAR were measured with and without 20ng/ml EGF. Culturing cells in the absence of EGF abolished EGFR depletion induced by AICAR, indicating a requirement for EGF ligand and most likely EGFR activation/turnover (**Figure 3.5, A**). Ligand stimulation is known to induce EGFR internalization followed by either receptor recycling or degradation (Huang et al., 2007). To establish whether AICAR can induce EGFR degradation due to ligand stimulation, a time point experiment was conducted in which EGF-starved 1CT+7 cells were stimulated with EGF ligand to follow receptor degradation kinetics. In **Figure 3.5, B**, 48 hour EGF-starved 1CT+7 cells treated with vehicle induced only a slight degree of EGFR degradation due to EGF stimulation for the indicated time points. However, EGF-starved 1CT+7 cells treated with AICAR for 24 hours prior to ligand stimulation provoked rapid and potent EGFR degradation (**Figure 3.5, B**). These results suggest that AICAR treatment leads to accelerated EGFR degradation in a ligand-dependent manner as opposed to receptor recycling back to the cell surface.

It was next reasoned whether AICAR treatment would lead to an increase in proteasomal-mediated degradation of EGFR protein. 1CT+7 cells were pre-treated with the proteasome inhibitor MG132 (10μM) for one hour prior to 24-hour AICAR treatment and collection of lysates at the indicated time points. MG132 pre-treatment resulted in a rescue of EGFR levels (**Figure 3.5, C**), suggesting that AICAR-induced EGFR depletion may be, at least partially, attributed to an increase in protein degradation by the proteasome (at a time frame between 12 and 24 hours post-treatment). Although the majority of EGFR proteins is stabilized due to proteasome inhibition in the presence of AICAR, the slight decrease in EGFR levels following 24 hour AICAR exposure in MG132-treated 1CT+7 cells may be attributed to the contributions by the lysosomal degradative pathway. To determine if AICAR enhances ubiquitination of EGFR, an ubiquitination assay was performed on 24-hour AICAR-treated 1CT+7 cells transiently expressing HA epitope-tagged ubiquitin. MG132 was used to prevent EGFR degradation and lysates were immunoprecipitated with an EGFR agarose-conjugated antibody. A considerable increase in EGFR ubiquitination (most likely polyubiquitination as indicated by an HA-positive smear) was observed following AICAR treatment (**Figure 3.5, D**).

Next, HCECs were cultured with increasing concentrations of EGF to determine if AICAR can prevent growth stimulated by EGF ligands. This experiment indicates that AICAR selectively inhibits EGF-induced proliferation in 1CT+7 cells (**Figure 3.5, E**) but not in diploid 1CT cells. These results demonstrate that EGF ligands contribute to the specific anti-proliferative effects of AICAR on aneuploid human cells. Treatment of 1CT cells with 10ng/ml EGF induced an approximate 2.6-fold growth response compared to a 4.3-fold increase in 1CT+7 cells. However, 1CT+7 cells treated with AICAR resulted in

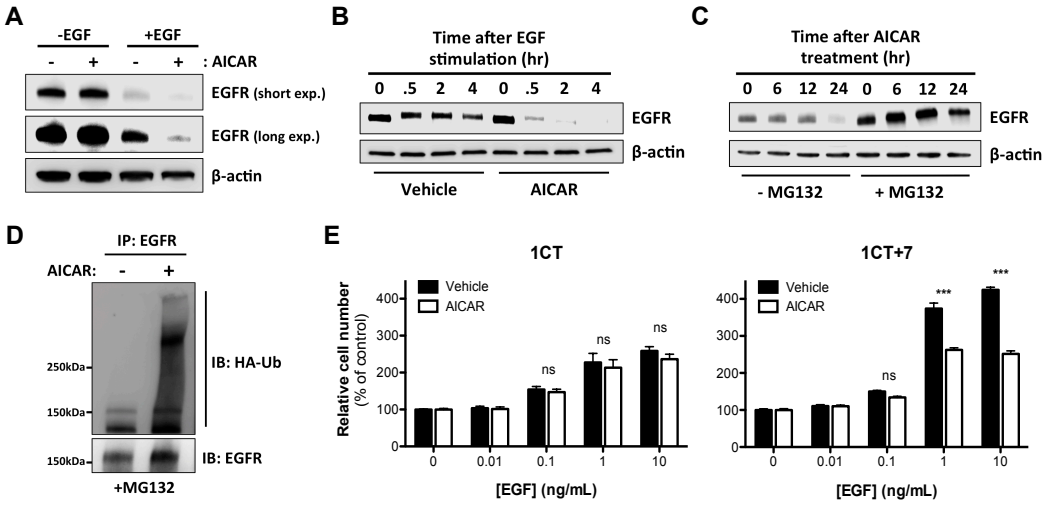

Figure 3.5. AICAR accelerates ubiquitination and ligand-dependent degradation of EGFR.

(A) 1CT+7 cells were treated with AICAR in the presence or absence of 20ng/mL EGF for 24 hours and lysates were analyzed by SDS-PAGE. In the absence of EGF ligand, AICAR has no effect on EGFR protein levels.

(B) EGF-starved 1CT+7 cells were treated with AICAR for 24 hours followed by 20ng/ml EGF stimulation for the indicated time points. AICAR accelerates ligand-induced receptor degradation compared to vehicle-treated cells.

(C) 1CT+7 cells were incubated with 10μM of the proteasome inhibitor MG132 for one hour prior to AICAR treatment for the following time points. Whole cell lysates were collected and analyzed by SDS-PAGE and probed for EGFR.

(D) 1CT+7 cells were transfected with HA-tagged ubiquitin and treated with 10μM MG132 and 0.25mM AICAR for 24 hours. Lysates were subjected to immunoprecipitation with an EGFR agarose-conjugated antibody and analyzed by SDS-PAGE.

(E) HCECs were treated with AICAR in increasing EGF concentrations for 5 days and cell numbers were assessed by CTG assay. AICAR selectively prevents EGF-induced proliferation in 1CT+7 cells.

Columns represent mean ± SEM (***$p<0.0001$, by two-tailed, unpaired Student's *t* test).

only a 2.5-fold increase in proliferation, reducing EGF-induced growth rates closer to those of diploid cells. Comparably, knockdown of EGFR in 1CT+7 cells using small interfering RNAs causes a growth inhibitory effect similar to AICAR treatment (data not shown).

Downregulation of EGFR by AICAR in human colorectal cancer cells in vitro and in vivo

To determine if AICAR-induced depletion of EGFR is specific towards HCECs, a panel of both CIN and microsatellite unstable (MIN) human CRC cell lines were treated with increasing concentrations of AICAR for 36 hours. A dose-dependent downregulation of EGFR upon treatment with AICAR was observed (**Figure 3.6, A**) in five out of six cancer cell lines tested. This effect also appears to be independent of CIN (SW480, HT29) versus MIN (HCT116, LoVo, DLD-1) status as EGFR downregulation was observed in cancer cells of both genetic backgrounds, although similar results were not detected in the pseudodiploid cell line HCT15. As previously shown (Tang et al., 2011), AICAR effectively reduces tumor volume in mouse xenograft models using CRC cell lines compared to mice treated with PBS control. Daily intraperitoneal injection of AICAR for 18 days reduces xenograft tumor volume by roughly 33% and 45% compared to vehicle-treated mice using the CRC cell lines LoVo and HT29, respectively (Tang et al., 2011). These tumors were then harvested, fixed, and histologically sectioned for EGFR analysis by immunohistochemistry. In agreement with the *in vitro* data, AICAR treatment reduced the intensity of EGFR staining in xenograft tumors *in vivo* compared to control-injected animals (**Figure 3.6, B**).

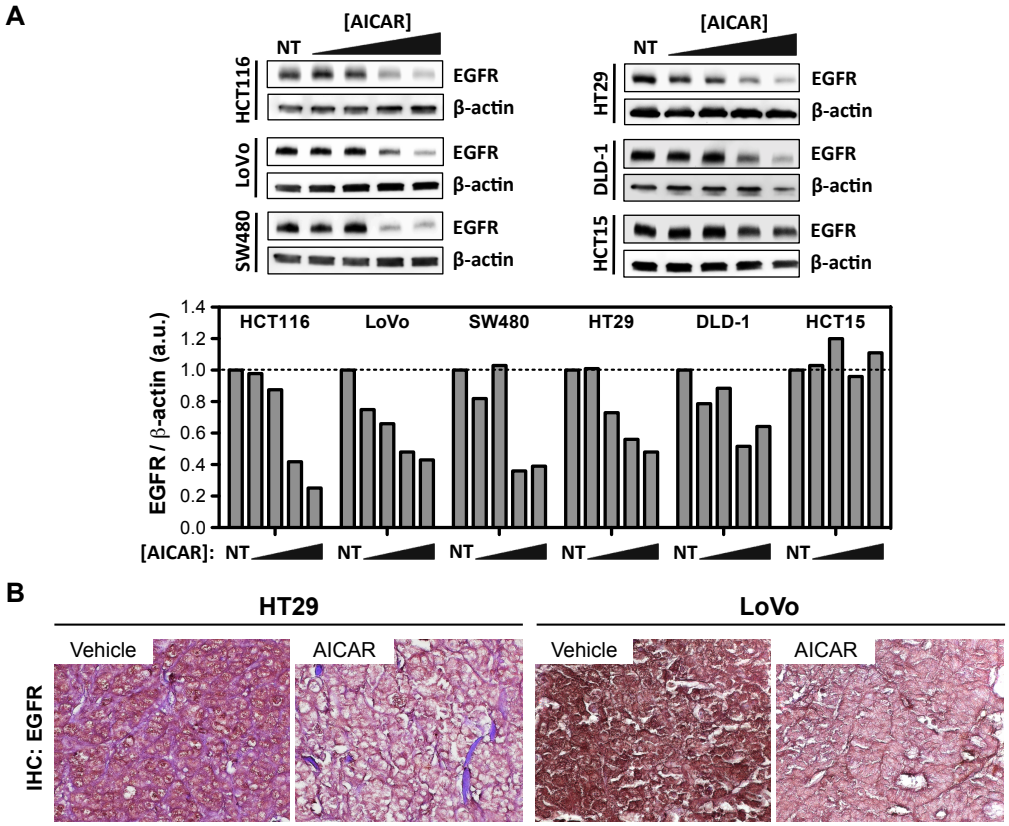

Figure 3.6. AICAR represses EGFR levels in a panel of human colorectal cancer cell lines in a dose-dependent manner *in vitro* and in xenograft tumor models *in vivo*.
(A) Six colon cancer cell lines were treated with increasing doses of AICAR (0, 0.1, 0.2, 0.4, and 0.8mM) for 36 hours and lysates were probed for EGFR. Bands were normalized to loading control and quantified relative to non-treated (NT) cells.
(B) Xenograft tumors were established from HT29 and LoVo cells and mice were treated daily with PBS vehicle or AICAR for 18 days after injection. Representative images of harvested tumor sections stained for EGFR by immunohistochemistry are shown (63x magnification).

It is important to note that most MIN cell lines also display some degree of aneuploidy, amplifications, and/or chromosomal rearrangements (Meltzer et al., 1994). Since the sensitivity of cell lines to AICAR does not appear to strongly correlate with EGFR expression levels or modal number of chromosomes per cell (**Figure 3.7**), further studies are required to more carefully evaluate the mechanisms involved in AICAR sensitivity and EGFR regulation. As previously reported (Tang et al., 2011) and in the current study, the increased sensitivity of non-transformed mouse and human cells to AICAR appears to correlate with an additional gain of a single chromosome (trisomic, 2n+1) whereas cancer cells represent a plethora of chromosomal abnormalities and other genetic alterations. Nonetheless, these data serve as initial observations in the use of AICAR as a chemopreventive or therapeutic agent against trisomy 7 cells through EGFR downregulation and perhaps in combination with AMPK activation.

Discussion

The discovery of aneuploid-specific compounds for the treatment of CIN-driven cancers is reliant on useful models to recapitulate the aneuploid state. I have employed an isogenic HCEC line that is distinctive at the karyotypic level: normal diploid versus trisomy 7 derived from identical cell populations. In this study, I provide data supporting AICAR as a prospective chemopreventive compound and further reveal for the first time that EGFR is a major target of AICAR in a trisomic, yet otherwise normal, non-malignant human epithelial cell line. Whether or not AICAR may be an effective therapeutic agent against EGFR-driven cancers (e.g. lung cancers) remains unknown.

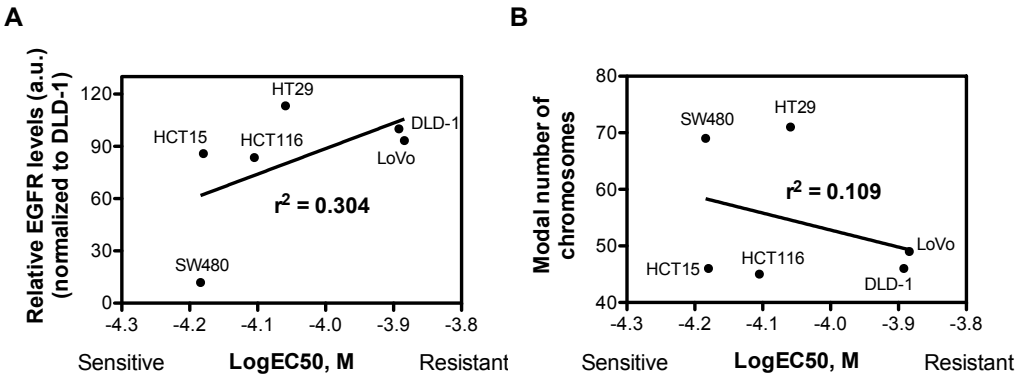

C

Cell Line	Status	LogEC$_{50}$, M	# of Chromosomes	EGFR Level
DLD-1	MIN	-3.892	46	100.0
HCT15	MIN	-4.18	46	85.9
HCT116	MIN	-4.105	45	83.5
LoVo	MIN	-3.884	49	93.3
HT29	CIN	-4.059	71	113.2
SW480	CIN	-4.184	69	11.8

Figure 3.7. Sensitivity to AICAR does not correlate with EGFR protein levels or chromosome number in human colon cancer cells.
(A) Relative EGFR expression levels were compared in six cell lines by western blot analysis (not shown), normalized to DLD-1, and plotted against the EC_{50} value of AICAR.
(B) Modal chromosome numbers per cell line are plotted against EC_{50} value of AICAR.
(C) Summary of findings from the panel of cancer cell lines tested.

Under optimal growth conditions, aneuploidy has been shown to be detrimental to cellular fitness in terms of proliferation rates compared to diploid cells (Torres et al., 2007; Williams et al., 2008). Evidence suggests that aneuploid cells develop an intrinsic stress response, independent of the alteration to a specific chromosome, which may assist them in thriving under selective pressures (Chen et al., 2012). One hypothesis to explain impaired proliferation is that additional chromosomes generate excess proteins (Pavelka et al., 2010) that in turn induce proteotoxic stress (Torres et al., 2007). These proteomic changes could therefore lead to compensatory genetic alterations in protein degradation pathways (e.g. the ubiquitin-proteasome pathway) to counteract the effects of imbalanced protein levels. For example, in budding yeast, aneuploid strains develop mutations in the deubiquitinating enzyme *UBP6* to compensate for the increased intracellular protein composition and this alteration is sufficient to improve their proliferation (Torres et al., 2010). In the present work, it is plausible that AICAR treatment may also be attenuating similar protein degradation pathways to revert overexpressed proteins generated by extra chromosomes to either normal or low levels that would otherwise provide proliferative cues (e.g. EGFR).

Figure 3.8 illustrates the current working model on the mechanism behind AICAR-induced growth inhibition. An enhanced dependency of 1CT+7 cells on EGFR signaling compared to diploid cells (Ly et al., 2011) had previously been reported. In the proposed schematic, EGF-ligand induced receptor activation and internalization is required for the intracellular activity of AICAR. Upon ligand binding and receptor sorting by endosomes, I hypothesize that AICAR indirectly accelerates EGFR ubiquitination and subsequent proteolysis. This reduces the recycling of receptors back to

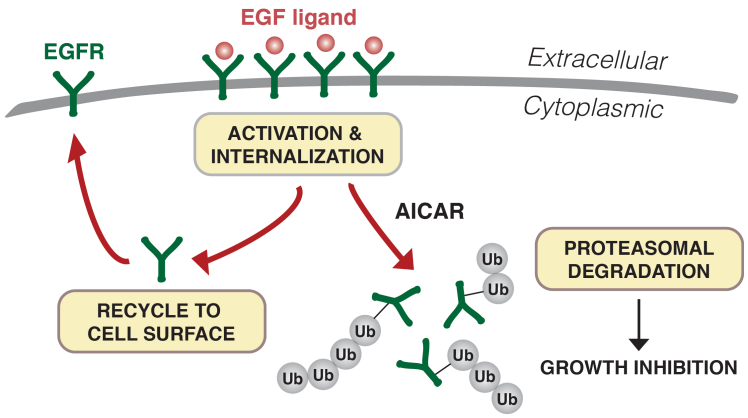

Figure 3.8. Proposed model for AICAR-induced EGFR depletion and growth inhibition. In the presence of EGF ligand, EGFR becomes autophosphorylated and internalized for sorting (endocytic pathway not shown for purpose of clarity). Rather than recycling receptors to the cell surface, I propose that AICAR promotes the ubiquitination and degradation of EGFR via the proteasome, leading to subsequent growth inhibition. The increased dependency of trisomy 7 cells on EGFR signaling may result in a differential toxicity to AICAR.

the cell surface and therefore diminishes sensitivity to EGF ligand. Further biochemical analysis is required to elucidate the exact mechanism of action and to uncover any unidentified pathways that may be involved in these events. It is also currently unclear the extent of which the lysosomal degradative pathway contributes to AICAR-mediated downregulation of EGFR.

Since trisomy 7 is found in a large fraction of premalignant lesions and the vast majority of human colorectal carcinomas, I hypothesized that 1CT cells cultured under defined, serum-depleted conditions acquired a third copy of chromosome 7 and upregulated EGFR levels, supporting a clonal expansion of "EGFR-addicted" 1CT+7 cells. Therefore, a more potent cytostatic effect is observed when inhibiting EGFR in oncogene-addicted cells (Gazdar et al., 2004) (i.e. the effect of cetuximab on 1CT+7 cells compared to 1CT). Interestingly, ectopic overexpression of EGFR in both normal human bronchial epithelial cells (HBEC) (Das et al., 2007) or in HCEC 1CT is insufficient to sensitize cells to AICAR (**Figure 3.9**). These results suggest that AICAR is more effective against EGFR-dependent cells and/or perhaps those that endogenously overexpress EGFR.

Cells typically respond to AICAR through phosphorylation and subsequent activation of AMPK, the best-known target of AICAR (Rattan et al., 2005). Although Tang *et al*. provided evidence of an AMPK-dependent cytostatic effect in aneuploid MEFs (Tang et al., 2011), they did not observe similar specificity when activating AMPK through an alternative method, such as treatment with the compound metformin, an indirect AMPK activator. I also observed that metformin did not specifically sensitize 1CT+7 cells (**Figure 3.10, A**) suggesting that the specificity of AICAR may be

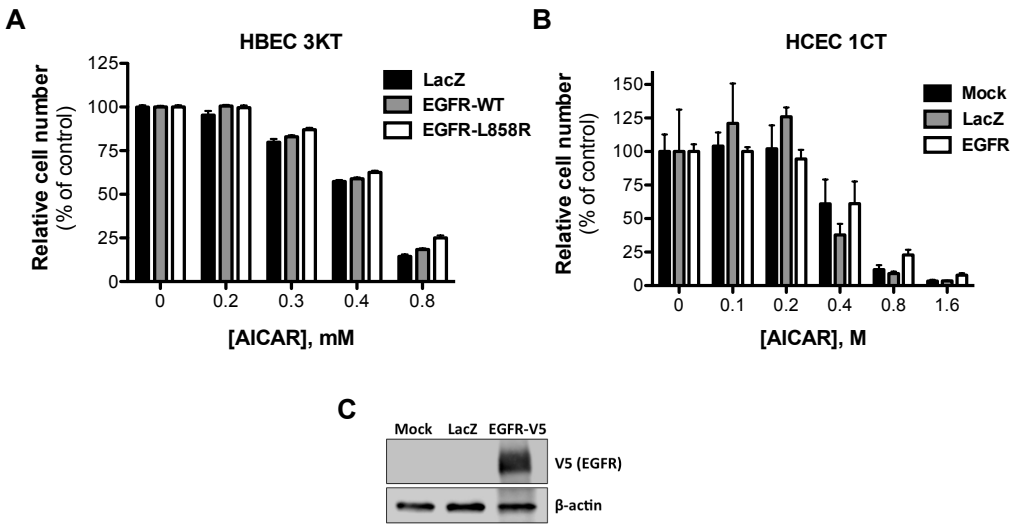

Figure 3.9. Overexpression of EGFR is insufficient to enhance AICAR sensitivity.
(A) Immortalized human bronchial epithelial cells expressing LacZ, wild-type EGFR, or L858R-mutant EGFR were treated with increasing doses of AICAR for 5 days.
(B) HCEC 1CT cells expressing LacZ or wild-type EGFR were treated with increasing doses of AICAR for 5 days.
(C) Western blot confirmation of ectopic EGFR protein expression in HCECs with an anti-V5 antibody.

independent of AMPK function. Furthermore, both HCEC lines were similarly responsive to mTOR repression-mediated growth inhibition using the compound Torin1 (**Figure 3.10, B**), indicating that the sensitivity of trisomy 7 cells to AICAR is also not regulated through the canonical mTOR pathway. EGFR degradation induced by AICAR could be either dependent on AMPK (treatment with AICAR leads to AMPK activation by LKB1 leading to EGFR depletion) or independent of AMPK (treatment with AICAR affects another pathway that leads to EGFR depletion). While there is no direct experimental evidence whether the effects of AICAR on EGFR are dependent on AMPK, I reasoned that AMPK, like LKB1, is not required for EGFR degradation since activation of AMPK (T172 phosphorylation) is dependent on LKB1 (Shaw et al., 2004). Because AMPK activation requires LKB1 and this data indicates that LKB1 is not required for EGFR degradation (**Figure 3.4**), these results collectively suggest that AICAR-induced EGFR depletion is independent of AMPK activation. Although activation of AMPK may play a large role in reducing cell proliferation induced by AICAR in some cells, the data reported here indicates that EGFR depletion may be an alternative mechanism of growth inhibition. AMPK activation and targeted proteolysis of EGFR could also be working collectively to reduce the growth of aneuploid cells.

These findings describe AICAR as a novel compound in regulating EGFR protein levels in both non-malignant and malignant genomically unstable cells, a potential therapeutic strategy in the chemoprevention of aneuploidy-driven CRC. AICAR selectively inhibits proliferation of 1CT+7 HCECs whereas diploid cells are largely unaffected. Furthermore, these effects are reversible (**Figure 3.3, D**) and EGFR levels are restored upon 24-hour washout. These results indicate that AICAR may be effective in

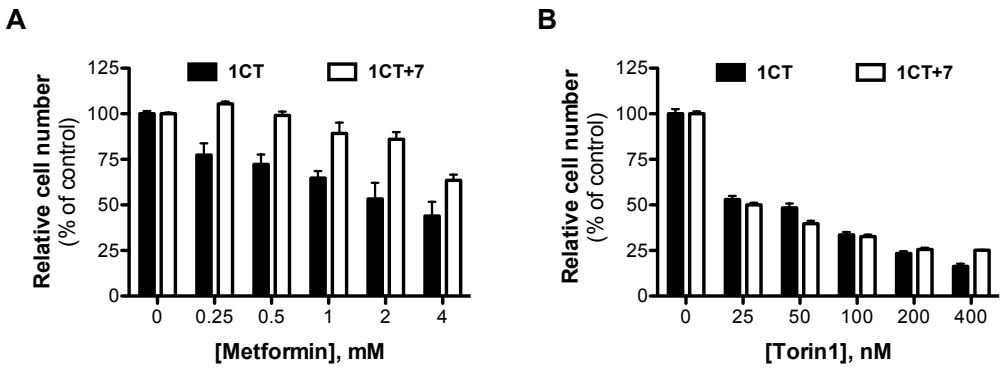

Figure 3.10. Treatment with an **(A)** alternative activator of AMPK (metformin) or **(B)** inhibition of the mTOR pathway (Torin1) does not selectively inhibit growth of 1CT+7 cells.

treating patients with colonic adenomas driven by aneuploidy with minimal toxicity to normal epithelial tissue. Since the human colon constantly undergoes rapid turnover, AICAR may be used to prevent the spontaneous growth of aneuploid cells until they are shedded at the apex of the colonic crypt (Lamprecht et al., 2002). Upon turnover-mediated abolishment of aneuploid cells from the colonic epithelium, AICAR treatment may be discontinued and EGFR levels will presumably be restored in normal tissue. Also noteworthy is that AICAR efficacy is dependent on the presence of EGF ligand, thus only affecting cycling cells in a mitogen-containing environment.

To conclude, I have identified AICAR as a novel regulator of EGFR signaling that potently prevents proliferation of a minimally aneuploid (trisomy 7) HCEC line. The downregulation of EGFR protein levels can be attributed to increased ubiquitination and proteasomal-mediated degradation in an EGF-dependent manner. I propose that this negative regulation of EGFR (in possible combination with AMPK activation) inhibits the growth of both malignant and non-malignant human colonic cells with unstable chromosome numbers. Future studies involve testing the effects of AICAR on a diverse set of aneuploid cancer cell lines, further elucidating the mechanism of preferential sensitivity to cells with genomic instability, and to determine critical pathways involved in AICAR-mediated EGFR regulation. Further analyses on a broad panel of aneuploid, non-transformed human cell lines are also unquestionably needed, although the field is currently limited by the lack of these cell-based models. Therefore, the development of new aneuploid systems using human cells or mouse models is of utmost importance towards therapeutic discovery in exploiting the aneuploid state for clinical benefit. This study provides further rationale for the potential clinical utility of AICAR as a

chemopreventive compound to patients predisposed or recurring from sporadic CRC or as a therapeutic agent to those currently diagnosed with CRC.

Materials and Methods

Cell culture & reagents

Culture conditions of HCECs have been previously described elsewhere (Roig et al., 2010). Briefly, HCECs are maintained in 2% oxygen/5% carbon dioxide conditions on Primaria dishes (BD Biosciences). 4:1 DMEM:Medium 199 (Hyclone, Thermo Scientific) is supplemented with 2% cosmic calf serum (Hyclone, Thermo Scientific) and 20ng/mL EGF (PeproTech). HCEC experiments are performed in serum-free, defined conditions in the presence of EGF unless otherwise stated. Human CRC cell lines are cultured with 10% serum. The identity of all cell lines were verified by DNA fingerprinting.

AICAR (Toronto Research Chemicals), metformin (Sigma), and MG132 (Torcris Biosciences) were dissolved in DMSO. RT-PCR primers for EGFR-tyrosine kinase domains were previously described elsewhere (Ly et al., 2011). siGENOME siRNAs targeting LKB1 or non-targeting controls were purchased from Dharmacon and reverse transfections were performed using RNAiMAX transfection reagent (Invitrogen) under manufacturer's instructions.

Growth assays

Cells (2×10^3) were seeded in 96-well clear-bottom plates in serum-free medium for 24 hours prior to the addition of vehicle or drug-containing medium. Five days post-drug treatment, CellTiter-Glo (Promega) reagent is added to each well per manufacturer's

instructions and shaken. Luminescent ATP levels were detected by an Envision plate reader (Perkin Elmer) and cell numbers are normalized to control wells.

For colony formation assays, cells were plated at clonal density (200-400 cells/10cm^2 dish) in 2% cosmic calf serum to promote low-density cell adhesion to plates. Twenty-four hours later, cells were washed with PBS and replaced with either vehicle or 0.25mM AICAR in serum-free medium. Fifteen days post-treatment, colonies were washed with PBS and stained with 6% glutaraldehyde/0.5% crystal violet solution for 30 minutes and counted.

Metabolic analysis

HCECs were seeded in six-well dishes at various densities (1-5 x 10^3 cells) in 2mL serum-free medium and replaced with 1mL vehicle or AICAR-containing medium 24 hours later. Cell culture supernatants were collected 48 hours post-treatment and centrifuged to exclude debris. Supernatants were analyzed using a BioProfile Basic-4 Automated Analyzer (Nova Biomedical) and values were normalized to cell-free medium incubated alongside drug-treated cells. Glucose consumption and lactate production is then normalized to the relative sum of total cell counts per hour over a 48-hour treatment period.

Western blot

Whole cell lysates were collected in Laemmli sample buffer and boiled. Equal amount of lysates were resolved on 4-15% polyacrylamide gels (BioRad) and transferred to PVDF. Membranes were then probed with the following primary antibodies: anti-EGFR (sc-03,

Santa Cruz), anti-Met (L41G3, Cell Signaling), anti-RalA (610221, BD Biosciences), anti-LKB1 (27D10, Cell Signaling), and anti-HA (C29F4, Cell Signaling). Anti-phospho-AMPK, phospho-ACC, and phospho-mTOR are from the AMPK and ACC sampler kit (9957, Cell Signaling). HRP-conjugated goat anti-mouse or anti-rabbit secondary antibodies (Jackson ImmunoResearch) were detected by SuperSignal West Femto Chemiluminescent Substrate kit (Thermo Scientific) and imaged on a G:Box (Syngene) gel documentation system. Bands were quantified using GeneTools (Syngene) software and normalized to loading controls.

Immunofluorescence and immunohistochemistry

For immunofluorescence, cells cultured in chamberslides were fixed in 4% paraformaldehyde for 10 minutes, permeabilized with 0.5% Triton-X, and blocked (10% goat serum, 3% BSA) for 5 minutes. Anti-EGFR primary antibody (sc-03) was diluted 1:50 in blocking solution and applied for 1 hour followed by goat-anti-rabbit FITC secondary for 1 hour. Cells were then stained for DAPI, mounted in Mowiol 4-88 (Calbiochem), and observed at 100x magnification.

Immunohistochemistry was performed on 5μm paraffin-embedded sections of Bouin-fixed HT29 and LoVo xenografted tumors following heat-induced antigen retrieval with 0.01M Sodium Citrate buffer, pH 6.0. Tumor formation and vehicle/AICAR treatment of immunocompromised mice was previously described elsewhere (Tang et al., 2011). Anti-EGFR primary antibody (sc-03) at a 1:200 dilution was applied overnight at 4ºC. Sections were then blocked using the Avidin/Biotin Blocking Kit (Vector Labs) and incubated with biotinylated secondary antibody,

streptavidin-conjugated HRP, and DAB reagents as described and supplied in the Peroxidase Detection System (Novocastra/Leica).

Ubiquitination assay

HCEC 1CT+7 (10^6) were reversed transfected with 1µg HA-tagged ubiquitin plasmid using Effectene Transfection Reagent (Qiagen) according to manufacturer's instructions in 2% serum medium. The next day, cells were washed with PBS and replaced with serum-free medium containing 0.25mM AICAR and 10µM MG132. After 24 hours, cells were washed with ice-cold PBS, collected in IP buffer (50mM Tris, 150mM NaCl, 10% glycerol, 1% Tween-20, protease/phosphatase inhibitors) and lysed for 30 minutes at 4°C followed by passage through a 27.5 gauge needle. Lysates were then immunoprecipitated with EGFR agarose-conjugated antibody (sc120AC, Santa Cruz) for two hours at 4°C followed by three washes. Samples were then boiled in the presence of SDS and resolved by 4-15% SDS-PAGE. Membranes were probed using anti-EGFR and anti-HA antibodies.

CHAPTER FOUR

DISCUSSION AND FUTURE DIRECTIONS

Measuring CIN as a Prognostic or Diagnostic Marker

Although aneuploidy can be detected in a large percentage of human tumors, chromosomal instability (CIN) status is not currently assessed in the clinic for diagnostic or prognostic purposes. Since the degree of CIN correlates with poor patient outcome in several different cancer types, including the colon (Walther et al., 2008), breast (Smid et al., 2011), ovary, and lung (Choi et al., 2009), measuring the degree of aneuploidy could be a practical approach to prognostic assessment (Ferreira et al., 2008). While the concept appears logical, the technical challenge remains as to how to most accurately and rapidly quantify CIN status from patient tumor samples in a cost efficient manner.

Current cytogenetic methods, which are further discussed below, for measuring aneuploidy include GTG-banding, fluorescent *in situ* hybridization (FISH), array comparative genomic hybridization (CGH), and the use of gene expression signatures in predicting clinical outcome (McGranahan et al., 2012). Unfortunately, there is no clear consensus as to which of these techniques may be most suitable for clinical applications as they are either labor intensive or expensive. Thus, there is currently a need to develop alternative methods for assessing CIN status, taking into account costs, accuracy, technical challenges, and limitations to develop the most optimal strategy. Further considerations include being able to deconstruct static (non-CIN) versus fluctuating

(CIN) aneuploid tumors and whether single cell resolution or whole population analyses are required.

GTG-banding, the oldest technique, involves staining condensed metaphase chromosomes with Giemsa dye. This straightforward method provides an overall look at the entire cellular ploidy status and can detect structural chromosomal aberration (i.e. inversions, translocations). Each chromosome can be visibly distinguished due to inherent differences in Giemsa staining patterns. FISH is another relatively economical method to evaluate specific aneuploidies or gene copy number variation (Calasanz et al., 2008). This technique utilizes a highly specific probe or set of probes (i.e. dual multicolor FISH) that hybridizes to defined chromosomal regions with DNA sequence complementarity, most often at the centromeres. These probes can then be easily visualized by fluorescence microscopy, and the number of foci observed represents the copy number for the specific sequence of interest. FISH is a moderately useful method to quantitate copy number at single cell resolution and inferences could be made regarding tumor heterogeneity by observing the cell-to-cell variability within patient samples (Speicher et al., 2005). The disadvantage of FISH is that it does not provide a complete view of the entire karyotype, but rather the ploidy status of specific chromosomes. For example, a colorectal tumor sample may undergo FISH analysis for the development of trisomy 7, but the status of other chromosomes would remain undefined. GTG-banding and FISH can economically measure CIN status at single cell resolution, although both are labor-intensive procedures and may not be suitable for the clinical setting.

In comparison to measurements from single cells, several other techniques allow for larger population-based analyses of CIN status and may be more useful in the clinic.

Array CGH utilizes several thousand probes spanning the genome to quantify copy number alterations to produce a "virtual karyotype" from a patients DNA sample (Le Scouarnec et al., 2012). Not only is array CGH an effective method for measuring whole chromosome duplications, but it also permits the detection of amplifications or deletions at specific loci. Bioinformatic analyses are also required for data normalization to a reference genome. Although array CGH can provide useful genomic information from patient samples, it is currently an expensive technique and not yet amenable for high-throughput use.

More recently, gene expression signatures have been developed to predict patient outcome (Carter et al., 2006). For example, the CIN70 signature consists of 70 genes derived from a breast cancer cohort study that associates transcript expression levels with tumor size, *ER* and *HER2* status, and tumor grade (Birkbak et al., 2011). Another example uses a 12-gene signature to predict breast cancer patient prognosis, similar to the currently used clinical diagnostic tests Oncotype DX or MammaPrint (Habermann et al., 2009; Mettu et al., 2010). One critical disadvantage of these methods includes the measurement of population karyotypes with no information regarding single cell status. Therefore, analysis by gene expression signatures generally will not allow for inferences concerning tumor heterogeneity and karyotypic diversity within a population of cells in a tumor sample. A technique that may soon gain widespread acceptance in the field is next generation sequencing (Navin et al., 2011), a method that has already identified chromothripsis as a new form of genomic instability.

Groups of compounds	Number of compounds in the group
Ellipticine/Ellipticinium/Olivacinium group	10
Fuchsine group	3
Cytochalasin group	3
2-propenamide,N-[variable]-3-(1,2,3,4,tetrahydro-6-methyl-2,4-dioxo-5-pyrimidinyl) group	6
Benzodithiophene-4,8-dione group	6
Combretastatin group	4
Antibiotics	13
Others	8
Total # of compounds:	53

Figure 4.1. Compound groups targeting cancer cell lines with highly complex karyotypes. The NCI60-drug sensitivity database was mined for correlations between karyotypic complexities against sensitivity to growth inhibiting compounds.

Figure adapted from Roschke et al, *Curr Drug Targets* 2010.

Targeting Aneuploid Cells as a Therapeutic Strategy

Targeting aneuploid cells for therapeutic or chemopreventive purposes is a feasible strategy to combat cancer. Tumors are often heterogeneous (Shackleton et al., 2009) and contain a mixture of cells with varying karyotypes. Although there are currently no treatment options for targeting aneuploidy in the clinic, eliminating tumor cells with an inappropriate number of chromosomes using selective compounds may represent a novel and potentially effective therapeutic option (McClelland et al., 2009). Fortunately, preliminary data from the National Cancer Institute (NCI) has provided proof-of-principle insight into selectively targeting cells with chromosomal alterations. Sixty human cancer cell lines (termed the NCI-60) were screened with 1,429 anticancer compounds for growth inhibition. These data has been interrogated for correlations between karyotypic complexities and compound sensitivity (Roschke et al., 2003; Wallqvist et al., 2005). Such interrogations has yielded seven groups of compounds that are more specific towards cancer lines with high karyotypic complexity compared to lines with simple karyotypes (**Figure 4.1**) (Roschke et al., 2010). These studies provided the first evidence that certain compounds can discern between cells that are more diploid-like compared to those that are highly aneuploid.

More recently, the heat shock protein 90 (Hsp90) inhibitor, 17-AAG, has been shown to selectively target trisomic MEFs (Tang et al., 2011). As previously mentioned, the most current and generally accepted proposal is that aneuploid cells undergo proteotoxic stress due to extra proteins generated from additional chromosomes. In turn, this stress can activate specific cellular responses, such as engaging protein degradation

pathways, in an attempt to overcome proteotoxic stress. The Hsp90 chaperone, which is upregulated in response to stress, is crucial in regulating protein folding and degradation (Scheibel et al., 1998). Interestingly, treatment of wild type yeast with an Hsp90 inhibitor induces CIN with high karyotypic diversity (Chen et al., 2012). Inhibition of Hsp90 through treatment with 17-AAG can ultimately lead to aneuploid cell death by disturbing a pathway in which it is dependent. For example, 17-AAG-induced Hsp90 inhibition can decrease endogenous protein folding and degradation, which allows for a build-up of stress responses and excess proteins that could ultimately result in cell death. Moreover, AICAR treatment also activates a stress response through AMPK, placing additional stress on aneuploid cells. Therefore, the shared commonality exploited between both AICAR and 17-AAG includes disturbances to stress response pathways, which may be a possible mechanism of action for selectivity over diploid cells.

Future Directions

Several important questions remain unanswered regarding the role of aneuploidy in cancer development. For example, which genes or pathways are aneuploid cells dependent on for survival or proliferation? An obvious experiment to address this question would be to conduct genome-wide RNAi studies to determine which loss-of-function genes can induce apoptosis or alter the proliferative rates of aneuploid cells. The genes identified in these studies should elucidate genetic pathways that may be targeted for therapeutic purposes. I have initiated a preliminary experiment to determine which depleted genes can synergize with aneuploidy to induce cell death. Briefly, pooled

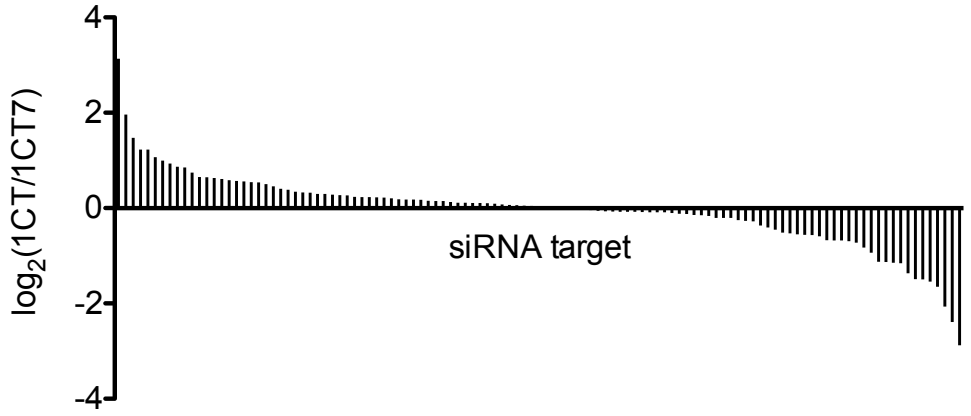

Figure 4.2. Overall viability distribution of focused siRNA screen targeting trisomy 7 cells for lethality. 1CT and 1CT+7 cells were individually transfected with pooled siRNAs targeting 115 genes and viability was measured after five days. siRNAs on the left-hand side represent those specifically toxic against trisomy 7, but not diploid, HCECs.

siRNAs targeting 115 individual genes were screened in HCEC 1CT and 1CT+7 for lethality over five days. A handful of genes were observed to cause decreased 1CT+7 viability with marginal effects on diploid HCECs, some of which include *ALDOA*, *CHEK1*, *PCF11*, and *POLR2A*. The overall distribution of all siRNAs screened is shown in **Figure 4.2**. Genome-wide RNAi screens could identify additional genes that may be exploitable for potential targeted therapy.

While this dissertation provides data supporting AICAR as an effective reagent against aneuploid cells *in vitro* and *in vivo*, its use as a therapy option may potentially be limited dependent on further testing. Thus, efforts have been initiated in discovering novel apoptosis-inducing compounds that are more specific and potent in targeting only aneuploid cells. To identify such compounds, I have piloted a preliminary high throughput chemical screen with an initial library of 8,000 compounds. In collaboration with the UT Southwestern High Throughput Screening core facility, conditions have been optimized to rapidly screen isogenic 1CT and 1CT+7 HCECs in 384-well plates with chemical libraries. In our initial experiments, 1CT+7 cells were individually screened for changes in viability with 8,000 compounds at a concentration of 5μM for five days. From this initial diversity library, 319 compounds were discovered to be broadly toxic against 1CT+7 cells. These 319 compounds were then cherry-picked and counter screened against both 1CT and 1CT+7 cells. Five compounds demonstrated specific and statistical lethality against 1CT+7 cells compared to diploid cells (**Figure 4.3**). In addition to this preliminary proof-of-principle screen, experiments examining the effects of a full 200,000 compound library are planned in the future. This full library contains stringently selected compounds that encompass a large range of structural diversity.

Further topics of interest include how the transcriptome and proteome differs between diploid and aneuploid cells. Approaches to be taken include microarray profiling and stable isotope labeling by amino acids in cell culture (SILAC) techniques to globally quantitate transcript and protein levels (Ong et al., 2002), respectively. Furthermore, whole genome DNA sequencing on the panel of HCECs generated by our laboratory is currently underway. We predict that this information will provide knowledge of mutations that may contribute towards the development of aneuploidy.

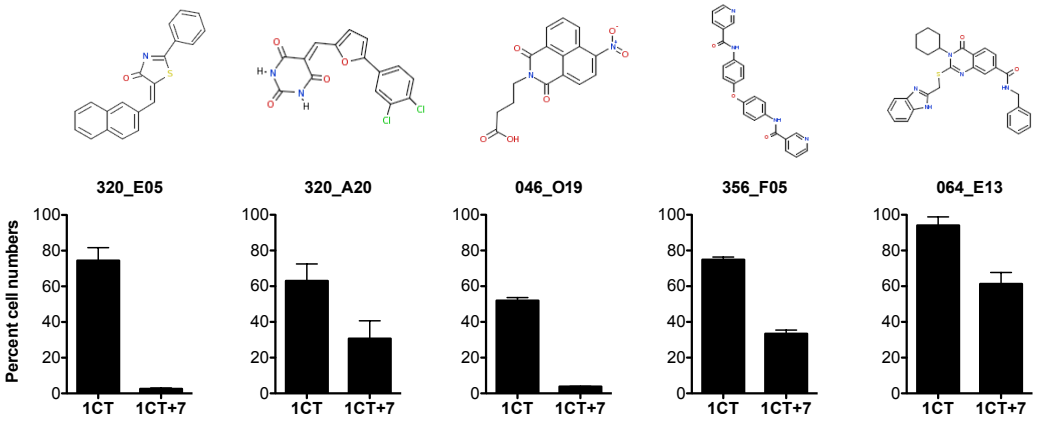

Figure 4.3. Preliminary high-throughput screening results from an initial 8,000 compound diversity library. The compounds shown here represent those that were statistically lethal against trisomy 7 cells compared to diploid cells. HCECs were treated for five days with 5μM compound followed by viability assessment.

CHAPTER FIVE

RNA INTERFERENCE SCREENING OF THE HUMAN COLORECTAL CANCER GENOME IDENTIFIES MULTIPLE TUMOR SUPPRESSORS REGULATING EPITHELIAL CELL INVASION

Introduction

Genomic sequencing of human tumor-derived DNA has identified a vast number of novel tissue-specific genetic mutations occurring at varying frequencies (Wood et al., 2007). Frequently mutated genes are informally referred to as driver alterations (or candidate cancer genes, *CAN*-genes), whereas those less frequently mutated are considered passenger alterations (Wood et al., 2007; Stratton 2011). With few exceptions, the majority of mutations are loss-of-function alterations and the ones that occur rarely are presumed to be a by-product of genomic instability or normal mutation rates that do not directly contribute to tumor progression (passengers) (Carter et al., 2009).

In addition to computational and biostatistical models for parsing driver from passenger mutations, the utility of biological assays to functionally interrogate cancer genomes is required to determine which of these mutations are able to contribute to a particular tumorigenic phenotype (i.e. anchorage-independent growth, resistance to apoptosis, enhanced invasion through extracellular matrices). Moreover, these assays can also decipher whether less frequently mutated genes are actively involved in cancer progression. Thus, the development of experimental methods to separate putative driver from passenger mutations is critical towards understanding which genes are directly

promoting tumorigenesis. Although sequencing of the human colorectal cancer (CRC) genome, in parallel with computational analyses, has detected 140 frequently mutated *CAN*-genes and up to ~700 mutations occurring at a lower frequency (passengers) (Wood et al., 2007), it is difficult to distinguish whether these mutations play a causal or incidental role in tumor development. The identification of those mutated genes with tumor-associated roles may therefore lead to novel therapeutic avenues as we transition towards an era of personalized medicine and targeted therapy.

Advances in RNA interference (RNAi) technologies have enabled loss-of-function screens to identify tumor suppressors in mammalian cells, the knockdown of which promotes an assayable cancer-associated phenotype(s) (Schlabach et al., 2008). Compared to whole-genome screens, RNAi screens focusing on specific gene sets obtained from cancer genome sequencing data are suitable for classifying potential driver from passenger alterations. To identify tumor suppressors of human CRC, we conducted a loss-of-function screen using a small interfering RNA (siRNA) library (Dharmacon, Lafayette, CO) targeting the most frequently mutated genes in CRC (*CAN*-genes) for the ability to permit cell invasion, a hallmark of cancer. The initial step in the progression of a localized tumor towards invasive and metastatic disease occurs when cells acquire the ability to invade through a basement membrane (Sethi et al., 2011).

In this screen, we utilized a modified Boyden chamber coated with Matrigel (BD Biosciences, San Jose, CA), a reconstituted extracellular matrix, to recapitulate these events (Albini et al., 1987) using normal migratory, yet non-invasive, epithelial cells. These screens were carried out with non-malignant, *Cdk4*- and *hTERT*-immortalized human colonic epithelial cells (HCEC) (Roig et al., 2010) in the background of either

TP53-knockdown (1CTP) using short hairpin RNAs (shRNA) or ectopic expression of oncogenic $KRAS^{V12}$ (1CTR) (Eskiocak et al., 2011). The gene sets used in this study (*CAN*-genes) were derived from a report by Wood *et al* (2007). According to this study, *APC, KRAS, TP53,* and *PIK3CA* are mutated most often across a panel of sequenced colon tumors.

Results

Figure 5.1.A represents a diagram of the screening scheme. Briefly, pooled siRNAs (four siRNAs per gene) were reverse-transfected into 1CTP and 1CTR HCECs in 2% serum growth medium for 24 h before cells were washed and serum-starved overnight. Cells transfected for 48 h were then harvested in serum-free medium and plated onto 24-well Matrigel-coated transwell filters (BD Biosciences, San Jose, CA). The bottom chamber is filled with 2% serum medium plus growth factors as a chemoattractant. After overnight incubation, invaded cells were then fixed for Hoechst staining (Invitrogen, Grand Island, NY). Images were taken at 10× with five fields imaged per well. Altogether, pooled siRNAs targeting 159 genes (140 *CAN*-genes plus 19 additional "passenger" genes that closely interacted with *CAN*-genes through interaction mapping [8]) were tested in two cell lines (1CTP and 1CTR) for the ability to enhance invasion *in vitro.*

The overall screening results are shown in **Figure 5.1.B** as a scatterplot wherein the x- and y-axis represent the fold changes in invasion in the background of 1CTP and 1CTR cells, respectively. siRNAs targeting the essential ubiquitin B (*UBB*) gene were

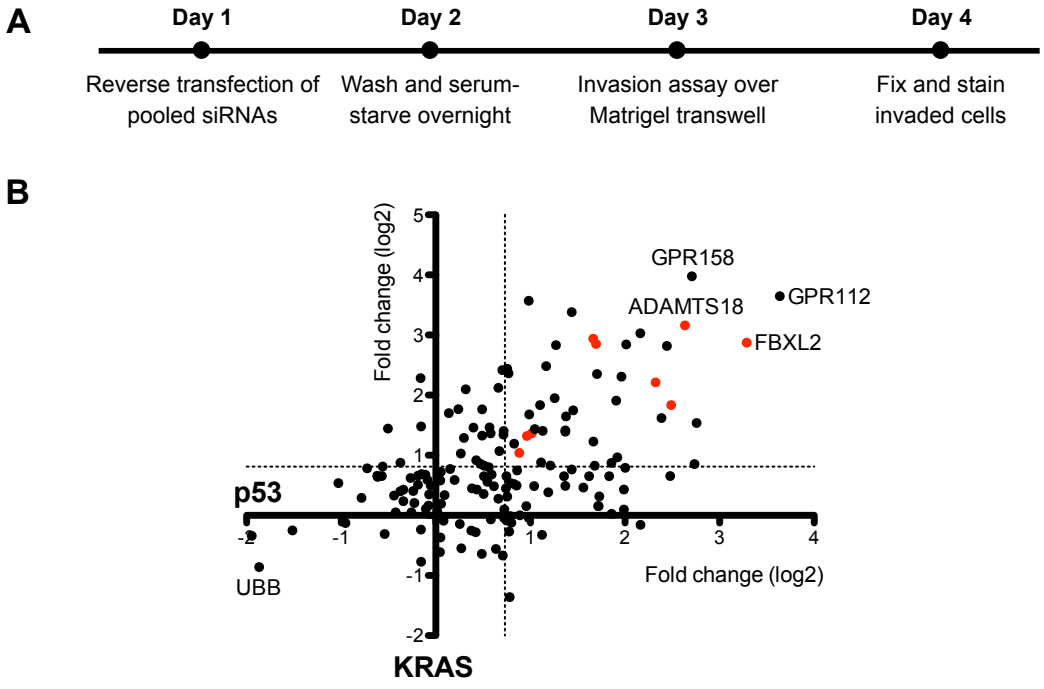

Figure 5.1. Identification of frequently mutated CRC tumor suppressors regulating cell invasion.

(A) Overall scheme of focused siRNA screen for tumor suppressors involved in regulating the invasive potential of normal cells. 1CTP (shRNA-*TP53*) and 1CTR (oncogenic-$KRAS^{V12}$ HCECs were reverse-transfected 48 h with pooled siRNAs prior to re-plating onto Matrigel-coated transwell filters. Invaded cells were Hoechst-stained and data were normal- ized to non-targeting siRNA control.

(B) Scatterplot of the overall screening results. The x-axis represents fold changes in invasion in 1CTP cells, whereas the y-axis represents those for 1CTR cells. Each dot represents a single gene targeted by pooled siRNAs (four siRNAs/gene) and red dots represent multifunctional tumor suppressor genes (listed in **G**). The dotted line represents the statistical cutoff point and is defined as three standard deviations.

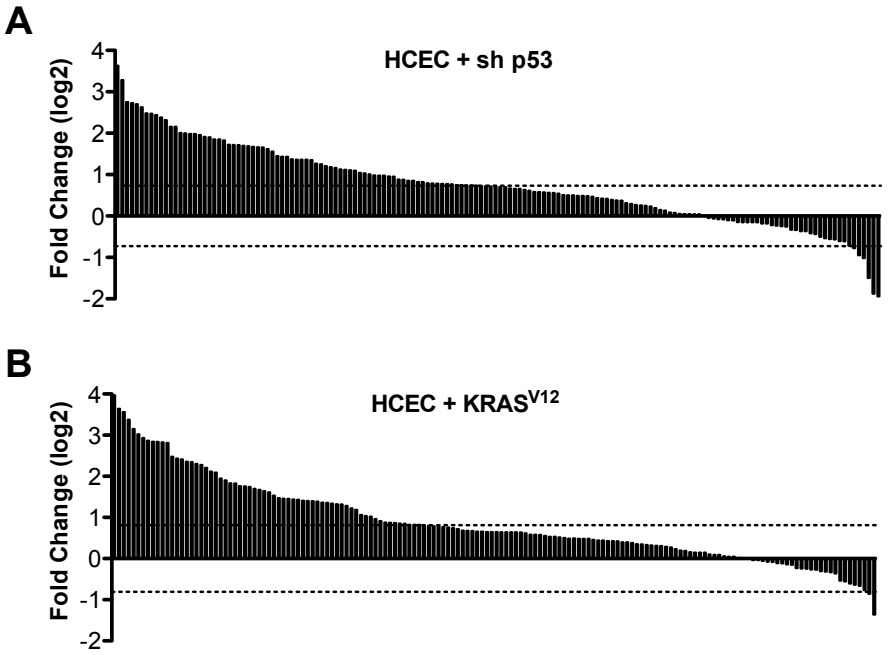

Figure 5.2. Overall distribution of all pooled siRNAs screened in **(A)** 1CTP and **(B)** 1CTR human colonic epithelial cells (HCECs) for changes in cell invasion. The dotted line represents the cutoff point of three standard deviations.

used to determine transfection efficiency and as a negative control, and a non-targeting control siRNA was used for normalization. A statistical cutoff point of three standard deviations was used to eliminate noise and false positives.

Depletion of 42 out of 159 (26.4%) screened genes promoted invasion in both cell backgrounds in a context-independent manner. The overall distribution of all siRNA pools screened in both backgrounds (calculated as changes in cell invasion) is depicted graphically in **Figure 5.2**. The results of the twenty most potent suppressors of invasion in each context are shown in **Figure 5.3**. Among these, knockdown of two G-protein coupled receptors (GPR112 and *GPR158)* with previously unidentified roles in cancer progression was among the most effective in inducing cell invasion. Moreover, **Figure 5.4.A** shows representative screening images of Hoechst-stained invaded cells on a transwell filter where depletion of *ADAMTS18* levels by pooled siRNAs induces context-independent cell invasion. Deconvolution of pooled *ADAMTS18* siRNAs revealed that three out of four siRNAs tested positive for increased cell invasion, strongly suggesting "on-target" effects of RNAi (**Figure 5.4.B-C**). Since stress fiber formation has been associated with cell migration and focal adhesion assembly that may promote cell invasion (Chrzanowska-Wodnicka et al., 1996), as a proof of principle experiment, we next determined whether *ADAMTS18* depletion could lead to rearrangements in the actin cytoskeleton. siRNA-mediated knockdown of *ADAMTS18* in 1CTP HCECs induced an approximate nine-fold increase in the number of cells positive for actin stress fiber formation compared to a non-targeting control siRNA (**Figure 5.4.D**).

Next, we sought to validate several of the identified hits using stable shRNA knockdowns (pGIPZ library, Open Biosystems, Lafayette, CO). We chose to retest five

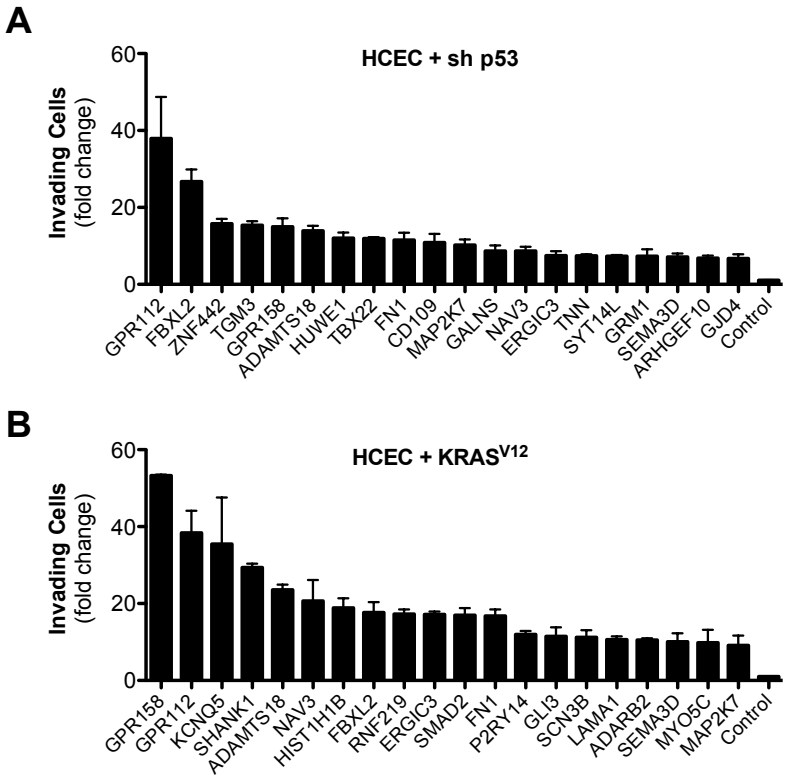

Figure 5.3. The top twenty most potent suppressors of invasion in **(A)** 1CTP and **(B)** 1CTR HCECs upon depletion by pooled siRNAs. Bar graphs are depicted as mean ± SEM.

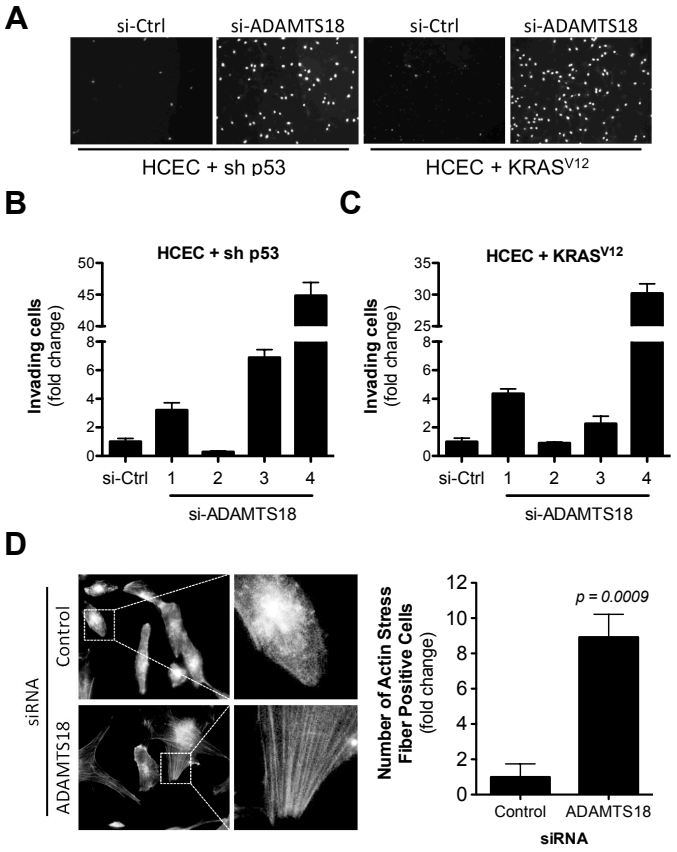

Figure 5.4. ***ADAMTS18*** **is a candidate tumor suppressor for CRC progression.**
(A) Representative images of Hoechst-stained invaded 1CTP and 1CTR cells with control siRNA or siRNA targeting the *ADAMTS18* gene.
(B-C) Deconvolution of pooled ADAMTS18 siRNAs in **(B)** 1CTP and **(C)** 1CTR HCECs for enhancements in cell invasion. Cells were transfected with individual siRNAs and tested for invasion as previously described.
(D) Depletion of ADAMTS18 using siRNAs induces the formation of F-actin stress fibers.
Bar graphs are depicted as mean ± SEM. P-values were calculated by two-tailed, unpaired Student's *t* test.

genes among each group that scored positive in the siRNA screen and five random genes that scored negative using two shRNAs per gene in 1CTP cells. A non-targeting shRNA was used for normalization. On average, shRNAs targeting genes that scored positive from the screen (black bars) resulted in a 2.3 ± 0.8-fold change in invasion compared to 0.6 ± 0.3-fold change using shRNAs against negatively scored genes (white bars) (**Figure 5.5**). Quantitative real-time PCR were performed on four of the positive hits (*FBXL2*, *HIST1H1B, HUWE1,* and *RNF219)* to determine shRNA knockdown efficiency. Seven out of eight hairpins caused marked reduction in target gene mRNA levels (**Figure 5.6**), with the exception of one shRNA targeting *HIST1H1B*.

Discussion

We have previously completed similar loss-of-function screens for tumor suppressors, the knockdown of which allows for bypass of anchorage-dependent proliferation restraints (i.e., growth in soft-agar) [8]. From those studies, we identified 52 context-independent regulators of soft-agar growth representing ~33% of all *CAN*-genes, an unexpectedly high percentage. Cross-analysis with this previously completed screen for soft-agar growth revealed that nine out of the 42 invasion-suppressing genes identified in the current study also permitted anchorage-independent growth upon knockdown (**Figure 5.7.A** and **Appendix A**). These nine over- lapping genes represent those mutated at a high frequency in human CRC with multiple tumorigenic phenotypes when depleted *in vitro* in a context-independent manner (**Figure 5.7.B**). Furthermore, the effect of these siRNAs on HCEC proliferation is shown in **Figure 5.8**.

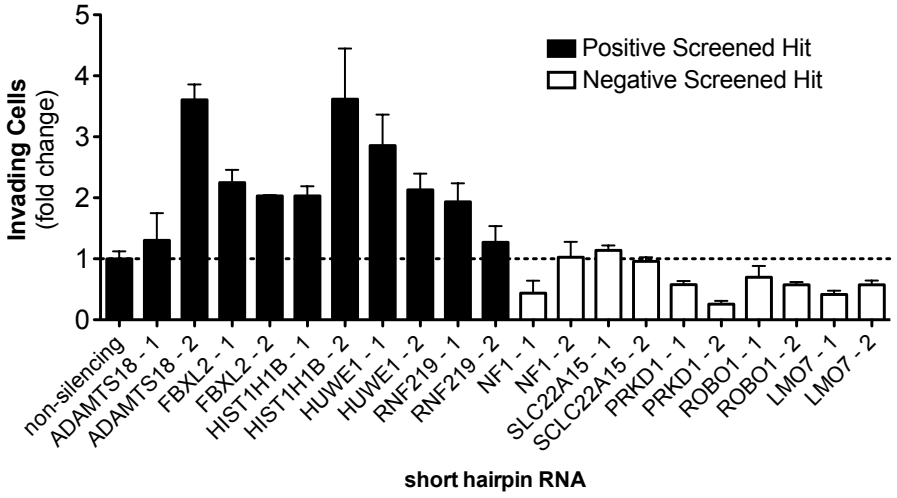

Figure 5.5. Screening results were partially validated in 1CTP cells using shRNA-mediated knockdown of five positive hits and five negative non-hits. Fold change in invasion is normalized to non-silencing shRNA. Bar graphs are depicted as mean ± SEM.

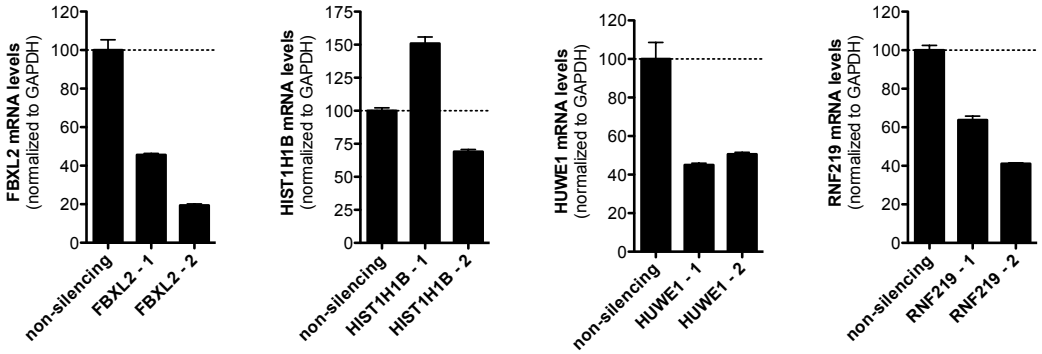

Figure 5.6. shRNA knockdown efficiency as assessed by quantitative real-time PCR. Total RNA isolated from the indicated cell lines infected with lentiviral shRNAs (Open Biosystems, pGIPZ library) were reverse transcribed and subjected to quantitative real-time PCR. GAPDH was used as an internal control and data are normalized to a non-silencing shRNA. Seven out of eight shRNAs tested displays marked reduction in target mRNA levels. Bar graphs are depicted as mean ± SEM.

One of the most potent suppressors of invasion that also conferred soft-agar growth upon RNAi-mediated knockdown is the *ADAMTS18* gene. *ADAMTS18* (a disintegrin and metalloproteinase with thrombospondin motifs 18) belongs to a family of ADAMTS peptidases with well-studied roles in extracellular matrix degradation and reorganization. Mutations in *ADAMTS18* have previously been linked to melanoma progression (Wei et al., 2010). *ADAMTS18* is mutated in 6% of colorectal carcinomas out of 193 sequenced tumors (The Cancer Genome Atlas), representing a large number of patients out of the ~140,000 annually diagnosed colon cancer cases in the United States alone (American Cancer Society).

In summary, these results allow for deconstructing driver and passenger alterations within a given tumor context characterized by cancer-associated phenotypes. Loss-of-function screening using RNAi provides a robust method to rapidly analyze the cellular effects of depleting specific genes identified from cancer genome sequencing efforts. While not comprehensive of all the genomic changes that occur in CRC, these studies are an initial step in validating and complementing bioinformatic approaches in selecting the most critical genes to pursue for future therapeutic discovery. The other multifunctional tumor suppressors identified from comparative analysis of the two independent screens include a group of ubiquitin ligases (*FBXL2*, *RNF219, HUWE1),* a histone protein (*HIST1H1B*), cell signaling components (*MAP2K7*, *PTPRD, TGFBR2),* and a subunit of transcription factor II D (*TAF2*). Future studies will involve screening candidate driver mutations for the ability to bypass CRC chemotherapy-induced apoptosis (i.e. mutations promoting resistance to 5-fluorouracil treatment).

A

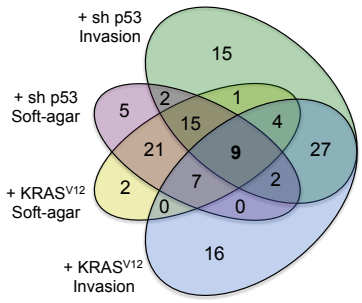

B

Context-independent multifunctional tumor suppressors

			Invasion (fold change ± SD)	
Gene	**Gene Name**	**Entrez Gene ID**	**TP53**	**KRAS**
ADAMTS18	A disintegrin and metalloproteinase with thrombospondin motif 18	170692	13.9 ± 2.6	23.6 ± 2.7
FBXL2	F-box and leucine-rich repeat protein 2	25827	26.7 ± 6.3	17.7 ± 5.3
HIST1H1B	Histone cluster 1, H1b	3009	5.3 ± .04	18.9 ± 4.9
RNF219	Ring finger protein 219	72486	5.4 ± 1.8	17.3 ± 2.3
HUWE1	HECT, UBA, and WWE domain containing 1, E3 ubiquitin ligase	10075	12.0 ± 2.8	6.3 ± 2.5
MAP2K7	Mitogen-activated protein kinase kinase 7	5609	10.2 ± 2.9	9.1 ± 5.1
PTPRD	Protein tyrosine phosphatase, receptor type, D	5789	2.8 ± 0.2	3.9 ± 1.5
TAF2	RNA polymerase II, TATA box binding protein-associated factor	170844	2.6 ± 0.3	3.7 ± 1.3
TGFBR2	Transforming growth factor, beta receptor 2	7048	2.4 ± 0.5	2.8 ± 1.2

Figure 5.7. Comparative analyses of two independent screens reveal multifunctional tumor suppressors within CRC mutated genes.

(A) Venn diagram of overlapping soft-agar growth and invasion suppressing genes in each cell background. Soft-agar hits were obtained from a previously published screen (Eskiocak et al). Nine genes were identified through comparative analysis of both screens. RNAi knockdown of these genes leads to multiple tumorigenic phenotypes.

(B) List of the nine context-independent multifunctional tumor suppressor hits. Knockdown of these nine genes enhances both anchorage-independent growth and invasion in two independent backgrounds *in vitro* (also shown as red dots in **Figure 5.1.B**).

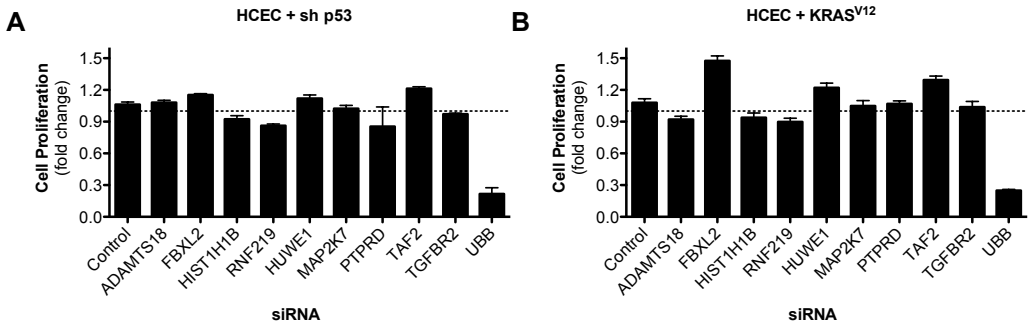

Figure 5.8. Transfections of pooled siRNAs targeting the context-independent multifunctional tumor suppressors do not drastically change proliferation of **(A)** 1CTP and **(B)** 1CTR HCECs after 96 hr transfection.

Materials and Methods

siRNA Transfection and Invasion Screening

Pooled siGENOME siRNAs (Dharmacon, Lafayette, CO) were reverse transfected into 1 x 10^5 1CTP and 1CTR HCECs using RNAiMAX per manufacturer's instructions. Briefly, siRNAs and RNAiMAX were diluted in OptiMEM medium and cells were resuspended and plated in 2% serum conditions. Twenty-four hours later, transfected cells were washed with PBS and replaced with serum-free medium overnight for starvation. For invasion assays, 24-well Matrigel-coated transwell filters (BD Biosciences, San Jose, CA) were thawed and rehydrated according to manufacturer's instructions. Transfected cells were collected, resuspended in 650µL serum-free medium, and 300µL were added to the top chamber in duplicates. The bottom chamber is filled with 600µL 2% serum medium plus growth supplements as a chemoattractant. After overnight incubation, non-invaded cells were scraped off with a cotton swab and wells were washed with PBS. Invaded cells were fixed for 5min in 10% neutral buffered formalin and stained for 10min with 10µg/mL Hoechst (Invitrogen, Grand Island, NY). Images were taken at 10X with five fields imaged per transwell.

Statistical Analysis

Two independent investigators counted the number of cells per field per transwell. These counts were averaged to calculate the fold change relative to control siRNAs. Any siRNA pools that induced a fold change in invasion greater than 3x standard deviations were considered significant.

F-actin Staining

1CTP HCECs were reverse transfected with siRNAs according to methods described above for three days before re-seeding into chamberslides. Cells were washed with PBS, fixed in 4% paraformaldehyde for 10min, and permeabilized with 0.1% Triton X-100. Fixed cells were then stained for F-actin using Alexa Fluor 488 phalloidin (Invitrogen, Grand Island, NY) according to manufacturers instructions.

Lentiviral shRNA Infection

293FT cells were transfected using PolyJet DNA transfection reagent (SignaGen Laboratories, Rockville, MD) with 1ug of the appropriate pGIPZ library vector (and 1ug of helper plasmids (pMD2G and psPAX2). Viral supernatants were collected 24 and 48 hrs post-transfection and cleared through a 0.45uM filter. 1CTP HCECs were infected for 4-6hrs with viral supernatants containing 4ug/mL polybrene (Sigma, St. Louis, MO) and selected with puromycin (Sigma, St. Louis, MO). Successfully infected cells were GFP positive and resistant to three-day puromycin selection.

Quantitative Real-Time PCR

Total RNA were isolated from semi-confluent HCECs using RNeasy Plus Mini Kit (Qiagen, Valencia, CA) and reverse transcribed using iScript cDNA Synthesis Kit (BioRad, Hercules, CA) according to manufacturers instructions. Primers were designed using PrimerBank (http://pga.mgh.harvard.edu/primerbank) and obtained from Sigma. Quantitative PCR were conducted in triplicate reactions using LightCycler 480 SYBR

Green I Master mix (Roche, Basel, Switzerland) and run on a LightCycler 480 Real-Time PCR System using the following amplification settings: 45 cycles at 95°C for 10sec, 60°C for 15sec, and 72°C for 40sec. The housekeeping gene GAPDH was used as an internal control and data were normalized to a non-silencing shRNA.

Proliferation Assay

HCECs were reverse transfected with pooled siRNAs in clear-bottom 96-well plates using the previously described method. Fresh culture medium were added to each well 48hrs post-transfection and cell viability were measured 96hrs post-transfection using CellTiter-Glo Luminescent Assay (Promega, Madison, WI) according to manufacturer's instructions. Luminescent ATP levels were detected by an Envision plate reader (Perkin-Elmer, Waltham, MA) and normalized to a non-targeting siRNA.

APPENDIX A

Comparative analyses of invasion and soft-agar growth suppressing genes

	Invasion*		**Soft-Agar Growth****	
Gene Name	**TP53**	**KRAS**	**TP53**	**KRAS**
ADAMTS18	+	+	+	+
FBXL2	+	+	+	+
HIST1H1B	+	+	+	+
HUWE1	+	+	+	+
MAP2K7	+	+	+	+
PTPRD	+	+	+	+
RNF219	+	+	+	+
TAF2	+	+	+	+
TGFBR2	+	+	+	+
SMAD2	+	+	+	-
ZMYM4	+	+	+	-
DTNB	+	+	-	+
KCNQ5	+	+	-	+
NAV3	+	+	-	+
SYNE1	+	+	-	+
ADARB2	+	+	-	-
ARHGEF10	+	+	-	-
CACNA2D3	+	+	-	-
CD109	+	+	-	-
CLSTN2	+	+	-	-
CUX1	+	+	-	-
EPHB6	+	+	-	-
ERGIC3	+	+	-	-
EVL	+	+	-	-
EYA4	+	+	-	-
FN1	+	+	-	-
GJD4	+	+	-	-
GLI3	+	+	-	-
GPR112	+	+	-	-
GPR158	+	+	-	-
KIAA1409	+	+	-	-

LAMA1	+	+	-	-
MMP2	+	+	-	-
OR51E1	+	+	-	-
P2RY14	+	+	-	-
PTPRU	+	+	-	-
RAPGEF4	+	+	-	-
SEMA3D	+	+	-	-
SHANK1	+	+	-	-
SMAD3	+	+	-	-
TGM3	+	+	-	-
ZNF442	+	+	-	-
ADAMTS15	+	-	+	+
C15orf2	+	-	+	+
CD248	+	-	+	+
CNTN4	+	-	+	+
COL3A1	+	-	+	+
ERCC6	+	-	+	+
FBXW7	+	-	+	+
GRM1	+	-	+	+
HAPLN1	+	-	+	+
MAPK8IP2	+	-	+	+
OBSCN	+	-	+	+
PRDM9	+	-	+	+
PRKDC	+	-	+	+
TIAM1	+	-	+	+
UHRF2	+	-	+	+
GUCY1A2	+	-	+	-
NOS3	+	-	+	-
GALNS	+	-	-	+
ABCB11	+	-	-	-
ADAMTSL3	+	-	-	-
AKAP6	+	-	-	-
ALK	+	-	-	-
BCL9	+	-	-	-
C10orf115	+	-	-	-
C10orf137	+	-	-	-
ERICH1	+	-	-	-

FAM193B	+	-	-	-
SMTN	+	-	-	-
STAB1	+	-	-	-
SYT14L	+	-	-	-
TBX22	+	-	-	-
TLR9	+	-	-	-
TNN	+	-	-	-
IRS4	-	+	+	+
KIAA0182	-	+	+	+
MAP2	-	+	+	+
SFRS6	-	+	+	+
SLC29A1	-	+	+	+
TCF7L2	-	+	+	+
TP53	-	+	+	+
CPAMD8	-	+	-	-
CSMD3	-	+	-	-
FBN2	-	+	-	-
GRID1	-	+	-	-
MKRN3	-	+	-	-
MYO5C	-	+	-	-
NUP210	-	+	-	-
P2RX7	-	+	-	-
PCDH11X	-	+	-	-
PIK3CA	-	+	-	-
PKNOX1	-	+	-	-
RET	-	+	-	-
ROBO1	-	+	-	-
RUNX1T1	-	+	-	-
SCN3B	-	+	-	-
SLC44A4	-	+	-	-
ADAMTS20	-	-	+	+
AKAP12	-	-	+	+
ATP13A1	-	-	+	+
ATP13A5	-	-	+	+
CHL1	-	-	+	+
F8	-	-	+	+
FAM161A	-	-	+	+

IGSF22	-	-	+	+
ITGAE	-	-	+	+
KIAA0556	-	-	+	+
KIAA2022	-	-	+	+
LMO7	-	-	+	+
MAP1B	-	-	+	+
NF1	-	-	+	+
PAK6	-	-	+	+
PHIP	-	-	+	+
PRKD1	-	-	+	+
PTEN	-	-	+	+
SH3TC1	-	-	+	+
TCERG1L	-	-	+	+
UQCRC2	-	-	+	+
GNAS	-	-	+	-
KRT73	-	-	+	-
MLL3	-	-	+	-
MYO19	-	-	+	-
NTNG1	-	-	+	-
CD46	-	-	-	+
DSCAML1	-	-	-	+
ABCA1	-	-	-	-
ACAN	-	-	-	-
ACSL5	-	-	-	-
ADAM29	-	-	-	-
APC	-	-	-	-
ARHGEF1	-	-	-	-
ARHGEF9	-	-	-	-
ATP11A	-	-	-	-
CD93	-	-	-	-
DPP10	-	-	-	-
EPHA3	-	-	-	-
EXOC4	-	-	-	-
FLNC	-	-	-	-
IGFBP3	-	-	-	-
KRAS	-	-	-	-
LCN9	-	-	-	-

LGR6	-	-	-	-
LRP2	-	-	-	-
MCM3AP	-	-	-	-
MYO18B	-	-	-	-
PCDHA9	-	-	-	-
PLB1	-	-	-	-
PLCG2	-	-	-	-
PRUNE2	-	-	-	-
PTPRS	-	-	-	-
RASGRF2	-	-	-	-
SLC22A15	-	-	-	-
SMAD4	-	-	-	-
SORL1	-	-	-	-
TTLL3	-	-	-	-
ZNF521	-	-	-	-
* Results identified from the current study				
** Results obtained from Eskiocak et al, *Cancer Research* 2011				

BIBLIOGRAPHY

Albini A, Iwamoto Y, Kleinman HK, Martin GR, Aaronson SA, Kozlowski JM, McEwan RN. 1987. A rapid in vitro assay for quantitating the invasive potential of tumor cells. Cancer Res 47: 3239-3245.

Aoki K, Aoki M, Sugai M, Harada N, Miyoshi H, Tsukamoto T, Mizoshita T, Tatematsu M, Seno H, Chiba T, Oshima M, Hsieh CL, Taketo MM. 2007. Chromosomal instability by beta-catenin/TCF transcription in APC or beta-catenin mutant cells. Oncogene 26: 3511-3520.

Aschenbach WG, Hirshman MF, Fujii N, Sakamoto K, Howlett KF, Goodyear LJ. 2002. Effect of AICAR treatment on glycogen metabolism in skeletal muscle. Diabetes 51: 567-573.

Baker DJ, Jin F, Jeganathan KB, van Deursen JM. 2009. Whole chromosome instability caused by Bub1 insufficiency drives tumorigenesis through tumor suppressor gene loss of heterozygosity. Cancer Cell 16: 475-486.

Bakhoum SF, Compton DA. 2012. Chromosomal instability and cancer: a complex relationship with therapeutic potential. J Clin Invest 122: 1138-1143.

Bakhoum SF, Thompson SL, Manning AL, Compton DA. 2009. Genome stability is ensured by temporal control of kinetochore-microtubule dynamics. Nat Cell Biol 11: 27-35.

Berrozpe G, Miro R, Caballin MR, Salvador J, Egozcue J. 1990. Trisomy 7 may be a primary change in noninvasive transitional cell carcinoma of the bladder. Cancer Genet Cytogenet 50: 9-14.

Birkbak NJ, Eklund AC, Li Q, McClelland SE, Endesfelder D, Tan P, Tan IB, Richardson AL, Szallasi Z, Swanton C. 2011. Paradoxical relationship between chromosomal instability and survival outcome in cancer. Cancer Res 71: 3447-3452.

Boman BM, Huang E. 2008. Human colon cancer stem cells: a new paradigm in gastrointestinal oncology. J Clin Oncol 26: 2828-2838.

Bomme L, Bardi G, Pandis N, Fenger C, Kronborg O, Heim S. 1994. Clonal karyotypic abnormalities in colorectal adenomas: clues to the early genetic events in the adenoma-carcinoma sequence. Genes Chromosomes Cancer 10: 190-196.

Bomme L, Lothe RA, Bardi G, Fenger C, Kronborg O, Heim S. 2001. Assessments of clonal composition of colorectal adenomas by FISH analysis of chromosomes 1, 7, 13 and 20. Int J Cancer 92: 816-823.

Boveri T. 2008. Concerning the origin of malignant tumours by Theodor Boveri. Translated and annotated by Henry Harris. J Cell Sci 121 Suppl 1: 1-84.

Briand P, Nielsen KV, Madsen MW, Petersen OW. 1996. Trisomy 7p and malignant transformation of human breast epithelial cells following epidermal growth factor withdrawal. Cancer Res 56: 2039-2044.

Calasanz MJ, Cigudosa JC. 2008. Molecular cytogenetics in translational oncology: when chromosomes meet genomics. Clin Transl Oncol 10: 20-29.

Carter H, Chen S, Isik L, Tyekucheva S, Velculescu VE, Kinzler KW, Vogelstein B, Karchin R. 2009. Cancer-specific high-throughput annotation of somatic mutations: computational prediction of driver missense mutations. Cancer Res 69: 6660-6667.

Carter SL, Eklund AC, Kohane IS, Harris LN, Szallasi Z. 2006. A signature of chromosomal instability inferred from gene expression profiles predicts clinical outcome in multiple human cancers. Nat Genet 38: 1043-1048.

Chen G, Bradford WD, Seidel CW, Li R. 2012. Hsp90 stress potentiates rapid cellular adaptation through induction of aneuploidy. Nature 482: 246-250.

Choi CM, Seo KW, Jang SJ, Oh YM, Shim TS, Kim WS, Lee DS, Lee SD. 2009. Chromosomal instability is a risk factor for poor prognosis of adenocarcinoma of the lung: Fluorescence in situ hybridization analysis of paraffin-embedded tissue from Korean patients. Lung Cancer 64: 66-70.

Chrzanowska-Wodnicka M, Burridge K. 1996. Rho-stimulated contractility drives the formation of stress fibers and focal adhesions. J Cell Biol 133: 1403-1415.

Cohen G, Mustafi R, Chumsangsri A, Little N, Nathanson J, Cerda S, Jagadeeswaran S, Dougherty U, Joseph L, Hart J, Yerian L, Tretiakova M, Yuan W, Obara P, Khare S, Sinicrope FA, Fichera A, Boss GR, Carroll R, Bissonnette M. 2006. Epidermal growth factor receptor signaling is up-regulated in human colonic aberrant crypt foci. Cancer Res 66: 5656-5664.

Crosnier C, Stamataki D, Lewis J. 2006. Organizing cell renewal in the intestine: stem cells, signals and combinatorial control. Nat Rev Genet 7: 349-359.

Cunningham D, Atkin W, Lenz HJ, Lynch HT, Minsky B, Nordlinger B, Starling N. 2010. Colorectal cancer. Lancet 375: 1030-1047.

Das AK, Chen BP, Story MD, Sato M, Minna JD, Chen DJ, Nirodi CS. 2007. Somatic mutations in the tyrosine kinase domain of epidermal growth factor receptor (EGFR) abrogate EGFR-mediated radioprotection in non-small cell lung carcinoma. Cancer Res 67: 5267-5274.

Delom F, Burt E, Hoischen A, Veltman J, Groet J, Cotter FE, Nizetic D. 2009. Transchromosomic cell model of Down syndrome shows aberrant migration, adhesion and proteome response to extracellular matrix. Proteome Sci 7: 31.

Dikic I. 2003. Mechanisms controlling EGF receptor endocytosis and degradation. Biochem Soc Trans 31: 1178-1181.

Eskiocak U, Kim SB, Ly P, Roig AI, Biglione S, Komurov K, Cornelius C, Wright WE, White MA, Shay JW. 2011. Functional parsing of driver mutations in the colorectal cancer genome reveals numerous suppressors of anchorage-independent growth. Cancer Res 71: 4359-4365.

Eskiocak U, Kim SB, Roig AI, Kitten E, Batten K, Cornelius C, Zou YS, Wright WE, Shay JW. 2010. CDDO-Me Protects against Space Radiation-Induced Transformation of Human Colon Epithelial Cells. Radiat Res 174(1): 27-36.

Esteller M, Sparks A, Toyota M, Sanchez-Cespedes M, Capella G, Peinado MA, Gonzalez S, Tarafa G, Sidransky D, Meltzer SJ, Baylin SB, Herman JG. 2000. Analysis of adenomatous polyposis coli promoter hypermethylation in human cancer. Cancer Res 60: 4366-4371.

Fearon ER. 2011. Molecular genetics of colorectal cancer. Annu Rev Pathol 6: 479-507.

Fearon ER, Vogelstein B. 1990. A genetic model for colorectal tumorigenesis. Cell 61: 759-767.

Fenton JI, Wolff MS, Orth MW, Hord NG. 2002. Membrane-type matrix metalloproteinases mediate curcumin-induced cell migration in non-tumorigenic colon epithelial cells differing in Apc genotype. Carcinogenesis 23: 1065-1070.

Ferreira BI, Alonso J, Carrillo J, Acquadro F, Largo C, Suela J, Teixeira MR, Cerveira N, Molares A, Gomez-Lopez G, Pestana A, Sastre A, Garcia-Miguel P, Cigudosa JC. 2008. Array CGH and gene-expression profiling reveals distinct genomic instability patterns associated with DNA repair and cell-cycle checkpoint pathways in Ewing's sarcoma. Oncogene 27: 2084-2090.

Fodde R, Kuipers J, Rosenberg C, Smits R, Kielman M, Gaspar C, van Es JH, Breukel C, Wiegant J, Giles RH, Clevers H. 2001. Mutations in the APC tumour suppressor gene cause chromosomal instability. Nat Cell Biol 3: 433-438.

Frey MR, Golovin A, Polk DB. 2004. Epidermal growth factor-stimulated intestinal epithelial cell migration requires Src family kinase-dependent p38 MAPK signaling. J Biol Chem 279: 44513-44521.

Garewal H, Meltzer P, Trent J, Prabhala R, Sampliner R, Korc M. 1990. Epidermal growth factor receptor overexpression and trisomy 7 in a case of Barrett's esophagus. Dig Dis Sci 35: 1115-1120.

Gazdar AF, Shigematsu H, Herz J, Minna JD. 2004. Mutations and addiction to EGFR: the Achilles 'heal' of lung cancers? Trends Mol Med 10: 481-486.

Giannelli G, Falk-Marzillier J, Schiraldi O, Stetler-Stevenson WG, Quaranta V. 1997. Induction of cell migration by matrix metalloprotease-2 cleavage of laminin-5. Science 277: 225-228.

Gordon DJ, Resio B, Pellman D. 2012. Causes and consequences of aneuploidy in cancer. Nat Rev Genet 13: 189-203.

Grade M, Becker H, Liersch T, Ried T, Ghadimi BM. 2006. Molecular cytogenetics: genomic imbalances in colorectal cancer and their clinical impact. Cell Oncol 28: 71-84.

Grady WM, Carethers JM. 2008. Genomic and epigenetic instability in colorectal cancer pathogenesis. Gastroenterology 135: 1079-1099.

Groden J, Thliveris A, Samowitz W, Carlson M, Gelbert L, Albertsen H, Joslyn G, Stevens J, Spirio L, Robertson M, et al. 1991. Identification and characterization of the familial adenomatous polyposis coli gene. Cell 66: 589-600.

Grossmann J, Walther K, Artinger M, Kiessling S, Steinkamp M, Schmautz WK, Stadler F, Bataille F, Schultz M, Scholmerich J, Rogler G. 2003. Progress on isolation and short-term ex-vivo culture of highly purified non-apoptotic human intestinal epithelial cells (IEC). Eur J Cell Biol 82: 262-270.

Guo D, Hildebrandt IJ, Prins RM, Soto H, Mazzotta MM, Dang J, Czernin J, Shyy JY, Watson AD, Phelps M, Radu CG, Cloughesy TF, Mischel PS. 2009. The AMPK agonist AICAR inhibits the growth of EGFRvIII-expressing glioblastomas by inhibiting lipogenesis. Proc Natl Acad Sci U S A 106: 12932-12937.

Habermann JK, Doering J, Hautaniemi S, Roblick UJ, Bundgen NK, Nicorici D, Kronenwett U, Rathnagiriswaran S, Mettu RK, Ma Y, Kruger S, Bruch HP, Auer G, Guo NL, Ried T. 2009. The gene expression signature of genomic instability in breast cancer is an independent predictor of clinical outcome. Int J Cancer 124: 1552-1564.

Habermann JK, Paulsen U, Roblick UJ, Upender MB, McShane LM, Korn EL, Wangsa D, Kruger S, Duchrow M, Bruch HP, Auer G, Ried T. 2007. Stage-specific alterations of the genome, transcriptome, and proteome during colorectal carcinogenesis. Genes Chromosomes Cancer 46: 10-26.

Hadjihannas MV, Bruckner M, Jerchow B, Birchmeier W, Dietmaier W, Behrens J. 2006. Aberrant Wnt/beta-catenin signaling can induce chromosomal instability in colon cancer. Proc Natl Acad Sci U S A 103: 10747-10752.

Hanahan D, Weinberg RA. 2011. Hallmarks of cancer: the next generation. Cell 144: 646-674.

Hassold T, Abruzzo M, Adkins K, Griffin D, Merrill M, Millie E, Saker D, Shen J, Zaragoza M. 1996. Human aneuploidy: incidence, origin, and etiology. Environ Mol Mutagen 28: 167-175.

Hoglund M, Gisselsson D, Hansen GB, Sall T, Mitelman F, Nilbert M. 2002. Dissecting karyotypic patterns in colorectal tumors: two distinct but overlapping pathways in the adenoma-carcinoma transition. Cancer Res 62: 5939-5946.

Huang F, Goh LK, Sorkin A. 2007. EGF receptor ubiquitination is not necessary for its internalization. Proc Natl Acad Sci U S A 104: 16904-16909.

Humphries A, Wright NA. 2008. Colonic crypt organization and tumorigenesis. Nat Rev Cancer 8: 415-424.

Iwaizumi M, Shinmura K, Mori H, Yamada H, Suzuki M, Kitayama Y, Igarashi H, Nakamura T, Suzuki H, Watanabe Y, Hishida A, Ikuma M, Sugimura H. 2009. Human Sgo1 downregulation leads to chromosomal instability in colorectal cancer. Gut 58: 249-260.

Johansson B, Heim S, Mandahl N, Mertens F, Mitelman F. 1993. Trisomy 7 in nonneoplastic cells. Genes Chromosomes Cancer 6: 199-205.

Kaplan KB, Burds AA, Swedlow JR, Bekir SS, Sorger PK, Nathke IS. 2001. A role for the Adenomatous Polyposis Coli protein in chromosome segregation. Nat Cell Biol 3: 429-432.

Komarova NL, Lengauer C, Vogelstein B, Nowak MA. 2002. Dynamics of genetic instability in sporadic and familial colorectal cancer. Cancer Biol Ther 1: 685-692.

Kopetz S, Chang GJ, Overman MJ, Eng C, Sargent DJ, Larson DW, Grothey A, Vauthey JN, Nagorney DM, McWilliams RR. 2009. Improved survival in metastatic colorectal cancer is associated with adoption of hepatic resection and improved chemotherapy. J Clin Oncol 27: 3677-3683.

Lamprecht SA, Lipkin M. 2002. Migrating colonic crypt epithelial cells: primary targets for transformation. Carcinogenesis 23: 1777-1780.

Lassmann S, Weis R, Makowiec F, Roth J, Danciu M, Hopt U, Werner M. 2007. Array CGH identifies distinct DNA copy number profiles of oncogenes and tumor suppressor genes in chromosomal- and microsatellite-unstable sporadic colorectal carcinomas. J Mol Med 85: 293-304.

Le Scouarnec S, Gribble SM. 2012. Characterising chromosome rearrangements: recent technical advances in molecular cytogenetics. Heredity 108: 75-85.

Lee AJ, Endesfelder D, Rowan AJ, Walther A, Birkbak NJ, Futreal PA, Downward J, Szallasi Z, Tomlinson IP, Howell M, Kschischo M, Swanton C. 2011. Chromosomal instability confers intrinsic multidrug resistance. Cancer Res 71: 1858-1870.

Leffler A, Ludwig M, Schmitt O, Busch LC. 1999. Germ cell migration and early development of the gonads in the trisomy 16 mouse--an animal model for Down's syndrome. Ann Anat 181: 247-252.

Lengauer C, Kinzler KW, Vogelstein B. 1997. Genetic instability in colorectal cancers. Nature 386: 623-627.

Lengauer C, Kinzler KW, Vogelstein B. 1998. Genetic instabilities in human cancers. Nature 396: 643-649.

Leung JY, Kolligs FT, Wu R, Zhai Y, Kuick R, Hanash S, Cho KR, Fearon ER. 2002. Activation of AXIN2 expression by beta-catenin-T cell factor. A feedback repressor pathway regulating Wnt signaling. J Biol Chem 277: 21657-21665.

Levkowitz G, Waterman H, Ettenberg SA, Katz M, Tsygankov AY, Alroy I, Lavi S, Iwai K, Reiss Y, Ciechanover A, Lipkowitz S, Yarden Y. 1999. Ubiquitin ligase activity and tyrosine phosphorylation underlie suppression of growth factor signaling by c-Cbl/Sli-1. Mol Cell 4: 1029-1040.

Levkowitz G, Waterman H, Zamir E, Kam Z, Oved S, Langdon WY, Beguinot L, Geiger B, Yarden Y. 1998. c-Cbl/Sli-1 regulates endocytic sorting and ubiquitination of the epidermal growth factor receptor. Genes Dev 12: 3663-3674.

Longva KE, Blystad FD, Stang E, Larsen AM, Johannessen LE, Madshus IH. 2002. Ubiquitination and proteasomal activity is required for transport of the EGF receptor to inner membranes of multivesicular bodies. J Cell Biol 156: 843-854.

Ly P, Eskiocak U, Kim SB, Roig AI, Hight SK, Lulla DR, Zou YS, Batten K, Wright WE, Shay JW. 2011. Characterization of aneuploid populations with trisomy 7 and 20 derived from diploid human colonic epithelial cells. Neoplasia 13: 348-357.

Ly P, Kim SB, Kaisani AA, Marian G, Wright WE, Shay JW. 2012. Aneuploid human colonic epithelial cells are sensitive to AICAR-induced growth inhibition through EGFR degradation. Oncogene.

Manchado E, Malumbres M. 2011. Targeting aneuploidy for cancer therapy. Cell 144: 465-466.

McClelland SE, Burrell RA, Swanton C. 2009. Chromosomal instability: a composite phenotype that influences sensitivity to chemotherapy. Cell Cycle 8: 3262-3266.

McGranahan N, Burrell RA, Endesfelder D, Novelli MR, Swanton C. 2012. Cancer chromosomal instability: therapeutic and diagnostic challenges. EMBO Rep 13: 528-538.

Meijer GA, Hermsen MA, Baak JP, van Diest PJ, Meuwissen SG, Belien JA, Hoovers JM, Joenje H, Snijders PJ, Walboomers JM. 1998. Progression from colorectal adenoma to carcinoma is associated with non-random chromosomal gains as detected by comparative genomic hybridisation. J Clin Pathol 51: 901-909.

Meltzer SJ, Yin J, Manin B, Rhyu MG, Cottrell J, Hudson E, Redd JL, Krasna MJ, Abraham JM, Reid BJ. 1994. Microsatellite instability occurs frequently and in both diploid and aneuploid cell populations of Barrett's-associated esophageal adenocarcinomas. Cancer Res 54: 3379-3382.

Messersmith WA, Ahnen DJ. 2008. Targeting EGFR in colorectal cancer. N Engl J Med 359: 1834-1836.

Mettu RK, Wan YW, Habermann JK, Ried T, Guo NL. 2010. A 12-gene genomic instability signature predicts clinical outcomes in multiple cancer types. Int J Biol Markers 25: 219-228.

Moran A, Ortega P, de Juan C, Fernandez-Marcelo T, Frias C, Sanchez-Pernaute A, Torres AJ, Diaz-Rubio E, Iniesta P, Benito M. 2010. Differential colorectal carcinogenesis: Molecular basis and clinical relevance. World J Gastrointest Oncol 2: 151-158.

Murphy G, Gavrilovic J. 1999. Proteolysis and cell migration: creating a path? Curr Opin Cell Biol 11: 614-621.

Musacchio A, Salmon ED. 2007. The spindle-assembly checkpoint in space and time. Nat Rev Mol Cell Biol 8: 379-393.

Navin N, Kendall J, Troge J, Andrews P, Rodgers L, McIndoo J, Cook K, Stepansky A, Levy D, Esposito D, Muthuswamy L, Krasnitz A, McCombie WR, Hicks J, Wigler M. 2011. Tumour evolution inferred by single-cell sequencing. Nature 472: 90-94.

Nishisho I, Nakamura Y, Miyoshi Y, Miki Y, Ando H, Horii A, Koyama K, Utsunomiya J, Baba S, Hedge P. 1991. Mutations of chromosome 5q21 genes in FAP and colorectal cancer patients. Science 253: 665-669.

Nowak MA, Komarova NL, Sengupta A, Jallepalli PV, Shih Ie M, Vogelstein B, Lengauer C. 2002. The role of chromosomal instability in tumor initiation. Proc Natl Acad Sci U S A 99: 16226-16231.

Ong SE, Blagoev B, Kratchmarova I, Kristensen DB, Steen H, Pandey A, Mann M. 2002. Stable isotope labeling by amino acids in cell culture, SILAC, as a simple and accurate approach to expression proteomics. Mol Cell Proteomics 1: 376-386.

Pavelka N, Rancati G, Zhu J, Bradford WD, Saraf A, Florens L, Sanderson BW, Hattem GL, Li R. 2010. Aneuploidy confers quantitative proteome changes and phenotypic variation in budding yeast. Nature 468: 321-325.

Pavelka N, Rancati G, Zhu J, Bradford WD, Saraf A, Florens L, Sanderson BW, Hattem GL, Li R. 2010. Aneuploidy confers quantitative proteome changes and phenotypic variation in budding yeast. Nature 468: 321-325.

Pino MS, Chung DC. 2010. The chromosomal instability pathway in colon cancer. Gastroenterology 138: 2059-2072.

Platzer P, Upender MB, Wilson K, Willis J, Lutterbaugh J, Nosrati A, Willson JK, Mack D, Ried T, Markowitz S. 2002. Silence of chromosomal amplifications in colon cancer. Cancer Res 62: 1134-1138.

Rajagopalan H, Lengauer C. 2004. Aneuploidy and cancer. Nature 432: 338-341.

Rajagopalan H, Nowak MA, Vogelstein B, Lengauer C. 2003. The significance of unstable chromosomes in colorectal cancer. Nat Rev Cancer 3: 695-701.

Rattan R, Giri S, Singh AK, Singh I. 2005. 5-Aminoimidazole-4-carboxamide-1-beta-D-ribofuranoside inhibits cancer cell proliferation in vitro and in vivo via AMP-activated protein kinase. J Biol Chem 280: 39582-39593.

Ricci-Vitiani L, Fabrizi E, Palio E, De Maria R. 2009. Colon cancer stem cells. J Mol Med (Berl) 87: 1097-1104.

Ried T, Knutzen R, Steinbeck R, Blegen H, Schrock E, Heselmeyer K, du Manoir S, Auer G. 1996. Comparative genomic hybridization reveals a specific pattern of chromosomal gains and losses during the genesis of colorectal tumors. Genes Chromosomes Cancer 15: 234-245.

Roig A.I. SJW. 2010. Immortalization of adult human colonic epithelial cells extracted from normal tissues obtained via colonoscopy. Nature Protocols 10.1038/nprot.2010.29

Roig AI, Eskiocak U, Hight SK, Kim SB, Delgado O, Souza RF, Spechler SJ, Wright WE, Shay JW. 2010. Immortalized epithelial cells derived from human colon biopsies express stem cell markers and differentiate in vitro. Gastroenterology 138: 1012-1021 e1011-1015.

Roschke AV, Kirsch IR. 2010. Targeting karyotypic complexity and chromosomal instability of cancer cells. Curr Drug Targets 11: 1341-1350.

Roschke AV, Tonon G, Gehlhaus KS, McTyre N, Bussey KJ, Lababidi S, Scudiero DA, Weinstein JN, Kirsch IR. 2003. Karyotypic complexity of the NCI-60 drug-screening panel. Cancer Res 63: 8634-8647.

Rusan NM, Peifer M. 2008. Original CIN: reviewing roles for APC in chromosome instability. J Cell Biol 181: 719-726.

Rustgi AK. 2007. The genetics of hereditary colon cancer. Genes Dev 21: 2525-2538.

Sareen D, McMillan E, Ebert AD, Shelley BC, Johnson JA, Meisner LF, Svendsen CN. 2009. Chromosome 7 and 19 trisomy in cultured human neural progenitor cells. PLoS One 4: e7630.

Scheibel T, Buchner J. 1998. The Hsp90 complex--a super-chaperone machine as a novel drug target. Biochem Pharmacol 56: 675-682.

Schlabach MR, Luo J, Solimini NL, Hu G, Xu Q, Li MZ, Zhao Z, Smogorzewska A, Sowa ME, Ang XL, Westbrook TF, Liang AC, Chang K, Hackett JA, Harper JW, Hannon GJ, Elledge SJ. 2008. Cancer proliferation gene discovery through functional genomics. Science 319: 620-624.

Schlessinger J. 2000. Cell signaling by receptor tyrosine kinases. Cell 103: 211-225.

Seiki M. 2002. The cell surface: the stage for matrix metalloproteinase regulation of migration. Curr Opin Cell Biol 14: 624-632.

Selmecki AM, Dulmage K, Cowen LE, Anderson JB, Berman J. 2009. Acquisition of aneuploidy provides increased fitness during the evolution of antifungal drug resistance. PLoS Genet 5: e1000705.

Sethi N, Kang Y. 2011. Unravelling the complexity of metastasis - molecular understanding and targeted therapies. Nat Rev Cancer 11: 735-748.

Shackelford DB, Shaw RJ. 2009. The LKB1-AMPK pathway: metabolism and growth control in tumour suppression. Nat Rev Cancer 9: 563-575.

Shackleton M, Quintana E, Fearon ER, Morrison SJ. 2009. Heterogeneity in cancer: cancer stem cells versus clonal evolution. Cell 138: 822-829.

Shaw RJ, Kosmatka M, Bardeesy N, Hurley RL, Witters LA, DePinho RA, Cantley LC. 2004. The tumor suppressor LKB1 kinase directly activates AMP-activated kinase and regulates apoptosis in response to energy stress. Proc Natl Acad Sci U S A 101: 3329-3335.

Sheltzer JM, Amon A. 2011. The aneuploidy paradox: costs and benefits of an incorrect karyotype. Trends Genet 27: 446-453.

Sheltzer JM, Blank HM, Pfau SJ, Tange Y, George BM, Humpton TJ, Brito IL, Hiraoka Y, Niwa O, Amon A. 2011. Aneuploidy drives genomic instability in yeast. Science 333: 1026-1030.

Sheltzer JM, Torres EM, Dunham MJ, Amon A. 2012. Transcriptional consequences of aneuploidy. Proc Natl Acad Sci U S A 109: 12644-12649.

Sieber OM, Heinimann K, Tomlinson IP. 2003. Genomic instability--the engine of tumorigenesis? Nat Rev Cancer 3: 701-708.

Siegel JJ, Amon A. 2012. New Insights into the Troubles of Aneuploidy. Annu Rev Cell Dev Biol.

Silva P, Barbosa J, Nascimento AV, Faria J, Reis R, Bousbaa H. 2011. Monitoring the fidelity of mitotic chromosome segregation by the spindle assembly checkpoint. Cell Prolif 44: 391-400.

Smid M, Hoes M, Sieuwerts AM, Sleijfer S, Zhang Y, Wang Y, Foekens JA, Martens JW. 2011. Patterns and incidence of chromosomal instability and their prognostic relevance in breast cancer subtypes. Breast Cancer Res Treat 128: 23-30.

Sotillo R, Hernando E, Diaz-Rodriguez E, Teruya-Feldstein J, Cordon-Cardo C, Lowe SW, Benezra R. 2007. Mad2 overexpression promotes aneuploidy and tumorigenesis in mice. Cancer Cell 11: 9-23.

Sotillo R, Schvartzman JM, Socci ND, Benezra R. 2010. Mad2-induced chromosome instability leads to lung tumour relapse after oncogene withdrawal. Nature 464: 436-440.

Speicher MR, Carter NP. 2005. The new cytogenetics: blurring the boundaries with molecular biology. Nat Rev Genet 6: 782-792.

Stappenbeck TS, Wong MH, Saam JR, Mysorekar IU, Gordon JI. 1998. Notes from some crypt watchers: regulation of renewal in the mouse intestinal epithelium. Curr Opin Cell Biol 10: 702-709.

Stephens PJ, Greenman CD, Fu B, Yang F, Bignell GR, Mudie LJ, Pleasance ED, Lau KW, Beare D, Stebbings LA, McLaren S, Lin ML, McBride DJ, Varela I, Nik-Zainal S, Leroy C, Jia M, Menzies A, Butler AP, Teague JW, Quail MA, Burton J, Swerdlow H, Carter NP, Morsberger LA, Iacobuzio-Donahue C, Follows GA, Green AR, Flanagan AM, Stratton MR, Futreal PA, Campbell PJ. 2011. Massive genomic rearrangement acquired in a single catastrophic event during cancer development. Cell 144: 27-40.

Stingele S, Stoehr G, Peplowska K, Cox J, Mann M, Storchova Z. 2012. Global analysis of genome, transcriptome and proteome reveals the response to aneuploidy in human cells. Mol Syst Biol 8: 608.

Stratton MR. 2011. Exploring the genomes of cancer cells: progress and promise. Science 331: 1553-1558.

Tang YC, Williams BR, Siegel JJ, Amon A. 2011. Identification of aneuploidy-selective antiproliferation compounds. Cell 144: 499-512.

Thompson SL, Bakhoum SF, Compton DA. 2010. Mechanisms of chromosomal instability. Curr Biol 20: R285-295.

Tighe A, Johnson VL, Taylor SS. 2004. Truncating APC mutations have dominant effects on proliferation, spindle checkpoint control, survival and chromosome stability. J Cell Sci 117: 6339-6353.

Torres EM, Dephoure N, Panneerselvam A, Tucker CM, Whittaker CA, Gygi SP, Dunham MJ, Amon A. 2010. Identification of aneuploidy-tolerating mutations. Cell 143: 71-83.

Torres EM, Sokolsky T, Tucker CM, Chan LY, Boselli M, Dunham MJ, Amon A. 2007. Effects of aneuploidy on cellular physiology and cell division in haploid yeast. Science 317: 916-924.

Torres EM, Williams BR, Amon A. 2008. Aneuploidy: cells losing their balance. Genetics 179: 737-746.

Tsafrir D, Bacolod M, Selvanayagam Z, Tsafrir I, Shia J, Zeng Z, Liu H, Krier C, Stengel RF, Barany F, Gerald WL, Paty PB, Domany E, Notterman DA. 2006. Relationship of gene expression and chromosomal abnormalities in colorectal cancer. Cancer Res 66: 2129-2137.

Upender MB, Habermann JK, McShane LM, Korn EL, Barrett JC, Difilippantonio MJ, Ried T. 2004. Chromosome transfer induced aneuploidy results in complex dysregulation of the cellular transcriptome in immortalized and cancer cells. Cancer Res 64: 6941-6949.

Wallqvist A, Huang R, Covell DG, Roschke AV, Gelhaus KS, Kirsch IR. 2005. Drugs aimed at targeting characteristic karyotypic phenotypes of cancer cells. Mol Cancer Ther 4: 1559-1568.

Walther A, Houlston R, Tomlinson I. 2008. Association between chromosomal instability and prognosis in colorectal cancer: a meta-analysis. Gut 57: 941-950.

Weaver BA, Cleveland DW. 2008. The aneuploidy paradox in cell growth and tumorigenesis. Cancer Cell 14: 431-433.

Weaver BA, Silk AD, Montagna C, Verdier-Pinard P, Cleveland DW. 2007. Aneuploidy acts both oncogenically and as a tumor suppressor. Cancer Cell 11: 25-36.

Wei X, Prickett TD, Viloria CG, Molinolo A, Lin JC, Cardenas-Navia I, Cruz P, Rosenberg SA, Davies MA, Gershenwald JE, Lopez-Otin C, Samuels Y. 2010. Mutational and functional analysis reveals ADAMTS18 metalloproteinase as a novel driver in melanoma. Mol Cancer Res 8: 1513-1525.

Williams BR, Amon A. 2009. Aneuploidy: cancer's fatal flaw? Cancer Res 69: 5289-5291.

Williams BR, Prabhu VR, Hunter KE, Glazier CM, Whittaker CA, Housman DE, Amon A. 2008. Aneuploidy affects proliferation and spontaneous immortalization in mammalian cells. Science 322: 703-709.

Wong SF. 2005. Cetuximab: an epidermal growth factor receptor monoclonal antibody for the treatment of colorectal cancer. Clin Ther 27: 684-694.

Wood LD, Parsons DW, Jones S, Lin J, Sjoblom T, Leary RJ, Shen D, Boca SM, Barber T, Ptak J, Silliman N, Szabo S, Dezso Z, Ustyanksky V, Nikolskaya T, Nikolsky Y, Karchin R, Wilson PA, Kaminker JS, Zhang Z, Croshaw R, Willis J, Dawson D, Shipitsin M, Willson JK, Sukumar S, Polyak K, Park BH, Pethiyagoda CL, Pant PV, Ballinger DG, Sparks AB, Hartigan J, Smith DR, Suh E, Papadopoulos N, Buckhaults P, Markowitz SD, Parmigiani G, Kinzler KW, Velculescu VE, Vogelstein B. 2007. The genomic landscapes of human breast and colorectal cancers. Science 318: 1108-1113.

Zhang J, Wang X, Zhao Y, Chen B, Suo G, Dai J. 2006. Neoplastic transformation of human diploid fibroblasts after long-term serum starvation. Cancer Lett 243: 101-108.

Zhuang Z, Park WS, Pack S, Schmidt L, Vortmeyer AO, Pak E, Pham T, Weil RJ, Candidus S, Lubensky IA, Linehan WM, Zbar B, Weirich G. 1998. Trisomy 7-harbouring non-random duplication of the mutant MET allele in hereditary papillary renal carcinomas. Nat Genet 20: 66-69.